รายงานวิจัยฉบับสมบูรณ์

โครงการ การควบคุมและบทบาทของระบบขนส่งโลหะ ต่อความอยู่รอดและการก่อโรคของเชื้อ *Agrobacterium tumefaciens*

โดย ดร. รจนา สุขชวลิต

เดือน มิถุนายน พ.ศ. 2561

สัญญาเลขที่ RSA5880010

รายงานวิจัยฉบับสมบูรณ์

โครงการ การควบคุมและบทบาทของระบบขนส่งโลหะ ต่อความอยู่รอดและการก่อโรคของเชื้อ *Agrobacterium tumefaciens*

ดร. รจนา สุขชวลิต
ห้องปฏิบัติการวิจัยเทคโนโลยีชีวภาพ
สถาบันวิจัยจุฬาภรณ์

สนับสนุนโดยสำนักงานกองทุนสนับสนุนการวิจัยและสถาบันวิจัยจุฬาภรณ์

บทคัดย่อ

รหัสโครงการ RSA5880010

ชื่อโครงการ การควบคุมและบทบาทของระบบขนส่งโลหะ ต่อความอยู่รอดและการก่อโรคของเชื้อ *Agrobacterium tumefaciens*

ชื่อนักวิจัย ดร. รจนา สุขชวลิต

E-mail addresss rojana@cri.or.th

ระยะเวลาโครงการ 3 ปี

คำหลัก: สังกะสี โคบอลต์ การรักษาสมดุล

Agrobacterium tumefaciens เป็นแบคทีเรียที่ก่อโรคปุ่มปม (crown gall tumor) ในพืช สังกะสีและโคบอลต์เป็นโลหะที่มีความจำเป็นต่อต่อการเจริญเติบโตของพืชและแบคทีเรีย แต่หากมีโลหะภายในเซลล์เกินความจำเป็นจะเป็นพิษต่อเซลล์ได้ แบคทีเรีย *A. tumefaciens* มีกลไกการรักษาสมดุลของสังกะสีภายในเซลล์โดยอาศัยการควบคุมระบบนำเข้าและส่งออกของสังกะสี ในสภาวะที่ขาดแคลนสังกะสีแบคทีเรีย *A. tumefaciens* มีระบบนำเข้าสังกะสีที่สำคัญสองระบบคือ TroCBA และ ZnuABC โดยการทำงานของระบบ TroCBA มีความสำคัญอย่างมากและทำงานร่วมกับโปรตีน ZinT ในขณะที่ระบบ ZnuABC จะเป็นเสมือนระบบสำรองกรณีที่ TroCBA ไม่สามารถทำงานได้ตามปกติ เมื่อสังกะสีเข้าสู่เซลล์แบคทีเรียแล้วการส่งต่อสังกะสีไปยังโปรตีนต่างๆโดยโปรตีน ZinT และ YciC ก็มีความสำคัญต่อการเจริญเติบโตในสภาวะที่ขาดแคลนสังกะสีเช่นกัน ในสภาวะที่มีสังกะสีมากเกินความต้องการของแบคทีเรีย โปรตีน Zur จะจับกับสังกะสีและทำหน้าที่ในการกดการแสดงออกของยีน *troCBA znuABC zinT* และ *yciC* เพื่อลดการนำสังกะสีเข้าเซลล์ ในขณะที่ โปรตีน ZntR เมื่อจับกับสังกะสีแล้วจะทำหน้าที่ไปกระตุ้นการแสดงออกของยีน *zntA* โดยโปรตีน ZntA จะทำหน้าที่ในการกำจัดสังกะสีออกนอกเซลล์ โคบอลต์เป็นโลหะจำเป็นซึ่งเป็นองค์ประกอบของวิตามินบี12 และโปรตีนหลายชนิด การมีปริมาณโคบอลต์มากเกินจะเป็นพิษกับเซลล์โดยก่อให้เกิดสารอนุมูลอิสระและกระทบต่อระบบควบคุมเหล็กภายในเซลล์ แบคทีเรีย *A. tumefaciens* มีกลไกลดระดับโคบอลต์โดยการขับโคบอลต์ออกด้วยโปรตีน DmeF การแสดงออกของยีน *dmeF* จะถูกกดโดยโปรตีน DmeR ในสภาวะที่ขาดแคลนโคบอลต์ เมื่อระดับโคบอลต์มีเกินความจำเป็นโคบอลต์จะไปจับกับโปรตีน DmeR และทำให้ไม่สามารถกดการแสดงออกของยีน *dmeF* เมื่อโปรตีน DmeF ถูกสร้างขึ้นก็เริ่มขับโคบอลต์ออกนอกเซลล์เพื่อรักษาระดับที่เหมาะสมของโคบอลต์ภายในเซลล์ของแบคทีเรีย

Abstract

Project Code: RSA5880010

Project Title: Regulation and role of transition metal transporters for the survival and virulence of *Agrobacterium tumefaciens*

Investigator: Dr. Rojana Sukchawalit

E-mail addresss rojana@cri.or.th

Project Period: 3 years

Keywords: zinc, cobalt, metal homeostasis

Both host and pathogen battle over access to essential metals including zinc and cobalt. However, metal overload is toxic to cells. Zinc homeostasis in *Agrobacterium tumefaciens* is maintained through controlling zinc uptake and zinc efflux systems. To survive under a wide range of zinc-deficient conditions, *A. tumefaciens* requires co-operation of Zur-regulated zinc acquisition systems, including two ABC-type zinc importers: TroCBA and ZnuABC and two zinc chaperones: ZinT and YciC. It was found that TroCBA and ZinT play dominant roles. While ZnuABC may function as a back-up system and is very important for supporting growth under zinc limitation when TroCBA is disrupted. When *A. tumefaciens* encounters conditions of severe zinc shortage, even if the high-affinity zinc uptake TroCBA and ZnuABC systems are still functioning, it need ZinT and YciC to effectively shuttle zinc ions to essential zinc-dependent proteins, in the periplasm and cytoplasm respectively, whose functions are required to cope with low-zinc stress. When intracellular zinc is overloaded, the complexes of Zn^{2+} with the zinc sensors are formed, Zur-Zn^{2+} and ZntR-Zn^{2+}. The Zur-Zn^{2+} complex represses the zinc uptake genes, whereas the ZntR-Zn^{2+} complex activates the zinc efflux gene, *zntA*. Consequently, the high-affinity zinc uptake systems, TroCBA and ZnuABC, are shut down, and excess zinc can be pumped out of the cytoplasm by a P_{1B}-type ATPase, ZntA. Cobalt is required by coenzyme B_{12}-dependent enzymes and several proteins. However, cobalt overload can cause cellular toxicity through catalyzing the generation of reactive oxygen species and leads to iron and glutathione depletion, thus disturbing iron homeostasis. To prevent intracellular cobalt overload-mediated toxicity, excessive amounts of cobalt are eliminated by DmeF (divalent metal efflux) protein. Transcription of *dmeF* gene is regulated by the transcriptional regulator DmeR. The binding of Co^{2+}causes conformational changes in DmeR resulting in dissociation from DNA, thus triggering the transcription of the *dmeF*.

สารบัญ

หน้า

หน้าสรุปโครงการ (Executive Summary)

RSA5880010-รจนา สุขชวลิต

การควบคุมและบทบาทของระบบขนส่งโลหะ ต่อความอยู่รอดและการก่อโรคของเชื้อ *Agrobacterium tumefaciens*

1. ความสำคัญและที่มาของปัญหา

Pathogens and hosts compete for essential metals such as iron, zinc, nickel and cobalt. Metal stress, either deficiency or excess, can be used as a host defence (Bezkorovainy, 1981; Ward & Conneely, 2004; Nairz *et al*., 2010; Botella *et al*., 2012; Fones & Preston, 2012). Under severe metal-limiting conditions, bacteria sequester metals from the environments via turn on high-affinity metal uptake systems (Andrews *et al*., 2003; Blencowe & Morby AP, 2003; Rodionov *et al*., 2006; Berntsson *et al*., 2010). When intracellular metal concentrations are overload, bacteria pump metals out of cells using various types of metal efflux systems (Nies, 2003; Guilhen *et al*., 2013). The balance of metal uptake and efflux in bacteria need to be tightly controlled in order to meet cellular demand and prevent metal toxicity. Therefore, metal transporters play an important role during bacterial infection and can have an impact on disease development (Stähler *et al*., 2006; Brenot *et al*., 2007; Klein & Lewinson, 2011; Botella *et al*., 2012; Lewis *et al*., 2012; Guilhen *et al*., 2013; Shafeeq *et al*., 2013). Study of bacterial metal transporters will facilitate the design of more effective antimicrobial agents or vaccine development (Yang *et al*., 2006; Couñago *et al*., 2012). Toward these applications, more research into a clear understanding of physiological functions and mechanisms of metal transporters as well as their roles for bacterial survival and virulence is needed.

The alpha-proteobacteria contain diverse group of organisms, including the human pathogen *Bartonella*, the animal pathogen *Brucella*, and the plant pathogen *Agrobacterium*. The transport of metals in alpha-proteobacteria is poorly understood. *Agrobacterium tumefaciens* is a Gram-negative, soil-born plant pathogen that causes crown gall tumor disease on dicotyledonous plants. Bacterial zinc uptake, ZnuABC and ZinT, are well studied in *Escherichia coli* and Salmonella *enterica* serovar Typhimurium. The ZnuABC is a high-affinity zinc transporter belonging to ATP-binding cassette family and plays a dominant role, while ZinT is a periplasmic zinc-binding protein that helps ZnuA in zinc transport through ZnuBC (Petrarca *et al*., 2010; Gabbiannelli *et al.*, 2011). It was found that *A. tumefaciens* ZnuABC did not play an apparent role whereas *A. tumefaciens* ZinT was more important and could function independently of ZnuABC (Bhubhanil *et al*., 2014). The loss of *A. tumefaciens* ZinT but not ZnuA and ZnuB, caused a slight reduction in the cellular zinc content, implying the existence of an additional high-affinity zinc uptake system. Zinc uptake and zinc efflux systems both help to maintain the intracellular zinc homeostasis. The research will particularly focus on the identification of additional zinc uptake system (Atu3180-Atu3179-Atu3178) and the investigation of zinc efflux systems (ZntR, ZntA and ZntB) in order to gain a better understanding of how *A. tumefaciens* maintains zinc homeostasis and the impact of these zinc transporters on bacterial survival and virulence.

Cobalt stress has been shown to affect iron homeostasis and Fe-S cluster is a major target of cobalt toxicity in *E. coli* and *S. enterica* (Barras and Fontecave, 2011). Since Fe-S clusters are required for function of many enzymes and proteins, damage of Fe-S cluster leads to production of non-functional proteins and thus disrupting many vital biological processes. Iron regulation in alpha-proteobacteria differs from many other bacteria in which the iron response regulator (Irr) and the rhizobial iron regulator (RirA) are the regulators of many iron-responsive genes under low iron and high iron conditions, respectively (Hibbing & Fuqua, 2011). Unlike Irr, RirA requires Fe-S cluster for its repression function. However, the effect of cobalt stress on RirA activity has not been reported. RirA was shown to be important for the survival and virulence of *A. tumefaciens* (Ngok-ngam *et al*., 2009). The research aims to determine the effect of a putative cobalt exporter (DmeRF) on controlling the cellular cobalt levels and to determine whether cobalt stress interferes with RirA activity which in turn may affect bacterial survival and virulence.

References

Alexeyev MF (1999) The pKNOCK series of broad-host-range mobilizable suicide vectors for gene knockout and targeted DNA insertion into the chromosome of gram-negative bacteria. *Biotechniques* 26:824-826, 828.

Andrews SC, Robinson AK & Rodríguez-Quiñones F (2003) Bacterial iron homeostasis. *FEMS Microbiol Rev* 27:215-237.

Barras F & Fontecave M. (2011) Cobalt stress in *Escherichia coli* and *Salmonella enterica*: molecular bases for toxicity and resistance. *Metallomics* 3:1130-1134.

Berntsson RP, Smits SH, Schmitt L, Slotboom DJ & Poolman B (2010) A structural classification of substrate-binding proteins. *FEBS Lett* 584:2606-2617.

Bezkorovainy A (1981) Antimicrobial properties of iron-binding proteins. *Adv Exp Med Biol* 135:139-154.

Bhubhanil S, Sittipo P, Chaoprasid P, Nookabkaew S, Sukchawalit R & Mongkolsuk S. (2014) Control of zinc homeostasis in *Agrobacterium tumefaciens* via *zur* and the zinc uptake genes *znuABC* and *zinT*. *Microbiology* doi: 10.1099/mic.0.082446-0.

Blencowe DK & Morby AP (2003) Zn(II) metabolism in prokaryotes. *FEMS Microbiol Rev* 27:291-311.

Botella H, Stadthagen G, Lugo-Villarino G, de Chastellier C & Neyrolles O. (2012) Metallobiology of host-pathogen interactions: an intoxicating new insight. *Trends Microbiol* 20:106-12.

Brenot A, Weston BF & Caparon MG (2007) A PerR-regulated metal transporter (PmtA) is an interface between oxidative stress and metal homeostasis in *Streptococcus pyogenes*. *Mol Microbiol* 63:1185-1196.

Cangelosi GA, Best EA, Martinetti G & Nester EW (1991) Genetic analysis of *Agrobacterium*. *Methods Enzymol* 204:384-397.

Couñago RM, McDevitt CA, Ween MP & Kobe B (2012) Prokaryotic substrate-binding proteins as targets for antimicrobial therapies. *Curr Drug Targets* 13:1400-1410.

Fones H & Preston GM (2012). The impact of transition metals on bacterial plant disease. *FEMS Microbiol Rev* 37:495-519.

Gabbianelli R, Scotti R, Ammendola S, Petrarca P, Nicolini L & Battistoni A. (2011) Role of ZnuABC and ZinT in *Escherichia coli* O157:H7 zinc acquisition and interaction with epithelial cells. *BMC Microbiol* 11:36.

Guilhen C, Taha MK & Veyrier FJ. (2013). Role of transition metal exporters in virulence: the example of Neisseria meningitidis. *Front Cell Infect Microbiol* 3:102.

Hibbing ME & Fuqua C (2011) Antiparallel and interlinked control of cellular iron levels by the Irr and RirA regulators of *Agrobacterium tumefaciens*. *J Bacteriol* 193: 3461-3472.

Kamoun S, Hamada W & Huitema E (2003) Agrosuppression: a bioassay for the hypersensitive response suited to high-throughput screening. *Mol Plant Microbe Interact* 16: 7-13.

Kitphati W, Ngok-ngam P, Suwanmaneerat S, Sukchawalit R & Mongkolsuk S (2007) *Agrobacterium tumefaciens fur* has important physiological roles in iron and manganese homeostasis, the oxidative stress response, and full virulence. *Appl Environ Microbiol* 73: 4760–4768.

Klein JS & Lewinson O (2011) Bacterial ATP-driven transporters of transition metals: physiological roles, mechanisms of action, and roles in bacterial virulence. *Metallomics* 3:1098-3108.

Kovach ME, Elzer PH, Hill DS, Robertson GT, Farris MA, Roop II RM & Peterson KM (1995) Four new derivatives of the broad-host-range cloning vector pBBR1MCS, carrying different antibiotic-resistance cassettes. *Gene* 166:175-176.

Lewis VG, Ween MP & McDevitt CA (2012) The role of ATP-binding cassette transporters in bacterial pathogenicity. *Protoplasma* 249:919-942.

Livak KJ & Schmittgen TD (2001) Analysis of relative gene expression data using real-time quantitative PCR and the $2^{-\Delta\Delta Ct}$ Method. *Methods* 25:402-408.

Luo ZQ, Clemente TE & Farrand SK (2001) Construction of a derivative of *Agrobacterium tumefaciens* C58 that does not mutate to tetracycline resistance. *Mol Plant-Microbe Interact* 14:98–103.

Nairz M, Schroll A, Sonnweber T & Weiss G (2010) The struggle for iron - a metal at the host-pathogen interface. *Cell Microbiol* 12:1691-1702.

Nies DH (2003) Efflux-mediated heavy metal resistance in prokaryotes. *FEMS Microbiol Rev* 27: 313-339.

Petrarca P, Ammendola S, Pasquali P & Battistoni A (2010) The Zur-regulated ZinT protein is an auxiliary component of the high-affinity ZnuABC zinc transporter that facilitates metal recruitment during severe zinc shortage. *J Bacteriol* 192:1553-1564.

Rodionov DA, Hebbeln P, Gelfand MS & Eitinger T. (2006) Comparative and functional genomic analysis of prokaryotic nickel and cobalt uptake transporters: evidence for a novel group of ATP-binding cassette transporters. *J Bacteriol* 188:317-327.

Sambrook J, Fritsch EF & Maniatis T (1989) *Molecular cloning*: *A Laboratory Manual*. Cold Spring Harbor, NY:Cold Spring Harbor Laboratory Pres

Shafeeq S, Kuipers OP & Kloosterman TG. (2013) The role of zinc in the interplay between pathogenic streptococci and their hosts. *Mol Microbiol* 88:1047-1057.

Stähler FN, Odenbreit S, Haas R, Wilrich J, Van Vliet AH, Kusters JG, Kist M & Bereswill S (2006) The novel *Helicobacter pylori* CznABC metal efflux pump is required for cadmium, zinc, and nickel resistance, urease modulation, and gastric colonization. *Infect Immun* 74:3845-3852.

Ward PP & Conneely OM (2004) Lactoferrin: role in iron homeostasis and host defense against microbial infection. *Biometals* 17:203-208.

Yang X, Becker T, Walters N & Pascual DW (2006) Deletion of *znuA* virulence factor attenuates *Brucella abortus* and confers protection against wild-type challenge. *Infect Immun* 74:3874-3879.

2. วัตถุประสงค์

2.1 To study regulation and roles of the *troBCA* operon in zinc homeostasis and virulence of *A. tumefaciens*.

2.2 To study regulation and roles of putative genes involved in zinc efflux (*zntR, zntA* and *zntB*) in zinc homeostasis and virulence of *A. tumefaciens*.

2.3 To study regulation and roles of putative genes involved in cobalt and nickel transport (*dmeR* and *dmeF*) in metal homeostasis and virulence of *A. tumefaciens*.

● **แผนการวิจัยตลอดโครง ระยะเวลาของโครงการ: 3 ปี** (1 กรกฎาคม พ.ศ. 2558 ถึงวันที่ 30 มิถุนายน พ.ศ. 2561)

	Year 1		Year 2		Year 3	
	1st half	2nd half	1st half	2nd half	1st half	2nd half
PART I						
1. Expression analysis of *zntA* and *zntB* in response to metals using qRT-PCR in order to determine metal-specific response of these genes.	↔					
2. Construction of mutant strains containing mutation either at *zntR*, *zntA* or *zntB*, and double mutations at *zntA* and *zntB*.	↔					
3. Construction of plasmids expressing functional gene either *zntA* or *zntB* for complementation.	↔					
4. Determine whether ZntR is the regulator of *zntA* and *zntB* by comparing expression levels of these genes in wild-type and *zntR* mutant using qRT-PCR.	↔					
5. Sensitivity test to metals using wild-type, mutants and complemented strains.	↔					
6. Determine total cellular metal content of the mutant strains compared to wild-type using ICP-MS.	↔					
7. Determine virulence of *zntR*, *zntA* and *zntB* mutants using *Nicotiana benthamiana* plants infected with wild-type, mutants and complemented strains.		↔				
PART II						
8. Determine whether zinc uptake genes (*zinT*, *znuABC* and *troBCA*) play a role in the response to oxidants. Oxidant sensitivity test in wild-type and mutant strains.		↔				
9. Determine whether zinc efflux genes (*zntR*, *zntA* and *zntB*) play a role in the response to oxidants. Oxidant sensitivity test in wild-type and mutant strains.		↔				
10. Manuscript preparation		↔				

	Year 1		Year 2		Year 3	
	1st half	2nd half	1st half	2nd half	1st half	2nd half
PART III						
1. RT-PCR analysis to determine whether Atu3180, Atu3179 and Atu3178 genes are co-transcribed.			↔			
2. Expression analysis of the *troBCA* operon in response to metals using qRT-PCR in order to determine metal-specific response of the *troBCA* operon.			↔			
3. Determine whether Zur is the regulator of the *troBCA* operon by comparing expression levels of *troBCA* in wild-type and *zur* mutant using qRT-PCR.			↔			
4. Construction of mutant strains containing a single mutation either at Atu3180 or Atu3178.			↔			
5. Construction of a plasmid expressing functional *troA* gene (Atu3178) for complementation and comparing role of TroA with other periplasmic zinc-binding proteins (ZinT and ZnuA).			↔			
6. Construction of double mutant strains containing mutations at Atu3180 in combination with either *zinT* or *znuA* in order to test whether these genes co-operate to transport zinc.				↔		
7. Sensitivity test to metals and a metal chelator EDTA using wild-type, mutants and complemented strains.				↔		
8. Determine total cellular metal content of wild-type and mutant strains using ICP-MS.				↔		
9. Determine roles of the *troBCA* operon in the virulence of *A. tumefaciens* using *Nicotiana benthamiana* plants infected with wild-type, mutants and complemented strains.				↔		
10. Preparation of manuscript				↔		

	Year 1		Year 2		Year 3	
	1st half	2nd half	1st half	2nd half	1st half	2nd half
PART IV						
1. RT-PCR analysis to determine whether *dmeR* and *dmeF* genes are co-transcribed.					↔	
2. Expression analysis of *dmeRF* in response to various metals using qRT-PCR in order to determine metal-specific response of *dmeRF*.					↔	
3. Construction of plasmids expressing functional gene either *dmeR* or *dmeF* for complementation.					↔	
4. Determine whether DmeR is the regulator of *dmeF* by comparing expression levels of *dmeF* in wild-type and *dmeR* mutant using qRT-PCR.					↔	
5. Sensitivity test to various metals using wild-type, mutants and complemented strains.					↔	
6. Determine total cellular metal content of the mutant strains compared to wild-type using ICP-MS.						↔
7. Determine virulence of *dmeR* and *dmeF* mutants using *Nicotiana benthamiana* plants infected with wild-type, mutants and complemented strains.						↔
8. Determine the influence of cobalt stress, which may result from the loss of *dmeF*, on the iron regulation by monitoring iron-responsive genes that are regulated by RirA and Irr using qRT-PCR.						↔
9. Determine whether cobalt stress, which may result from the loss of *dmeF*, affects activity of Fe-S proteins including *soxR* and aconitase.						↔
10. Manuscript preparation						↔

3. ผลงานวิจัย

3.1 To study regulation and roles of putative genes involved in zinc efflux (*zntR, zntA* and *zntB*) in zinc homeostasis and virulence of *A. tumefaciens*.

3.1.1 *A. tumefaciens zntR* mediates the induction of *zntA* in response to cadmium, zinc and cobalt.

The expression of *A. tumefaciens zntA* and *zntB* in response to zinc levels was determined using qRT-PCR analysis. In the wild-type strain (WT), the expression of *zntA*, but not *zntB*, was increased after treatments with 100, 500 and 750 μM $ZnCl_2$ **(Fig. 1a**). The zinc-mediated induction of *zntA* was abolished in the *zntR* mutant strain (ZR1423), suggesting that *zntR* activates *zntA* (**Fig. 1a**). The loss of zinc-induced *zntA* expression was able to be restored in the complemented strain (ZR1423/pZNTR) (**Fig. 2a**). Next, the metal-specific response of *zntA* was determined using WT cells grown in LB individually supplemented with 250 μM $CdCl_2$, $CoCl_2$, $CuSO_4$, $FeCl_3$, $MgCl_2$, $MnCl_2$, $NiCl_2$, $PbSO_4$ or $ZnCl_2$. The results shown in **Fig. 1b** suggest that Cd (∼100-fold) was the best inducer, followed by Zn (∼14-fold) and Co (∼8-fold), while other metals induced less than 3-fold *zntA* expression (Ni and Pb) or had no effect (Cu, Fe, Mg and Mn). The expression of *zntB* was not affected by the *zntR* mutation (**Fig. 2a**), and *zntB* expression was not strikingly changed upon treatment with zinc (**Fig. 1a**) or other metals (**Fig. 2b**).

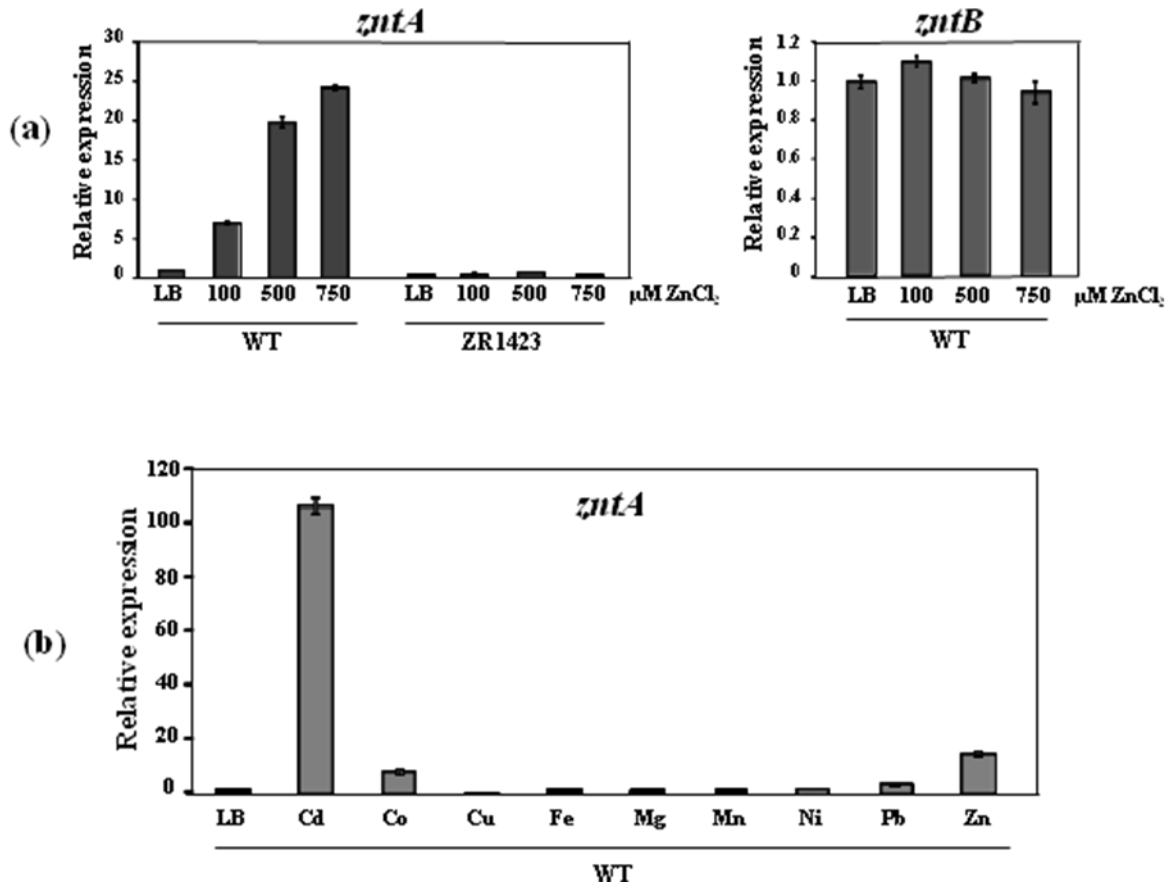

FIG. 1. (a) Transcription analyses of *zntA* and *zntB* in response to increased zinc levels using qRT-PCR. Wild-type (WT) and the *zntR* mutant (ZR1423) cells were grown to the log phase in LB medium supplemented with 100, 500 and 750 μM $ZnCl_2$ for 15 min. The expression of the target genes was normalized to 16S rRNA, and the fold-changes in gene expression were assessed relative to WT cells grown in LB (regarded as 1). The experiment was performed in biological triplicate, and the error bars indicate the standard deviations.

(b) qRT-PCR analysis of *zntA* expression in response to various metals. WT cells were grown in LB medium to the log phase and individually supplemented with 250 μM of $CdCl_2$, $CoCl_2$, $CuSO_4$, $FeCl_3$, $MgCl_2$, $MnCl_2$, $NiCl_2$, $PbNO_3$ or $ZnCl_2$ for 15 min. The fold-changes in gene expression were assessed relative to cells grown in LB (regarded as 1).

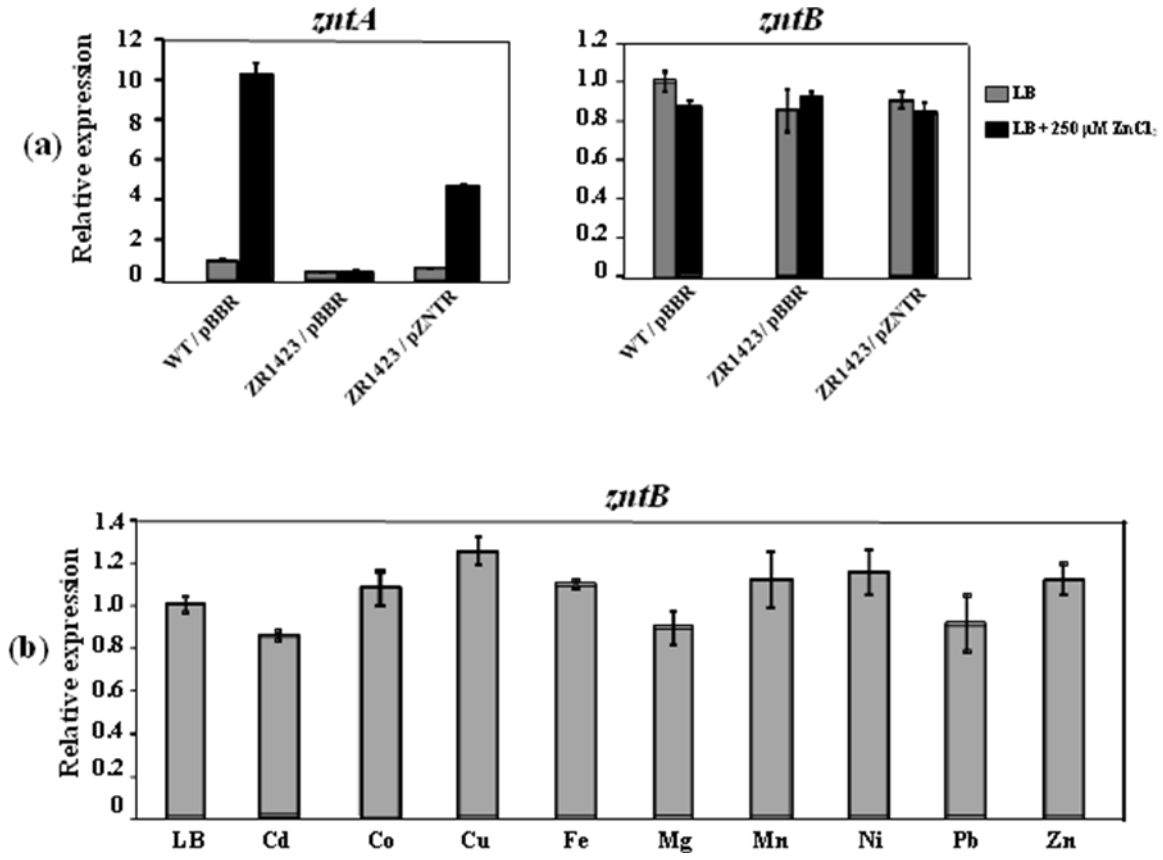

FIG. 2. (a) qRT-PCR analysis of *zntA* and *zntB* expression in wild-type (WT) and ZR1423 (*zntR* mutation) strains carrying the plasmid vector pBBR. The mutant strain was complemented with multi-copies of the *zntR* gene from the plasmid pZNTR. Log-phase cells grown in LB were either untreated or treated with 250 μM $ZnCl_2$ for 15 min. The expression of *zntA* and *zntB* was normalized to that of 16S rRNA, and the fold-changes in gene expression were assessed relative to those in WT/pBBR grown in LB (regarded as 1). The experiment was performed in biological triplicate, and the error bars indicate the standard deviations.

(b) qRT-PCR analysis of *zntB* expression in response to various metals. Log-phase WT cells were grown in LB medium individually supplemented with 250 μM of $CdCl_2$, $CoCl_2$, $CuSO_4$, $FeCl_3$, $MgCl_2$, $MnCl_2$, $NiCl_2$, $PbNO_3$ or $ZnCl_2$ for 15 min. The fold-changes in gene expression were assessed relative to the cells grown in LB (regarded as 1).

3.1.2 ZntR and ZntA are required for resistance to cadmium, zinc and cobalt. Next, the *zntR* (ZR1423) and *zntA* (ZA141) mutant strains were generated, and the metal sensitivity was determined (**Fig. 3**). The results showed that the ZR1423 strain was ~10^2-fold more sensitive to 50 μM $CdCl_2$ and 450 μM $ZnCl_2$ than WT (**Fig. 3**). The loss of *zntA* severely affected cell tolerance to cadmium and zinc. The ZA141strain was ~10^4-fold more sensitive to 450 μM $ZnCl_2$ than WT, while a low concentration (50 μM) of $CdCl_2$ completely inhibited the growth of ZA141 (**Fig. 3**). Furthermore, the strains ZR1423 and ZA141 also exhibited ~10-fold more sensitivity to $CoCl_2$ than WT (**Fig. 3**). The sensitive phenotypes of the *zntR* (ZR1423/pBBR) and *zntA* (ZA141/pBBR) mutant strains to $CdCl_2$, $ZnCl_2$ and $CoCl_2$ could be reversed in the complemented strains (ZR1423/pZNTR and ZA141/pZNTA) (**Fig. 4**). However, the resistance to other metals ($CuSO_4$, $FeCl_3$, $MgCl_2$, $MnCl_2$, $NiCl_2$ and $PbSO_4$) was similar in WT and the mutants ZR1423 and ZA141. These results demonstrated that *A. tumefaciens zntR* and *zntA* are important for the detoxification of cadmium, zinc and cobalt. In addition, strain ZRA15 (*zntR* and *zntA* mutations) did not show increased metal sensitivity when compared to ZA141 (*zntA* mutation) (**Fig. 4**), suggesting that the phenotype of ZRA15 was likely due to the loss of *zntA*. This notion was supported by the fact that the metal-sensitive phenotype of ZRA15 could be completely reversed by complementation with *zntA* carried on the plasmid, pZNTA (**Fig. 4**).

3.1.3 ZntB plays no role in zinc resistance under the tested conditions. It has been reported that *Salmonella enteric* serovar Typhimurium ZntB mediates the efflux of Zn^{2+} and Cd^{2+}, and the *zntB* mutant shows increased sensitivity to zinc and cadmium (Worlock & Smith, 2002). The single inactivation of *A. tumefaciens zntB* (ZB141) had no effect on cell tolerance to cadmium, zinc, cobalt (**Fig. 3**) and other metals ($CuSO_4$, $FeCl_3$, $MgCl_2$, $MnCl_2$, $NiCl_2$ and $PbSO_4$). The metal sensitivity was also tested in the double mutation strain (ZAB141) and the WT strain expressing multi-copies of *zntB* (WT/pZNTB). Mutations at *zntB* and *zntA* (ZAB141) showed no additional effect on the sensitivity to cadmium, zinc and cobalt compared with the single *zntA* mutation (ZA141) (**Fig. 3**). Moreover, the WT/pZNTB strain showed resistance to cadmium, zinc and cobalt similar to the WT strain carrying the empty vector. Under the tested conditions, *A. tumefaciens zntB* did not show an apparent role for metal resistance.

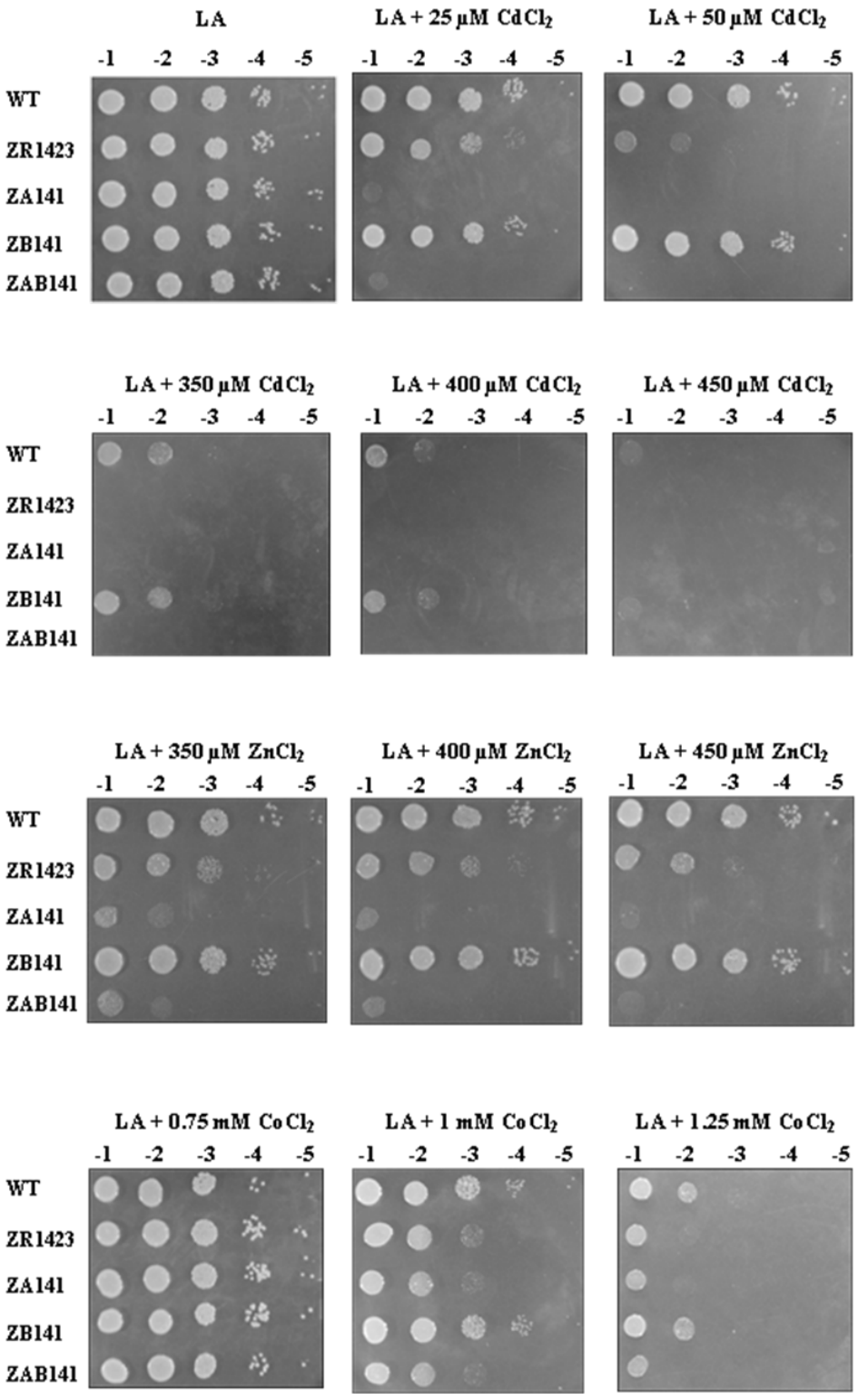

FIG. 3. Sensitivity to metals. Wild type (WT), ZR1423 (*zntR* mutation), ZA141 (*zntA* mutation), ZB141 (*zntB* mutation) and ZAB141 (*zntA* and *zntB* mutations). Log-phase cells grown in LB medium were adjusted, serial diluted and spotted onto plates containing LA, LA+$CdCl_2$ (25, 50, 350, 400 and 450 μM), LA+$ZnCl_2$ (350, 400 and

450 μM) and LA+$CoCl_2$ (0.75, 1 and 1.25 mM). The ten-fold serial dilutions are indicated, and the plates were incubated at 28 °C for 48 h.

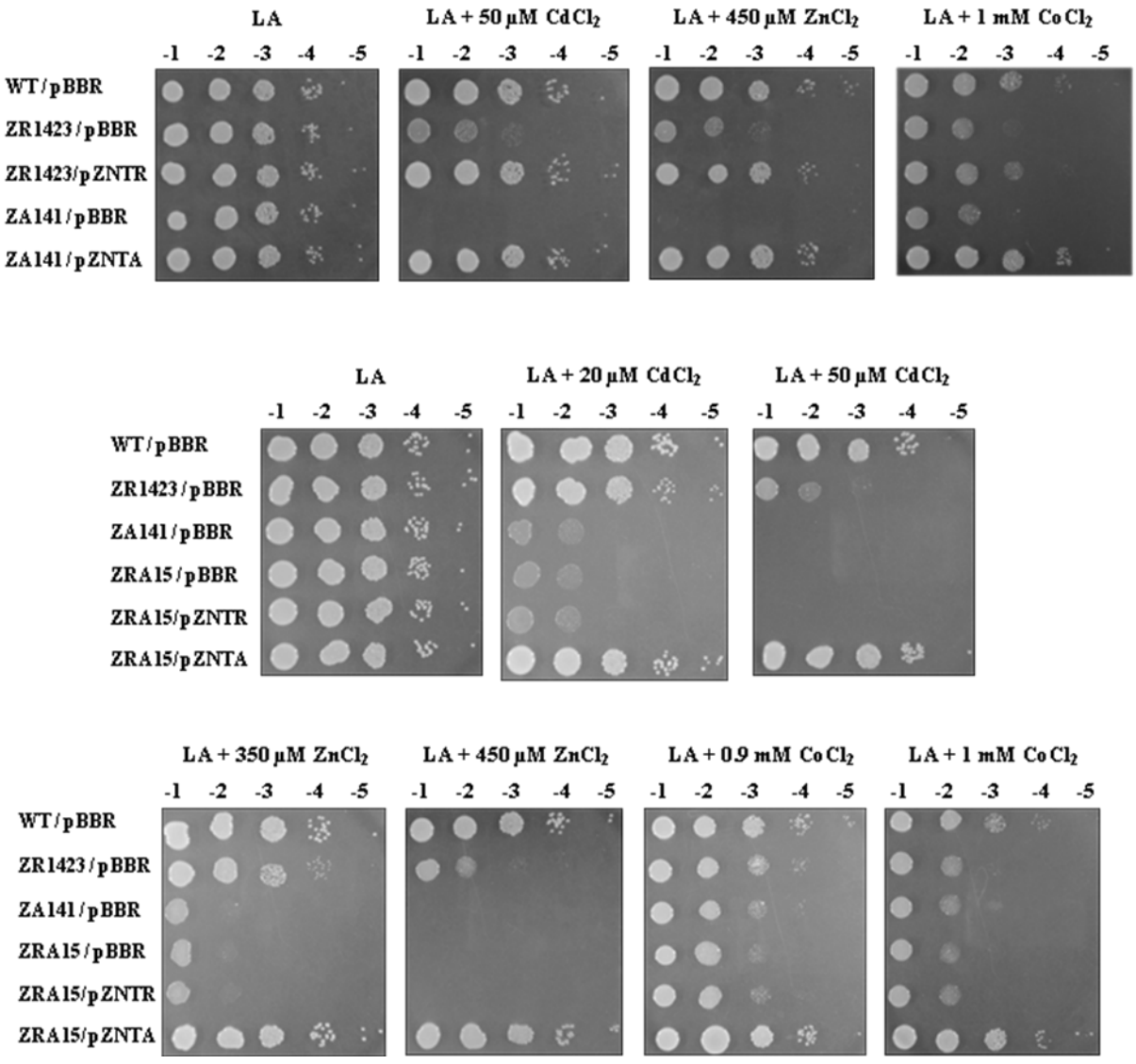

FIG. 4. Sensitivity to metals. Wild-type (WT), ZR1423 (*zntR* mutation), ZA141 (*zntA* mutation) and ZRA15 (*zntR* and *zntA* mutations) strains carrying the plasmid vector pBBR. The mutant strains were complemented with multi-copies either of the *zntR* or *zntA* gene from the plasmids pZNTR and pZNTA, respectively. Cells grown in LB medium were adjusted, serial diluted and spotted onto plates containing LA, LA+20 μM $CdCl_2$, LA+50 μM $CdCl_2$, LA+350 μM $ZnCl_2$, LA+450 μM $ZnCl_2$, LA+0.9 mM $CoCl_2$ and LA+1 mM $CoCl_2$. The ten-fold serial dilutions are indicated, and the plates were incubated at 28 °C for 48 h.

3.1.4 The *zntA* mutant showed a striking increase in the accumulation of cadmium and zinc. The ICP-MS analysis was performed to determine the metal content in WT and mutant strains (**Fig. 5**). The cells were grown in LB medium individually supplemented with 50 μM of $CoCl_2$, $CuSO_4$, $FeCl_3$, $MnCl_2$, $NiCl_2$ or $ZnCl_2$. However, $CdCl_2$ was used at 10 μM due to the Cd-hyper-sensitivity of the mutant strains (ZR1423, ZA141 and ZAB141, **Fig. 3**). The *zur* (zinc uptake regulator) mutant strain (SPP12) (Bhubhanil *et al*., 2014c) was used as a control, which showed the increased accumulation of zinc (∼5-fold, Fig. 3). The inactivation of *zntR* (ZR1423) led to the increased accumulation of Cd (∼1.5-fold), while the levels of other metals were similar to those in WT (**Fig. 5**). The loss of *zntA* increased the accumulation of Cd (∼4-fold), Zn (∼2-fold) and Mn (∼1.2-fold) compared with WT, and WT showed higher levels of Co (∼1.6-fold) and Fe (∼1.2-fold) than the *zntA* mutant (ZA141) (**Fig. 5**). The *zntB* mutation had a lesser effect on the metal content than the *zntA* mutation, as only the Cu and Mn contents in the *zntB* mutant (ZB141) were slightly changed relative to WT (**Fig. 5**). In addition, the accumulation of Ni in all of the mutants and WT was similar. The striking increase in the accumulation of Cd and Zn in the *zntA* mutant suggests that ZntA is an exporter of Cd and Zn ions.

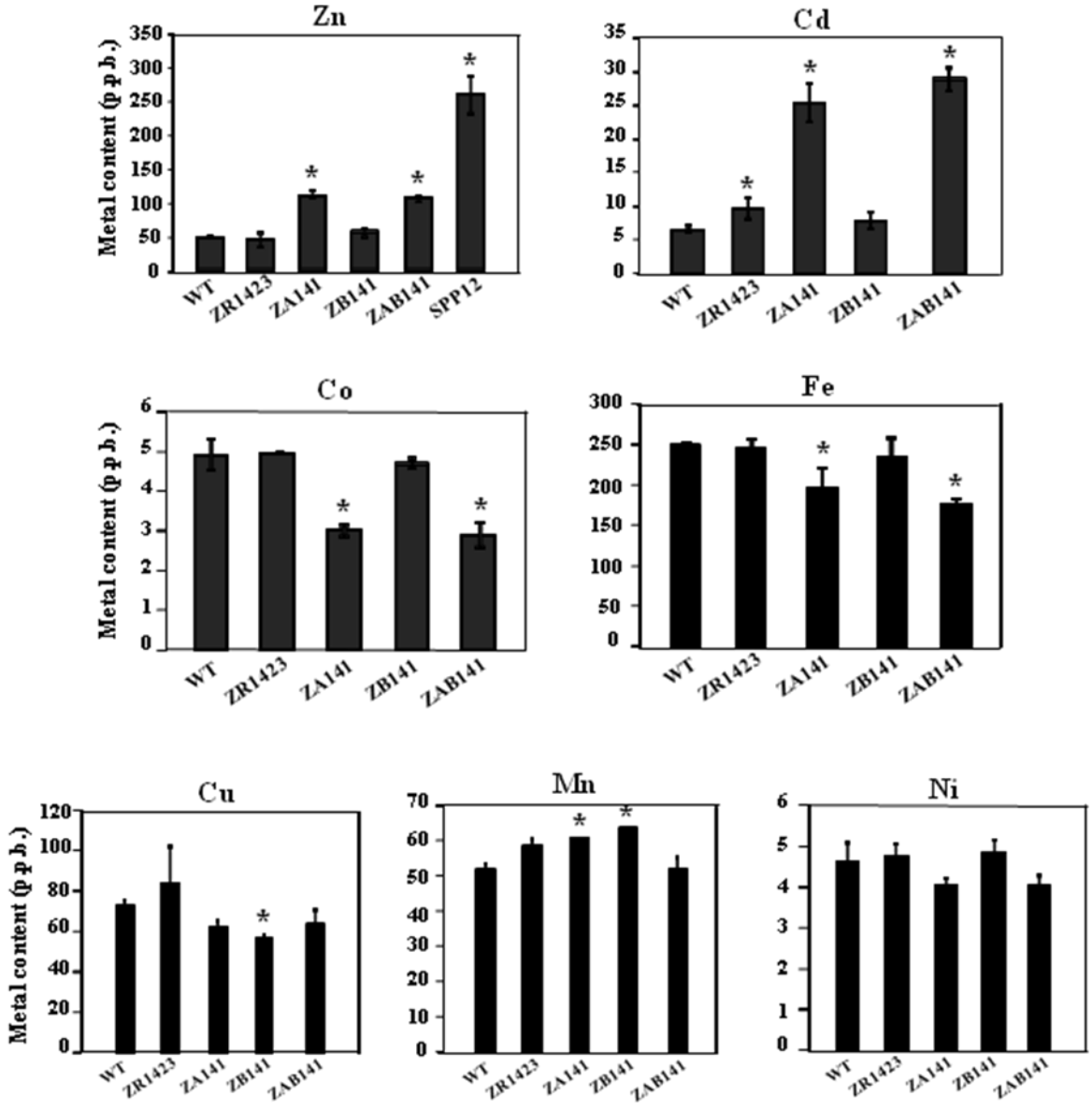

FIG. 5. Determination of metal contents using ICP-MS. Wild-type (WT), ZR1423 (*zntR* mutation), ZA141 (*zntA* mutation), ZB141 (*zntB* mutation) ZAB141, (*zntA* and *zntB* mutations) and SPP12 (*zur* mutation) cells were grown in LB medium individually supplemented with 10 μM of $CdCl_2$ and 50 μM of $CoCl_2$, $CuSO_4$, $FeCl_3$, $MnCl_2$, $NiCl_2$ or $ZnCl_2$ at 28 °C for 24 h. The total metal contents were measured using ICP-MS. The results are shown as the means of biological triplicate samples, and the error bars indicate the standard deviations. The bars marked with * are significantly different from WT ($P < 0.05$ in an unpaired Student's *t*-test).

3.1.5 Roles of zinc uptake and export systems in H_2O_2 resistance. Zinc-mediated protection against H_2O_2 stress has been reported in *B. subtilis* (Gaballa & Helmann, 2002) and *S. enteric* (Cerasi *et al*., 2014). Thus, to examine whether the disruption of the zinc exporter or deregulation of zinc uptake in *A. tumefaciens* affected the ability of cells to survive under H_2O_2 stress, the H_2O_2 sensitivity test was performed. The ZR1423, ZA141 and SPP12 strains displayed more tolerance to H_2O_2 than WT (LA+H_2O_2 and LA+H_2O_2+$ZnCl_2$, **Fig. 6a**). However, the mechanism for enhanced-H_2O_2 resistance in the *A. tumefaciens* mutants (ZR1423, ZA141 and SPP12) remains unknown.

3.1.6 The inactivation of either *zntR* or *zntA* did not affect the virulence of *A. tumefaciens*. *A. tumefaciens* causes crown gall disease through the insertion of T-DNA from the tumour-inducing (Ti) plasmid into the plant genome (Zhu *et al.*, 2000). The virulence of the mutant strains (ZR1423 and ZA141) compared with WT was examined after infecting *N. benthamiana* petioles. The results showed that tumour formation on *N. benthamiana* petioles infected with the mutant strains and WT was similar (**Fig. 6b**). These results suggested that *zntR* and *zntA* are not important for *A. tumefaciens* virulence in infecting the *N. benthamiana* host plant.

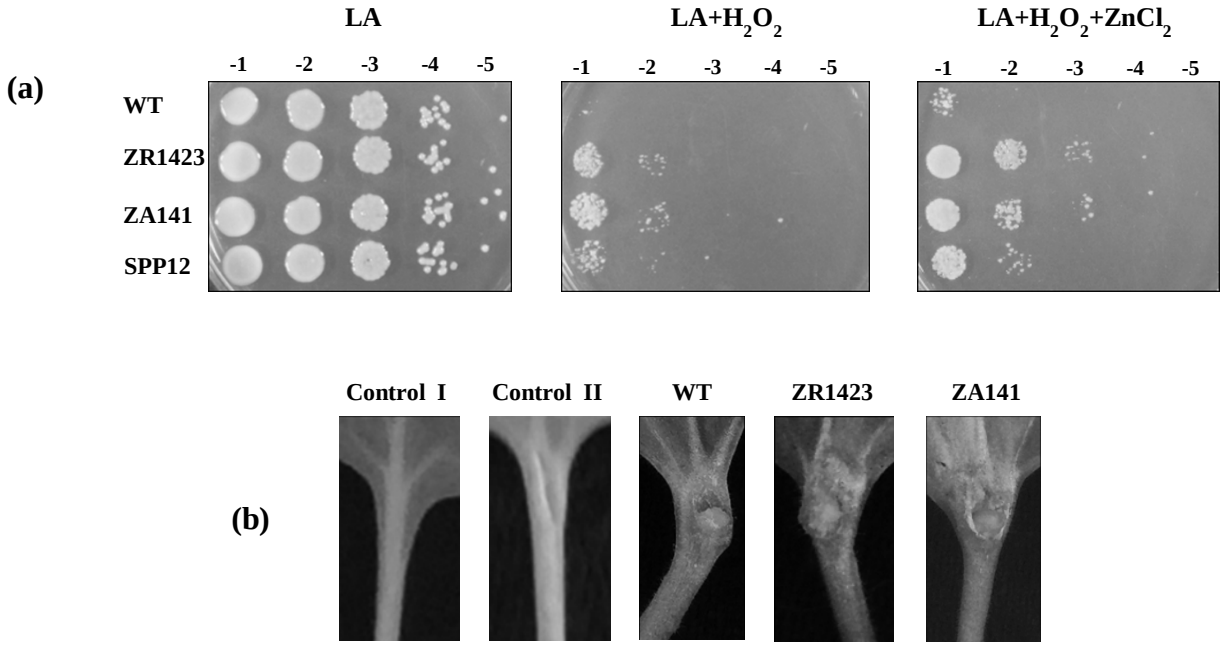

FIG. 6. (a) Sensitivity to H_2O_2. Wild type (WT), ZA141 (*zntA* mutation) ZR1423 (*zntR* mutation) and SPP12 (*zur* mutation). Cells grown in LB medium were adjusted, serial diluted and spotted onto plates containing LA, LA+275 μM H_2O_2 and LA+275 μM H_2O_2+50 μM $ZnCl_2$. Ten-fold serial dilutions are indicated, and the plates were incubated at 28 °C for 48 h.

(b) Virulence assay using young *Nicotiana benthamiana* plants. *A. tumefaciens* strains carrying the plasmid pCMA1 were grown in IB 5.5 medium containing 300 μM of acetosyringone (AS) and used to inoculate wounded *N. benthamiana* petioles. Fifteen petioles were tested for each bacterial strain. Tumour formation was observed at

4 weeks after inoculation. Representative petioles are shown. Control I: without inoculation. Control II: inoculation of wounded petiole with IB 5.5 + 300 µM AS.

3.1.7 Material and Methods

Bacterial strains and growth conditions. The bacterial strains and plasmids used in the present study are shown in **Table 1**. *A. tumefaciens* and *Escherichia coli* were aerobically grown at 28 °C and 37 °C, respectively, in Luria-Bertani (LB) medium. LA refers to LB medium containing 1.5% agar. The growth conditions and antibiotic concentrations used in the present study have been previously described (Bhubhanil *et al*., 2014a). Minimal AB medium (containing per litre: K_2HPO_4, 3 g; NaH_2PO_4, 1.15 g; NH_4Cl, 1 g; $MgSO_4 \cdot 7H_2O$, 0.3 g; KCl, 0.15 g; $CaCl_2$, 0.01 g; $FeSO_4 \cdot 7H_2O$, 2.5 mg; glucose, 0.45 %) and induction broth, pH 5.5 (IB 5.5), were prepared as previously reported (Bhubhanil *et al*., 2014a; Cangelosi *et al*., 1991).

Molecular techniques. General molecular techniques were performed using standard protocols (Sambrook *et al*., 1989). The primers are listed in **Table 2**. DNA sequencing was performed to confirm the sequence of the cloned DNA (Macrogen, Korea). Plasmid DNA was transferred into *A. tumefaciens* strains by electroporation (Cangelosi *et al*., 1991).

Construction of *zntR*, *zntA*, *zntB* and double mutant strains. The mutant strains were generated using a single homologous recombination method (Ngok-ngam *et al*., 2009). The *A. tumefaciens zntR* (Atu0888), *zntA* (Atu0843) and *zntB* (Atu0731) genes were individually disrupted. Primer pairs for gene inactivation (**Table 2**) were used to amplify the internal coding regions of *zntR*, *zntA* and *zntB*, and the PCR products were cloned into pKNOCK-Km, generating pKNOCKmZNTR, pKNOCKmZNTA and pKNOCKmZNTB, respectively. The plasmids were electroporated into the WT strain, and the *zntR* (ZR1423), *zntA* (ZA141) and *zntB* (ZB141) mutant strains were selected on LA containing 30 µg ml^{-1} of kanamycin (Km).

To generate the ZAB141 strain (disruption of both *zntA* and *zntB* genes), the PCR fragment corresponding to the internal coding region of *zntB* was cloned into pKNOCK-Gm, generating the plasmid pKNOCKZNTB. The plasmid was electroporated into the mutant ZA141 strain, and the mutant ZAB141 was selected on LA containing 60 µg ml^{-1} of gentamicin (Gm) and 30 µg ml^{-1} of Km.

To generate the ZRA15 strain (disruption of both *zntR* and *zntA* genes), the PCR fragment corresponding to the internal coding region of *zntA* was cloned into pKNOCK-Gm, generating the plasmid pKNOCKZNTA. The plasmid was electroporated into the mutant ZR1423 strain, and the mutant ZRA15 strain was selected on LA containing 60 µg ml^{-1} of gentamicin (Gm) and 30 µg ml^{-1} of Km. All the mutant strains were confirmed through Southern blot analysis.

Construction of plasmids expressing functional *zntR*, *zntA* and *zntB* genes. DNA fragments of full-length *zntR*, *zntA* and *zntB* were PCR amplified using genomic WT DNA as a template, gene-specific primer pairs for complementation (**Table 2**) and Pfu DNA polymerase (Fermentas). The PCR products were cloned into *Sma*I-digested pBBR1MCS-4 (Kovach *et al*., 1995), generating the plasmids pZNTR, pZNTA and pZNTB, respectively.

Quantitative real-time PCR (qRT-PCR) analysis. qRT-PCR was performed as previously described (Bhubhanil *et al*., 2014b). Log-phase cells grown in LB were either untreated or treated with various metals for 15 min prior to harvest. The metals $CdCl_2$, $CoCl_2$, $CuSO_4$, $FeCl_3$, $MgCl_2$, $MnCl_2$, $NiCl_2$ and $ZnCl_2$ were used at a final concentration of 100, 250, 500 or 750 μM. The gene-specific primers for *zntA*, *zntB* and 16S rRNA are listed in Table S1. The relative gene expression was determined using the $2^{-\Delta\Delta Ct}$ method. The fold-changes in gene expression are expressed relative to the untreated control as previously described (Livak & Schmittgen, 2001). The data were reported as the means of biological triplicates ± SD.

Sensitivity to metals and H_2O_2. The dilution method (Ngok-ngam *et al*., 2009) was used for the metal sensitivity test. Log-phase cells grown in LB medium were adjusted, serially diluted and spotted onto plates containing LA, LA + $CdCl_2$ (25, 50, 350, 400 and 450 μM), LA + $CoCl_2$ (0.75, 1 and 1.25 mM), LA + $ZnCl_2$ (350, 400 and 450 μM) and LA +275 μM H_2O_2 in the absence or presence of 50 μM $ZnCl_2$. The plates were subsequently incubated at 28 °C for 48 h. Each strain was examined in duplicate, and each experiment was repeated at least twice.

Measurement of the total cellular metal content. Cells were grown in LB individually supplemented with 10 μM $CdCl_2$ and 50 μM $CoCl_2$, $CuSO_4$, $FeCl_3$, $MnCl_2$, $NiCl_2$ or $ZnCl_2$ at 28 °C for 24 h. The cells were washed three times with 50 mM potassium phosphate buffer, pH 7.0 (KPB), and 10 mM ethylenediaminetetraacetic acid (EDTA). The cells were subsequently washed twice with 50 mM KPB and resuspended in KPB to achieve an OD_{600} of 1. The cell suspension (2.5 ml) was used for sample preparation, and the metals were measured in parts per billion (p.p.b.) using an inductively coupled plasma mass spectrometer (ICP-MS), as previously described (Bhubhanil *et al*., 2014a). The data were reported as the means of biological triplicates ± SD.

Virulence assay. *A. tumefaciens* strains carrying plasmid pCMA1 were used to infect young *Nicotiana benthamiana* plants according to a previously described protocol (Kamoun *et al*., 2003). Log-phase cells grown in LB were washed and resuspended in an IB 5.5 medium containing 300 μM acetosyringone (AS). The cells were incubated at 28 °C with shaking for 20 min, harvested and adjusted to an OD_{600} of 1 in IB 5.5 + 300 μM AS. A 5-μl aliquot of the cell suspension was used to inoculate a wounded *N. benthamiana* petiole; 15 petioles were tested for each bacterial strain. Deformation of the petiole (crooked petiole phenotype, tumour formation) was observed at 4 weeks after inoculation.

Table 1. Strains and plasmids used in this study

Ap^r, ampicillin resistance; Gm^r, gentamicin resistance; Km^r, kanamycin resistance

Strain or plasmid	Relevant characteristics	Reference or source
Agrobacterium tumefaciens		
NTL4	Wild-type (WT) strain, a Ti plasmid-cured derivative of strain C58	Luo *et al*. (2001)
SPP12	*zur*::pKNOCK-Gm, Gm^r	Bhubhanil *et al*. (2014c)
ZA141	*zntA*::pKNOCK-Km, Km^r	This study
ZB141	*zntB*::pKNOCK-Km, Km^r	This study
ZAB141	*zntA*::pKNOCK-Km, Km^r and *zntB*::pKNOCK-Gm, Gm^r	This study
ZR1423	*zntR*::pKNOCK-Km, Km^r	This study
Escherichia coli		
DH5α	Host for general DNA cloning	Grant *et al.* (1990)
BW20767	Host for plasmids pKNOCK-Gm and pKNOCK-Km	Metcalf *et al*. (1996)
Plasmids for gene inactivation		
pKNOCK-Gm	Suicide vector, Gm^r	Alexeyev (1999)
pKNOCK-Km	Suicide vector, Km^r	Alexeyev (1999)
pKNOCKmZNTA	Internal coding region of *zntA* cloned into pKNOCK-Km, Km^r	This study
pKNOCKmZNTB	Internal coding region of *zntB* cloned into pKNOCK-Km, Km^r	This study
pKNOCKmZNTR	Internal coding region of *zntR* cloned into pKNOCK-Km, Km^r	This study
pKNOCKZNTB	Internal coding region of *zntB* cloned into pKNOCK-Gm, Gm^r	This study
Plasmids for complementation		
pBBR1MCS-4	Expression vector, Ap^r (pBBR)	Kovach *et al*. (1995)
pZNTA	Full-length *zntA* cloned into pBBR1MCS-4, Ap^r	This study
pZNTB	Full-length *zntB* cloned into pBBR1MCS-4, Ap^r	This study
pZNTR	Full-length *zntR* cloned into pBBR1MCS-4, Ap^r	This study
Plasmid for the virulence assay		
pCMA1	pTiC58*traM*::*nptII*, Km^r	Hwang *et al*. (1995)

Table 2. Primers used in this study

Gene-primer name and purpose	Sequence (5'→3')
Gene inactivation	
zntA-BT4121	CATGCTGGCCAATCGCACGC
zntA-BT4122	CAGCGTGGCGACGATGAAGG
zntB-BT4328	GCGACCGCTTCATCATCACC
zntB-BT4329	ATCAGGGTGAGTACGGTGCG
zntR-BT4091	ATCCGACCTCGAAAGGCTGG
zntR-BT4092	CAATGGGAGACGATGCGTTC
Complementation	
zntA-BT4489	ATGAATATTTCGACACGCGGC
zntA-BT4490	AAAGCTGGGGTCAGGTTTTGC
zntB-BT4492	ATGGATCTCATAACGCCCAC
zntB-BT4493	TTGCTGTCACAAGATACGCG
zntR-BT4487	ATGCTGTCCATCGGTGAACTG
znuR-BT4488	GCTTTAGCGGTTCAATGCTCG
qRT-PCR	
16S rRNA-BT1421	GAATCTACCCATCTCTGCGG
16S rRNA-BT1422	AAGGCCTTCATCACTCACGC
zntA-BT4121	CATGCTGGCCAATCGCACGC
zntA-BT4122	CAGCGTGGCGACGATGAAGG
zntB-BT4533	CGAGATGCCTGACGGTTTCG
zntB-BT4534	GCAGGAATGCCGTCATCAGC

References

Alexeyev, M. F. (1999). The pKNOCK series of broad-host-range mobilizable suicide vectors for gene knockout and targeted DNA insertion into the chromosome of gram-negative bacteria. *Biotechniques* 26, 824-826, 828.

Bhubhanil, S., Chamsing, J., Sittipo, P., Chaoprasid, P., Sukchawalit, R. & Mongkolsuk, S. (2014a). Roles of *Agrobacterium tumefaciens* membrane-bound ferritin (MbfA) in iron transport and resistance to iron under acidic conditions. *Microbiology* 160, 863-871.

Bhubhanil, S., Niamyim, P., Sukchawalit, R. & Mongkolsuk, S. (2014b). Cysteine desulphurase-encoding gene *sufS2* is required for the repressor function of RirA and oxidative resistance in *Agrobacterium tumefaciens*. *Microbiology* 160, 79-90.

Bhubhanil, S., Sittipo, P., Chaoprasid, P., Nookabkaew, S., Sukchawalit, R. & Mongkolsuk, S. (2014c). Control of zinc homeostasis in *Agrobacterium tumefaciens* via *zur* and the zinc uptake genes *znuABC* and *zinT. Microbiology* 160, 2452-2463.

Cangelosi, G. A., Best, E. A., Martinetti, G. & Nester, E. W. (1991). Genetic analysis of *Agrobacterium*. *Methods Enzymol* 204, 384-397.

Cerasi, M., Liu, J. Z., Ammendola, S., Poe, A. J., Petrarca, P., Pesciaroli, M., Pasquali, P., Raffatellu, M. & Battistoni, A. (2014). The ZupT transporter plays an important role in zinc homeostasis and contributes to *Salmonella enterica* virulence. *Metallomics* 6, 845-853.

Gaballa, A. & Helmann, J. D. (2002). A peroxide-induced zinc uptake system plays an important role in protection against oxidative stress in *Bacillus subtilis*. *Mol Microbiol* 45, 997-1005.

Grant, S. G., Jessee, J., Bloom, F. R. & Hanahan, D. (1990). Differential plasmid rescue from transgenic mouse DNAs into *Escherichia coli* methylation-restriction mutants. *Proc Natl Acad Sci USA* 87, 4645-4649.

Kovach, M. E., Elzer, P. H., Hill, D. S., Robertson, G. T., Farris, M. A., Roop II, R. M. & Peterson, K. M. (1995). Four new derivatives of the broad-host-range cloning vector pBBR1MCS, carrying different antibiotic-resistance cassettes. *Gene* 166, 175-176.

Kamoun, S., Hamada, W., Huitema, E. (2003). Agrosuppression: a bioassay for the hypersensitive response suited to high-throughput screening. *Mol Plant Microbe Interact* 16: 7-13.

Livak, K. J. & Schmittgen, T. D. (2001). Analysis of relative gene expression data using real-time quantitative PCR and the $2^{-\Delta\Delta Ct}$ Method. *Methods* 25, 402-408.

Luo, Z. Q., Clemente, T. E. & Farrand, S. K. (2001). Construction of a derivative of *Agrobacterium tumefaciens* C58 that does not mutate to tetracycline resistance. *Mol Plant-Microbe Interact* 14, 98–103.

Metcalf, W. W., Jiang, W., Daniels, L. L., Kim, S. K., Haldimann, A. & Wanner, B. L. (1996). Conditionally replicative and conjugative plasmids carrying *lacZ* alpha for cloning, mutagenesis, and allele replacement in bacteria. *Plasmid* 35, 1-13.

Ngok-ngam, P., Ruangkiattikul, N., Mahavihakanont, A., Virgem, S. S., Sukchawalit, R. & Mongkolsuk, S. (2009). Roles of *Agrobacterium tumefaciens* RirA in iron regulation, oxidative stress response and virulence. *J Bacteriol* 191, 2083-2090.

Sambrook, J., Fritsch, E. F. & Maniatis, T. (1989). *Molecular Cloning: a Laboratory Manual*, Cold Spring Harbor, NY: Cold Spring Harbor Laboratory.

Worlock, A. J. & Smith, R. L. (2002). ZntB is a novel Zn2+ transporter in *Salmonella enterica* serovar Typhimurium. *J Bacteriol* 184, 4369-4373.

Zhu, J., Oger, P. M., Schrammeijer, B., Hooykaas, P. J., Farrand, S. K. & Winans, S. C. (2000). The bases of crown gall tumorigenesis. *J Bacteriol* 182, 3885-3895.

3.2 To study regulation and roles of the *troBCA* operon in zinc homeostasis and virulence of *A. tumefaciens*.

3.2.1 *A. tumefaciens troC* (Atu3180), *troB* (Atu3179) and *troA* (Atu3178) genes are co-transcribed.

The *A. tumefaciens* C58 genome contains a cluster of genes consisting of Atu3178, Atu3179 and Atu3180 that are annotated as a putative zinc/manganese ABC transport system (http://www.genome.jp/kegg-bin/show_organism?org=atu). Atu3178 encodes a periplasmic substrate-binding protein belonging to the TroA (transport-related operon) superfamily. Atu3179 (*troB*) encodes a permease, and Atu3180 (*troC*) encodes an ATP-binding protein. Hereafter, these genes were named *troA*, *troB* and *troC*, respectively. Atu3181 is a gene that has a transcription orientation opposite to that of the *troCBA* operon and encodes a putative metal chaperone, YciC, belonging to the COG0523 family of GTPases (Haas *et al*., 2009). The *A. tumefaciens* genome sequence analysis (Wood *et al*., 2001) revealed that the gene arrangement in the *tro* operon starts with *troC* (Atu3180) followed by *troB* (Atu3179) and *troA* (Atu3178) (**FIG. 1**), and these genes may be co-transcribed. Reverse transcription PCR **(**RT-PCR) analysis was performed confirming that *troC*, *troB* and *troA* are co-transcribed (**FIG. 2**).

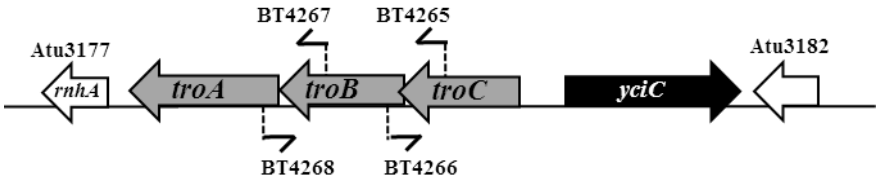

FIG. 1 The genomic context of *A. tumefaciens troCBA* operon. The *rnhA* (Atu3177) gene encoding a ribonuclease H is located downstream of the *troCBA* operon. The Atu3182 gene encoding a hypothetical protein with unknown function is located downstream of the *yciC* gene. Primer sets used to amplify the junctions between *troC* and *troB* (BT4265 and BT4266) and between *troB* and *troA* (BT4267 and BT4268) with RT-PCR analysis are indicated.

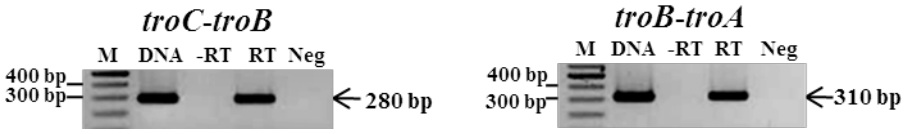

FIG. 2 RT-PCR analysis. RNA was isolated from log-phase cells of wild-type NTL4 grown in LB and treated with 1 mM EDTA for 15 min. Primer sets were used to amplify the junctions between *troC* and *troB* (BT4265 and BT4266) and between *troB* and *troA* (BT4267 and BT4268). Abbreviations: M, a 100-bp ladder marker; DNA, NTL4 chromosomal DNA template (a positive control); -RT, reaction without reverse transcriptase (a DNA contamination control); RT, reaction with reverse transcriptase; Neg, the PCR reaction without template (a negative control). The expected sizes of the PCR products are indicated.

3.2.2 The *A. tumefaciens troCBA* operon is inducible with zinc depletion. Expression of the *troC* gene was determined using quantitative real-time PCR (qRT-PCR). As expected for genes involved in metal acquisition, expression of *troC* in wild-type NTL4 was inducible (~10^3-fold) by the metal chelator EDTA compared to untreated cells. To investigate the metal-specific response of *troC*, repression of the EDTA-induced expression by various metals was determined. It was found that Zn^{2+} was the most potent metal ion that could repress the EDTA-induced expression of *troC* (**FIG. 3**) compared to other metals, including cadmium, cobalt, copper, iron, magnesium, manganese and nickel. These results demonstrated that the *A. tumefaciens troCBA* operon is inducible, more specifically by zinc depletion, which supported the view that *A. tumefaciens* TroCBA is involved in zinc acquisition.

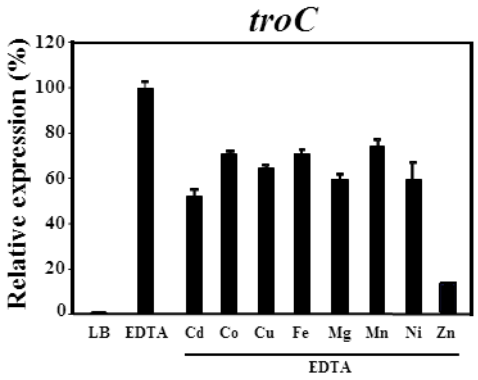

FIG. 3 Induction of *troC* is specific to zinc limitation. Expression analysis of *troC* was determined by qRT-PCR. RNA samples were isolated from log-phase cells of wild-type NTL4 strain grown in LB medium. The expression of *troC* was normalized to 16S rRNA. Wild-type NTL4 cells grown in LB medium and under metal-limiting conditions (LB + 1 mM EDTA). Metals ($CdCl_2$, $CoCl_2$, $CuSO_4$, $FeCl_3$, $MnCl_2$, $NiCl_2$ or $ZnCl_2$) were supplemented at a final concentration of 0.45 mM. The expression levels are presented as a percentage and are relative to those in cells grown in LB + 1 mM EDTA (100%).

3.2.3 *A. tumefaciens* Zur negatively regulates the *troCBA* operon. The *A. tumefaciens troCBA* operon was predicted to be controlled by Zur (zinc uptake regulator) due to the presence of a Zur box in their promoter region (Haas *et al*., 2009). However, the regulation has not been experimentally verified. Expression of *troC* was determined using qRT-PCR. The *troC* gene was constitutively expressed at high levels in the *zur* mutant but was suppressed when complemented with pZUR (**FIG. 4**). These results supported the view that *A. tumefaciens* Zur negatively regulates the *troCBA* operon.

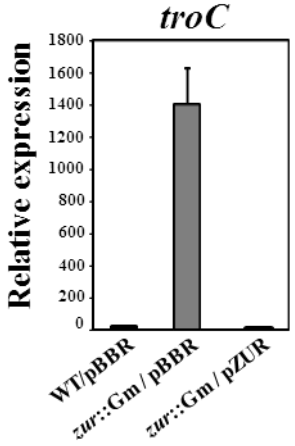

FIG. 4 Expression analysis of *troC* using qRT-PCR. RNA samples were isolated from log-phase cells of wild-type NTL4 (WT/pBBR), the *zur* mutant (*zur*::Gm/pBBR) and the complemented strain (*zur*::Gm/pZUR) grown in LB medium. pBBR is the plasmid vector. pZUR is the plasmid containing a functional *zur* gene. The expression of *troC* was normalized to 16S rRNA, and the fold changes in gene expression in *zur*::Gm/pBBR and *zur*::Gm/pZUR are relative to those in wild-type WT/pBBR (regarded as one). The experiment was performed in biological triplicate, and error bars indicate the standard deviations.

3.2.4 Construction of the *troC* mutant strain. The mutant strain was constructed using a single homologous recombination method as described previously (Kitphati *et al*., 2007). The internal coding region of *troC* [BT3751 (5′-TGAAACCGCTCGGCGGTGAG-3′) and BT3752 (5′-CTGCGCATCCTGCAACATGG-3′), 293 bp)] was amplified by PCR using the specific primers indicated in the parenthesis. The PCR product was cloned into the unique SmaI site of pKNOCK-Gm (Alexeyev, 1999). The resulting plasmid pKNOCKTROC was electroporated into wild-type NTL4 (a Ti plasmid-cured derivative of strain C58 with an internal deletion of the *tetA-tetR* locus) (Luo *et al*., 2001). The *troC* mutant (*troC*::Gm) was selected on LA plates containing 60 μg/ml gentamicin (Gm). The *A. tumefaciens* mutant strain was confirmed by Southern blot analysis (**FIG. 5**). Chromosomal DNA was isolated from wild-type NTL4 and the *troC*::Gm strain, and digested with PvuI (**FIG. 5A**). The 293 bp PCR product containing the internal coding region of *troC* gene was labeled with non-radioactive DIG and used as a probe. The expected size of 2,654 bp and 4,687 bp fragments were detected from wild-type NTL4 and the *troC*::Km strain, respectively (**FIG. 5B**).

(A) **(B)**

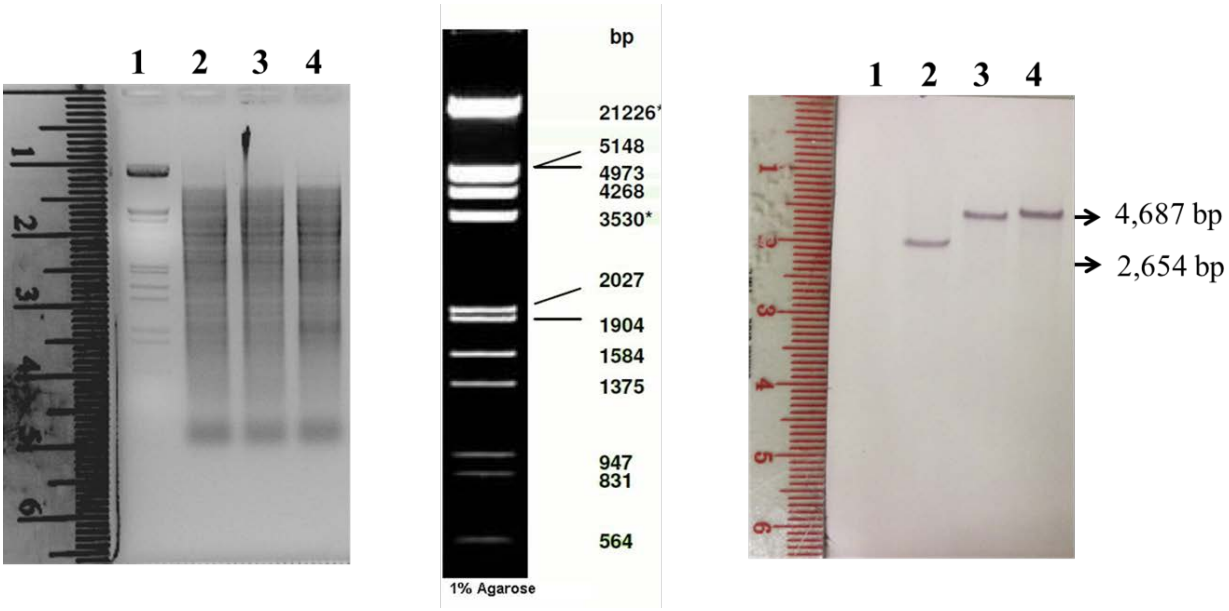

FIG. 5 Southern blot analysis Lane 1: DNA marker; lane 2: wild-type NTL4; lanes 3 and 4; the *troC* mutant (*troC*::Km).

3.2.5 The *troC* mutant is hypersensitive to EDTA treatment.

The *troC*::Gm mutant strain was constructed to assess the physiological function of *troC*. Growth was determined under metal limitation in the presence of 1.2 Mm EDTA. Inactivation of *troC* caused cells to become hypersensitive to EDTA. The *troC* mutant was ~10^2-fold more sensitive to 1.2 mM EDTA than WT (**Fig. 6**) and could be fully rescued by the addition of 50 μM $ZnCl_2$ (**Fig. 6**, EDTA + Zn) but not by other metals **(Fig. 6).** The results demonstrated that *A. tumefaciens troC* is important for zinc acquisition that responds specifically to zinc limitation.

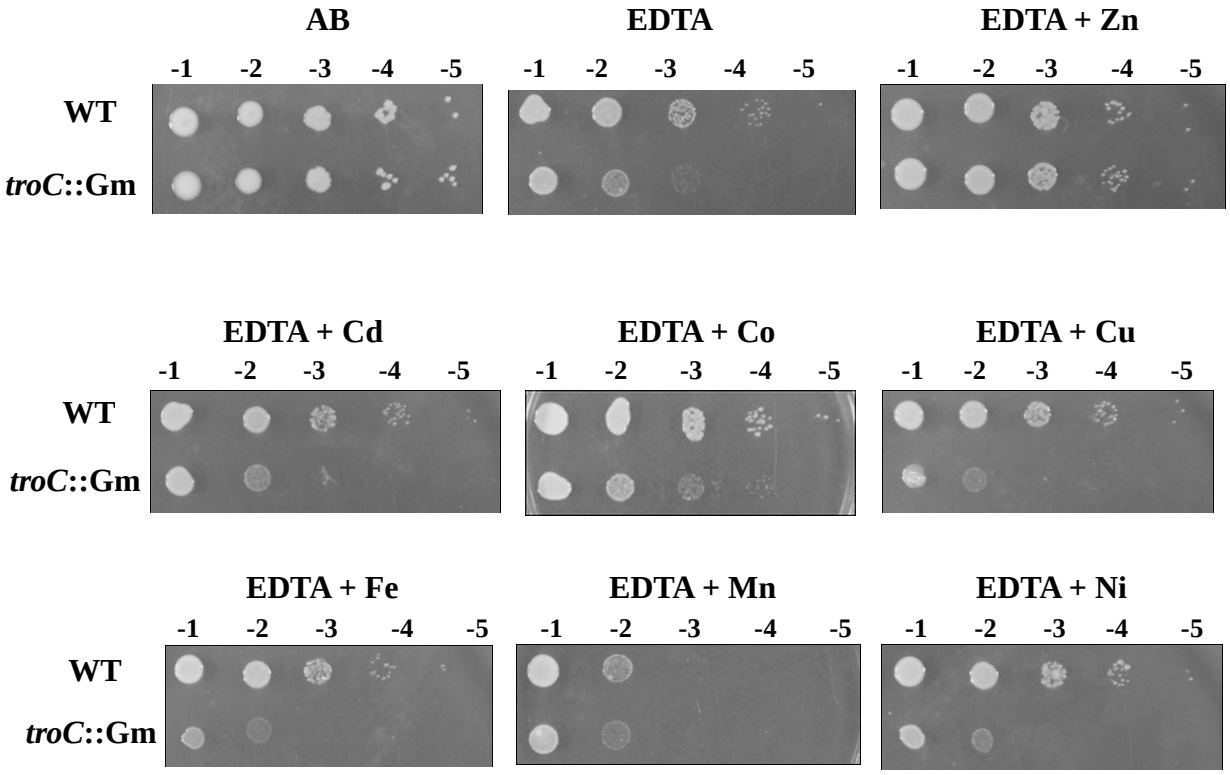

FIG. 6 Sensitivity to EDTA. Wild-type (WT) and the *troC* mutant (*troC*::Gm) cells were adjusted, serially diluted and spotted onto plates containing a minimal medium AB, AB + 1.2 mM EDTA and AB + 1.2 mM EDTA supplemented with 50 μM of $ZnCl_2$, $CdCl_2$, $CoCl_2$, $CuSO_4$, $FeCl_3$, $MnCl_2$ or $NiCl_2$ plates. Tenfold serial dilutions are indicated. The plates were incubated at 28°C for 48 h.

3.2.6 The important role of ZnuA is revealed when TroCBA is disrupted. In other bacteria, the ZnuABC is the major zinc uptake. Inactivation of either *znuA* or *znuAB* had no detectable effect on the growth of *A. tumefaciens* under zinc limiting-conditions (Bhubhanil *et al*., 2014c). However, disruption of *znuA* in combination with *troC* (*troC*::Gm *znuA*::Km) led to a growth defect of *A. tumefaciens* in a minimal AB medium and hyper-sensitivity to EDTA **(Fig. 7).** The growth defect of *troC*::Gm *znuA*::Km could be rescued by zinc supplementation (1.2 mM EDTA + Zn, **Fig. 7).** The results demonstrated that *A. tumefaciens* ZnuABC system is very important for supporting growth under zinc limitation in the absence of the TroCBA system. This indicates that *A. tumefaciens* ZnuABC may function as a back-up system for high-affinity zinc uptake. It is also possible that the two transporters function optimally under different conditions such as different pHs.

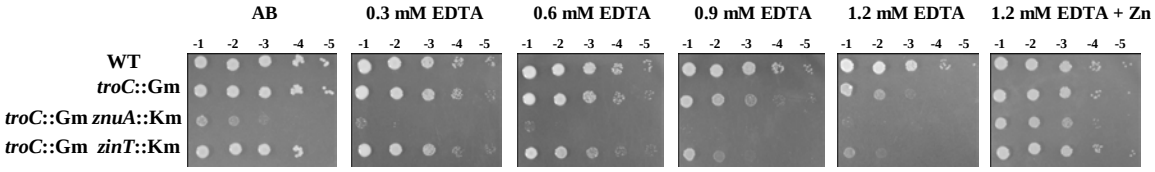

FIG. 7 Sensitivity to EDTA. Wild-type (WT), the *troC* mutant (*troC*::Gm), *troC*::Gm *znuA*::Km and *troC*::Gm *zinT*::Km cells were adjusted, serially diluted and spotted onto plates containing a minimal medium AB, AB + EDTA (0.3, 0.6, 0.9 and 1.2 mM) and AB + 1.2 mM EDTA + 50 µM of $ZnCl_2$. Tenfold serial dilutions are indicated. The plates were incubated at 28°C for 48 h.

3.2.7 ZinT may interact with TroCBA. Unlike other bacteria, it has been reported previously that *A. tumefaciens* ZinT functions independently of ZnuABC (Bhubhanil *et al*., 2014c). The inactivation of *zinT* caused a reduction in the total zinc content and hypersensitivity to EDTA (Bhubhanil *et al*., 2014c). To test the possibility of interaction between *A. tumefaciens* ZinT (a periplasmic protein) and TroCBA in zinc transport, the *troC*::Gm *zinT*::Km strain (mutations in *troC* and *zinT*) was generated, and its sensitivity to EDTA was determined. The *troC*::Gm (*troC* mutation) and *troC*::Gm *zinT*::Km (*troC* and *zinT* mutations) strains were ∼10^2-fold and ∼10^3-fold, respectively, more sensitive to 1.2 mM EDTA than WT (**Fig. 8**). Moreover, the EDTA-hypersensitive phenotype of *troC*::Gm *zinT*::Km could not be reversed to *troC*::Gm by complementation with the plasmid pZINT (**Fig. 8**), but the EDTA-hypersensitive phenotype of *zinT*::Gm (*zinT* mutation) could be fully restored by pZINT (**Fig. 8**). These results suggested that TroCBA is required for the function of *A. tumefaciens* ZinT.

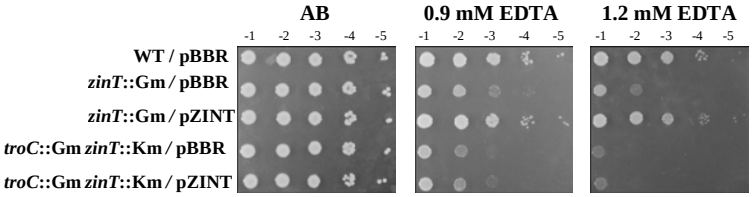

FIG. 8 Sensitivity to EDTA. Wild-type (WT), *zinT*::Gm and *troC*::Gm *zinT*::Km cells were adjusted, serially diluted and spotted onto plates containing a minimal medium AB, AB + EDTA (0.9 and 1.2 mM). Tenfold serial dilutions are indicated. The plates were incubated at 28°C for 48 h. The mutant strains were complemented with functional *zinT* from the plasmid pZINT or with a plasmic vector pBBR.

3.2.8 Decreased zinc levels in the EDTA-hypersensitive mutants. Total zinc content in the mutant strains compared to WT was determined using ICP-MS **(Fig. 9).** The lowest levels of intracellular zinc were detected in the *troC*::Gm *znuA*::Km strain and the *troC*::Gm *zinT*::Km strains < *troC*::Gm < *zinT*::Gm strain (**Fig. 9**).

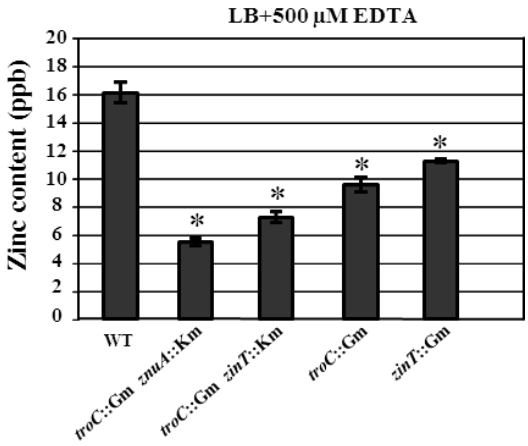

FIG. 9 Intracellular zinc content was determined using ICP-MS. Wild-type (WT) and the mutant strains, *troC*::Gm *znuA*::Km, *troC*::Gm *zinT*::Km, *troC*::Gm and *zinT*::Gm, were grown in LB + 500 µM EDTA for 24 h. The results are shown as the mean of samples in triplicate, and error bars indicate the standard deviations. The bars marked with * are significantly different from WT ($P < 0.05$ in an unpaired Student's *t*-test).

3.2.9 Virulence assay. *N. benthamiana* plants were infected with WT and the mutant strains carrying pCMA1 (a tumor-inducing plasmid). The mutant strains, including *troC*::Gm (*troC* mutation) and *troC*::Gm *zinT*::Km were tested. The *A. tumefaciens* strains were grown under metal limitation in LB + 500 µM EDTA for 24 h and used to infect plants. However, all the mutants caused tumors on the infected plants and were similar to WT (**Fig. 10**). Unfortunately, several attempts were made, the *troC*::Gm *znuA*::Km strain carrying pCMA1 could not be selected; thus the virulence of the *troC*::Gm *znuA*::Km was not determined.

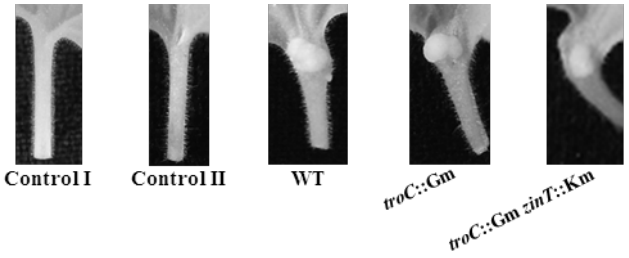

FIG. 10 Virulence assay. Tumor formation on the petioles of the *N. benthamiana* plants infected with WT and the mutant strains: *troC*::Gm and *troC*::Gm *zinT*::Km grown in IB 5.5 medium containing 300 µM of acetosyringone (AS). Control I: without inoculation. Control II: inoculation of wounded petiole with IB 5.5 + 300 µM AS.

Material and Methods

Bacterial strains and growth conditions. The bacterial strains and plasmids are shown in **Table 1**. *A. tumefaciens* and *Escherichia coli* were aerobically grown at 28 °C and 37 °C, respectively, in Luria-Bertani (LB) medium. LA refers to LB medium containing 1.5% agar. The growth conditions and antibiotic concentrations used in the present study have been previously described (Bhubhanil *et al*., 2014a).

Molecular techniques. General molecular techniques were performed using standard protocols (Sambrook *et al.*, 1989). DNA sequencing was performed to confirm the sequence of the cloned DNA (Macrogen, Korea). Plasmid DNA was transferred into *A. tumefaciens* strains by electroporation (Cangelosi *et al*., 1991).

Reverse transcription PCR (RT-PCR). Total RNA was extracted from cells grown in LB at 28^{o}C for 4 h and then treated with 1 mM EDTA for 15 min using a modified hot phenol method (Ngok-ngam *et al*., 2009). RT-PCR was performed as previously described (Ngok-ngam *et al*., 2009). Primer sets were used for amplifying the junction of *troC-troB* [BT4265 (5′-AGGCGCGTCATTTCCACGAG-3′) and BT4266 (5′-TGAGGCTCATGCGCCGCAAC-3′), 280 bp] and *troB-troA* [BT4267 (5′- GCATGGTCTCCTGCTTTGCC-3′) and BT4268 (5′-CGATGATCGAGAAGCTGGCC-3′), 310 bp]. PCR products were visualized using gel electrophoresis on a 1.8% agarose gel with ethidium bromide staining.

Quantitative real-time PCR (qRT-PCR) analysis. qRT-PCR was performed as previously described (Bhubhanil *et al*., 2014b). Log-phase cells grown in LB were not treated or treated with metal and a metal chelator for 15 min prior to harvest. The metals $CdCl_2$, $CoCl_2$, $CuSO_4$, $FeCl_3$, $MgCl_2$, $MnCl_2$, $NiCl_2$ and $ZnCl_2$ were used at a final concentration of 0.45 mM. The metal chelator used was ethylenediaminetetraacetic acid (EDTA, 1 mM). Gene-specific primers for *troC* [BT3751 (5′-TGAAACCGCTCGGCGGTGAG-3′) and BT3752 (5′-CTGCGCATCCTGCAACATGG-3′), 293 bp)], and 16S rRNA gene [BT1421 (5′-GAATCTACCCATCTCTGCGG-3′) and BT1422 (5′-AAGGCCTTCATCACTCACGC-3′), 280 bp] were used. The amount of a specific mRNA target was normalized to the amount of a housekeeping gene 16S rRNA. Fold changes in gene expression are relative to untreated samples from wild-type NTL4 using the $2^{-\Delta\Delta Ct}$ method (Livak & Schmittgen, 2001). The data were reported as the means of biological triplicates ± SD.

Construction of plasmids expressing functional *troA* and *troCBA* for complementation. DNA fragments of full-length *troA* [BT4626 (5′-ATGTTCAGAACCTTCCGATT-3′) and BT4627 (5′-GAAACTGTGCGTTTTACTGG-3′), 837 bp], *troCBA* [BT3809 and BT4627 (5′-GAAACTGTGCGTTTTACTGG-3′), 2747 bp] were amplified by PCR

using *Pfu* DNA polymerase (Fermentas) and the specific primers. The PCR products were cloned into SmaI-digested pBBR1MCS-4 (Kovach *et al*., 1995), generating pTROA and pTROCBA, respectively.

Construction of the double mutation strains (*troC*::Gm *znuA*::Km and *troC*::Gm *zinT*::Km). The plasmid pKNOCKmZNUA (Bhubhanil *et al*., 2014c) was electroporated into the *troC* mutant strain (*troC*::Gm), generating the *troC*::Gm *znuA*::Km strain (disruption of both *troC* and *znuA* genes), which was selected on LB agar (LA) plates containing 60 μg/ml Gm and 30 μg/ml Km. The plasmid pKNOCKmZINT was constructed by PCR amplification of the internal coding region of *zinT* (238 bp) using primers BT3747 (5′-TGACGGACTGGGAAGGCGAC-3′) and BT3748 (5′-ATCTCCTGGCCGTCGCTGAC-3′), which was then cloned into SmaI-digested pKNOCK-Km (Alexeyev, 1999). The plasmid pKNOCKmZINT was electroporated into the *troC* mutant strain, generating the *troC*::Gm *zinT*::Km strain (*troC* and *zinT* mutations).

EDTA sensitivity test. Log-phase cells grown in LB were adjusted, serially diluted and spotted onto plates containing AB medium and AB + EDTA (0.3, 0.6, 0.9, 1, 1.1, and 1.2 mM) according to the protocol previously described (Bhubhanil *et al*., 2014c). In some experiments, AB + 1.2 mM EDTA plates were individually supplemented with 50 μM of $ZnCl_2$, $CdCl_2$, $CoCl_2$, $CuSO_4$, $FeCl_3$, $MgCl_2$, $MnCl_2$ or $NiCl_2$. The plates were then incubated at 28°C for 48 h. Each strain was tested in duplicate, and the experiment was repeated at least twice.

Measurement of the total cellular zinc content. Zinc ions were measured in parts per billion (ppb) using an inductively coupled plasma mass spectrometer (ICP-MS), as previously described (Bhubhanil *et al*., 2014c). Samples were prepared from cells grown in LB + 500 μM EDTA at 28°C for 24 h. The data are reported as the means of biological triplicates ± SD.

Virulence assay. *A. tumefaciens* strains carrying plasmid pCMA1 were used to infect young *Nicotiana benthamiana* plants as previously described (Bhubhanil *et al*., 2014c). Cells grown in LB + 500 μM EDTA at 28°C for 24 h were washed and resuspended in induction broth (Cangelosi *et al*., 1991), pH 5.5 (IB 5.5) + 300 μM acetosyringone (AS). The cells were incubated at 28°C with shaking for 20 min, harvested and adjusted to an OD_{600} of 0.1 in IB 5.5 + 300 μM AS. A 5-μl aliquot of the cell suspension was inoculated into a wounded *N. benthamiana* petiole. Each bacterial strain was used to infect fifteen petioles. Tumor formation at 4 weeks after infection was assessed.

References

Alexeyev, M. F. 1999. The pKNOCK series of broad-host-range mobilizable suicide vectors for gene knockout and targeted DNA insertion into the chromosome of gram-negative bacteria. *Biotechniques* 26, 824-826, 828.

Bhubhanil S, Chamsing J, Sittipo P, Chaoprasid P, Sukchawalit R, Mongkolsuk S. 2014a. Roles of *Agrobacterium tumefaciens* membrane-bound ferritin (MbfA) in iron transport and resistance to iron under acidic conditions. Microbiology 160:863-871.

Bhubhanil S, Niamyim P, Sukchawalit R, Mongkolsuk S. 2014b. Cysteine desulphurase-encoding gene *sufS2* is required for the repressor function of RirA and oxidative resistance in *Agrobacterium tumefaciens*. Microbiology 160:79-90.

Bhubhanil, S., Sittipo, P., Chaoprasid, P., Nookabkaew, S., Sukchawalit, R. & Mongkolsuk, S. 2014c. Control of zinc homeostasis in *Agrobacterium tumefaciens* via *zur* and the zinc uptake genes *znuABC* and *zinT. Microbiology* 160, 2452-2463.

Cangelosi, G. A., Best, E. A., Martinetti, G. & Nester, E. W. 1991. Genetic analysis of *Agrobacterium*. *Methods Enzymol* 204, 384-397.

Grant, S. G., Jessee, J., Bloom, F. R. & Hanahan, D. 1990. Differential plasmid rescue from transgenic mouse DNAs into *Escherichia coli* methylation-restriction mutants. *Proc Natl Acad Sci USA* 87, 4645-4649.

Kovach, M. E., Elzer, P. H., Hill, D. S., Robertson, G. T., Farris, M. A., Roop II, R. M. & Peterson, K. M. 1995. Four new derivatives of the broad-host-range cloning vector pBBR1MCS, carrying different antibiotic-resistance cassettes. *Gene* 166, 175-176.

Haas CE, Rodionov DA, Kropat J, Malasarn D, Merchant SS, de Crécy-Lagard V. 2009. A subset of the diverse COG0523 family of putative metal chaperones is linked to zinc homeostasis in all kingdoms of life. BMC Genomics. 10:470. doi: 10.1186/1471-2164-10-470.

Kitphati, W, Ngok-ngam P, Suwanmaneerat S, Sukchawalit R, Mongkolsuk S. 2007. *Agrobacterium tumefaciens fur* has important physiological roles in iron and manganese homeostasis, the oxidative stress response, and full virulence. Appl. Environ. Microbiol. 73:4760-4768.

Livak KJ, Schmittgen TD. 2001. Analysis of relative gene expression data using real-time quantitative PCR and the $2^{-\Delta\Delta Ct}$ Method. Methods 25:402-408.

Luo, Z. Q., Clemente, T. E. & Farrand, S. K. 2001. Construction of a derivative of *Agrobacterium tumefaciens* C58 that does not mutate to tetracycline resistance. *Mol Plant-Microbe Interact* 14, 98–103.

Metcalf, W. W., Jiang, W., Daniels, L. L., Kim, S. K., Haldimann, A. & Wanner, B. L. 1996. Conditionally replicative and conjugative plasmids carrying *lacZ* alpha for cloning, mutagenesis, and allele replacement in bacteria. *Plasmid* 35, 1-13.

Ngok-ngam P, Ruangkiattikul N, Mahavihakanont A, Virgem SS, Sukchawalit R, Mongkolsuk S. 2009. Roles of *Agrobacterium tumefaciens* RirA in iron regulation, oxidative stress response and virulence. J. Bacteriol. 191:2083-2090.

Sambrook, J., Fritsch, E. F. & Maniatis, T. 1989. *Molecular Cloning: a Laboratory Manual*, Cold Spring Harbor, NY: Cold Spring Harbor Laboratory.

Wood DW, Setubal JC, Kaul R, Monks DE, Kitajima JP, Okura VK, Zhou Y, Chen L, Wood GE, Almeida NF Jr, Woo L, Chen Y, Paulsen IT, Eisen JA, Karp PD, Bovee D Sr, Chapman P, Clendenning J, Deatherage G, Gillet W, Grant C, Kutyavin T, Levy R, Li MJ, McClelland E, Palmieri A, Raymond C, Rouse G, Saenphimmachak C, Wu Z, Romero P, Gordon D, Zhang S, Yoo H, Tao Y, Biddle P, Jung M, Krespan W, Perry M, Gordon-Kamm B, Liao L, Kim S, Hendrick C, Zhao ZY, Dolan M, Chumley F, Tingey SV, Tomb JF, Gordon MP, Olson MV, Nester EW. 2001. The genome of the natural genetic engineer *Agrobacterium tumefaciens* C58. Science 294:2317-2323.

Table 1. Bacterial strains and plasmids

Strain or plasmid	Relevant characteristics	Reference or source
Agrobacterium tumefaciens		
NTL4	Wild-type (WT) strain, a Ti plasmid-cured derivative of strain C58	Luo *et al*. (2001)
zur::Gm	*zur*::pKNOCK-Gm, Gm^r	Bhubhanil *et al*. (2014c)
zinT::Gm	*zinT*::pKNOCK-Gm , Gm^r	Bhubhanil *et al*. (2014c)
znuA::Gm	*znuA*::pKNOCK-Gm, Gm^r	Bhubhanil *et al*. (2014c)
troC::Gm	*troC*::pKNOCK-Gm, Gm^r	This study
troC::Gm *znuA*::Km	*troC*::pKNOCK-Gm and *znuA*::pKNOCK-Km, Gm^r and Km^r	This study
troC::Gm *zinT*::Km	*troC*::pKNOCK-Gm and *zinT*::pKNOCK-Km, Gm^r and Km^r	This study
Escherichia coli		
DH5α	Host for general DNA cloning	Grant *et al*. (1990)
BW20767	Host for plasmids pKNOCK-Gm and pKNOCK-Km	Metcalf *et al*. (1996)
Plasmids for gene inactivation		
pKNOCK-Gm	Suicide vector, Gm^r	Alexeyev (1999)
pKNOCK-Km	Suicide vector, Km^r	Alexeyev (1999)
pKNOCKTROC	Internal coding region of *troC* cloned into pKNOCK-Gm, Gm^r	This study
pKNOCKmZINT	Internal coding region of *zinT* cloned into pKNOCK-Km, Km^r	This study
Plasmids for complementation		
pBBR1MCS-4	Expression vector, Ap^r (pBBR)	Kovach *et al*. (1995)
pZUR	Full-length *zur* cloned into pBBR1MCS-4, Ap^r	Bhubhanil *et al*. (2014c)
pZNUA	Full-length *znuA* cloned into pBBR1MCS-4, Ap^r	Bhubhanil *et al*. (2014c)
pZINT	Full-length *zinT* cloned into pBBR1MCS-4, Ap^r	Bhubhanil *et al*. (2014c)
pTROA	Full-length *troA* cloned into pBBR1MCS-4, Ap^r	This study
pTROCBA	Full-length *troCBA* cloned into pBBR1MCS-4, Ap^r	This study

Ap^r, ampicillin resistance; Gm^r, gentamicin resistance; Km^r, kanamycin resistance

3.3 To study regulation and roles of putative genes involved in cobalt and nickel transport (*dmeR* and *dmeF*) in metal homeostasis and virulence of *A. tumefaciens*.

3.3.1 The *dmeR* and *dmeF* genes are co-transcribed.

The arrangement of the *dmeR* (Atu0890) and *dmeF* (Atu0891) genes is shown in **Fig. 1A**. *A. tumefaciens dmeRF* is flanked by the Atu0889 and Atu0892 genes encoding proteins with unknown function. The *dmeR* and *dmeF* genes are co-transcribed as confirmed through RT-PCR analysis (**Fig. 1B**).

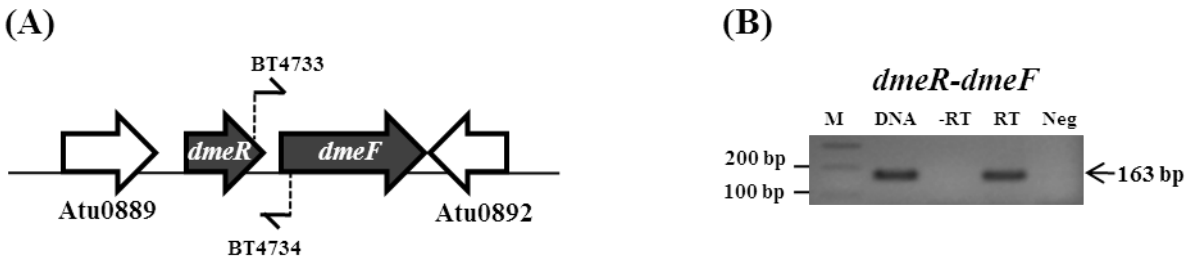

FIG. 1. (A) Gene organization of *A. tumefaciens dmeRF*. The *dmeR* (Atu0890) gene is located upstream of the *dmeF* (Atu0891) gene, separated by 78 bp. The Atu0889 and Atu0892 genes encode proteins of unknown function. The location of primers BT4733 and BT4734 used for RT-PCR analysis is indicated. **(B) Reverse transcription PCR (RT-PCR) analysis.** RNA was isolated from log-phase cells of the wild-type NTL4 strain grown in LB medium and induced with 500 μM $CoCl_2$ for 15 min, then treated with DNaseI, followed by treatment with reverse transcriptase (RT) or being untreated (-RT, a DNA-contamination control). Chromosomal DNA from NTL4 cells was amplified using the primers BT4733 and BT4734 used as a positive control (DNA). Neg is a reaction without template used as a negative control. The expected size of the PCR product is indicated. M is a 100-bp ladder marker.

3.3.2 The *A. tumefaciens dmeRF* operon is inducible by cobalt and nickel.

The expression of the *A. tumefaciens dmeF* gene was increased by cobalt and nickel treatment (10, 100 and 250 μM) in a dose-dependent manner (**Fig. 2A**), with cobalt serving as a better inducer. The expression of *dmeF* in response to various metals was determined using qRT-PCR (**Fig. 2B**). At a high concentration of 500 μM, $CoCl_2$ and $NiCl_2$ caused induction of $dmeF_{At}$ expression by ~30-fold and ~20-fold, respectively, while other metals, including $CuSO_4$, $FeCl_3$, $MnCl_2$ and $ZnCl_2$, caused a less than 2-fold induction.

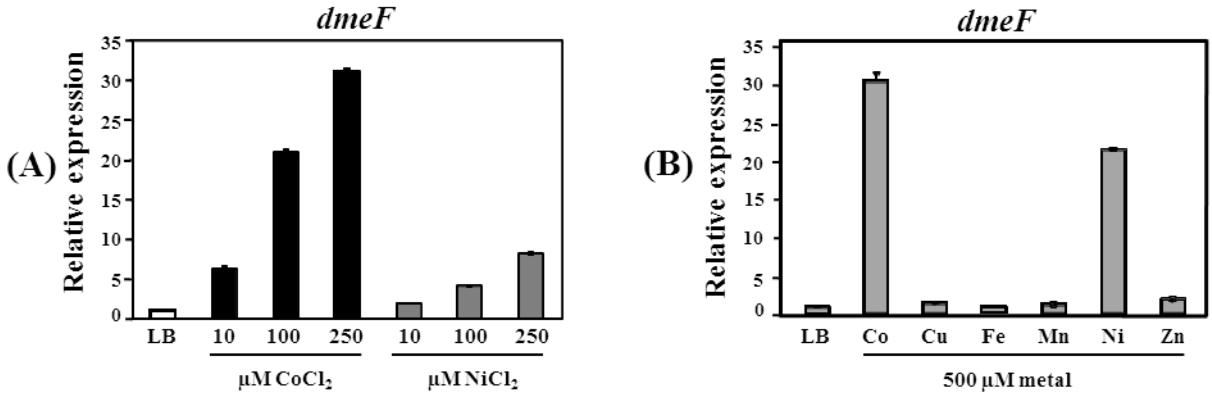

FIG. 2. Induction of *dmeF* by various metals examined through quantitative real-time PCR (qRT-PCR) analysis. Log-phase NTL4 cells grown in LB were either untreated or treated with $CoCl_2$, $CuSO_4$, $FeCl_3$, $MnCl_2$, $NiCl_2$ or $ZnCl_2$ for 15 min. The fold-changes in *dmeF* expression are expressed relative to the untreated control (LB, regarded as 1). The experiment was performed in biological triplicate, and the error bars indicate the standard deviations.

3.3.3 The *dmeRF* operon is negatively regulated by DmeR.

The DR151 (*dmeR* mutation) and DF156 (*dmeF* mutation) strains were generated to determine the functions of the transcriptional regulator DmeR and the CDF-type DmeF transporter. To test whether DmeR regulates the expression of *dmeRF*, the pDmeRF-lacZ (*dmeRF* promoter-*lacZ* transcriptional fusion) plasmid was constructed and transferred into wild-type NTL4 (WT), mutant and the complemented strains, and β-galactosidase (β-Gal) activity was measured (**Fig. 3**). The β-Gal activity obtained from the mutant strain DR151 (DR151/pBBR, ~1.25 U mg protein^{-1}) was higher than that from untreated WT cells (WT/pBBR, ~0.27 U/mg protein) and WT treated with 500 μM $CoCl_2$ for 30 min (~0.59 U/mg protein). The high levels of β-Gal activity observed in DR151 could be suppressed by expressing the functional *dmeR* gene from the multicopy plasmid pDmeR (DR151/pDmeR, ~0.03 U/mg protein), but not pDmeF (DR151/pDmeF, ~1.24 U/mg protein). In contrast to DR151, the level of β-Gal activity produced from DF156 (DF156/pBBR, ~0.33 U/mg protein) was similar to that from WT. These results demonstrated that DmeR is the repressor of the *dmeRF* operon.

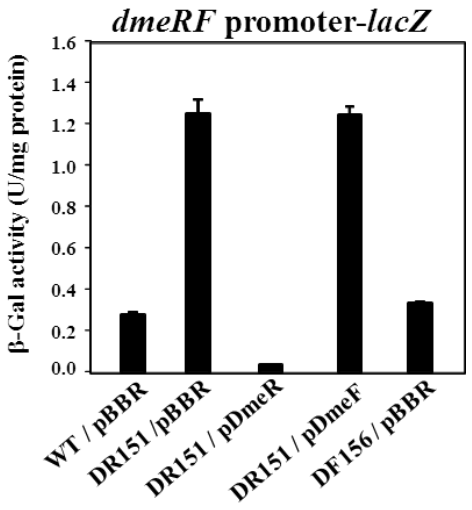

FIG. 3. β-Gal activity assay. β-Gal activities were determined from log-phase cells carrying the pDmeRF-lacZ plasmid grown in LB medium. The cells were wild-type NTL4 (WT) and the mutant strain DR151 (*dmeR* mutation) containing a plasmid vector (pBBR) or functional *dmeR* and *dmeF* genes from the multicopy plasmids pDmeR and pDmeF, respectively. The error bars indicate the standard deviations.

3.3.4 The *dmeF* mutant strain is hyper-sensitive to cobalt and nickel and exhibits increased cellular accumulation of these metals. The sensitivity of the WT and DF156 (*dmeF* mutation) strains to various metals was determined. The DF156 strain was more sensitive to 600 µM $CoCl_2$ (10^3-fold) and 1.2 mM $NiCl_2$ (10^3-fold) than WT (**Fig. 4**). However, the levels of sensitivity to other metals, including $CuSO_4$, $FeCl_3$, $MnCl_2$ and $ZnCl_2$, were similar in WT and DF156 (data not shown). The hyper-sensitive phenotype of DF156 could be reversed by complementation with functional *dmeF* from the multicopy plasmid pDmeF (**Fig. 4**).

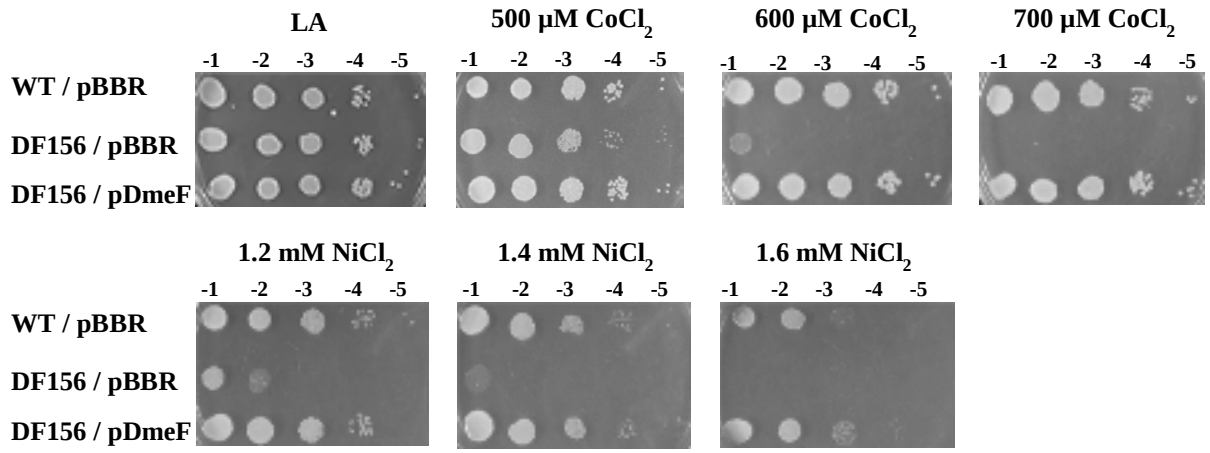

FIG. 4. Sensitivity to cobalt and nickel. Log-phase cells grown in LB were adjusted, serially diluted and spotted onto LA plates containing $CoCl_2$ (500, 600 and 700 µM) and $NiCl_2$ (1.2, 1.4 and 1.6 mM). WT and DF156 (*dmeF* mutation) strains containing a plasmid vector (pBBR) or functional *dmeF* from the multicopy plasmid pDmeF. Ten-fold serial dilutions are indicated.

Inductively coupled plasma mass spectrometry analysis was performed to determine the accumulation of metals in WT and DF156. The results showed that DF156 exhibited an apparently greater increase in intracellular cobalt (4-fold) and nickel (3-fold) contents than WT (**Fig. 5**). The iron content in DF156 was slightly lower than that in WT, whereas the levels of copper, manganese and zinc were similar in DF156 and WT (**Fig. 5**). These results demonstrated that DmeF plays an important role in the detoxification of cobalt and nickel in *A. tumefaciens* and supported the view that DmeF acts as an exporter of cobalt and nickel.

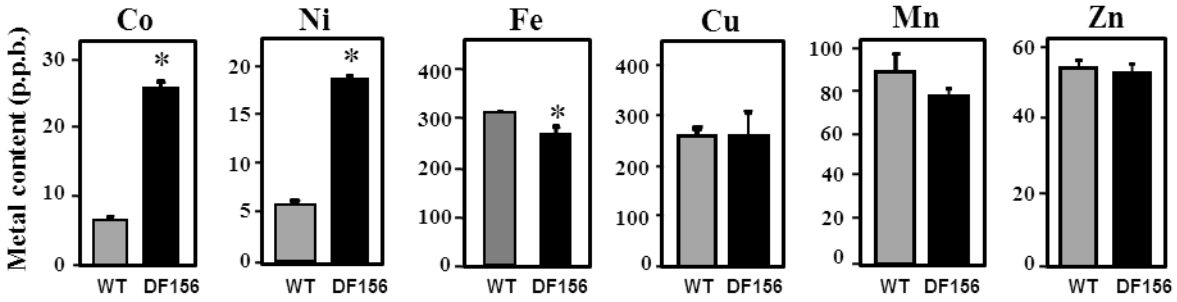

FIG. 5. Measurement of intracellular metal contents using inductively coupled plasma mass spectrometry. WT and DF156 (*dmeF* mutation) cells were grown in LB individually supplemented with 100 μM $CoCl_2$, $NiCl_2$, $FeCl_3$,$CuSO_4$, $MnCl_2$ or $ZnCl_2$. Bars marked with * are significantly different from WT ($P < 0.05$ in an unpaired Student's *t*-test). The error bars indicate the standard deviations.

3.3.5 Disruption of *dmeF* does not affect the virulence of *A. tumefaciens*. The effect of inactivation of *dmeF* on *A. tumefaciens* virulence was tested. *N. benthamiana* plants were infected with log-phase WT and DF156 cells grown in LB medium. Tumor formation was similar in plants infected with WT and DF156 (**Fig. 6**), suggesting that loss of *dmeF* does not affect the ability of *A. tumefaciens* to cause disease in the host plant *N. benthamiana* under the tested conditions.

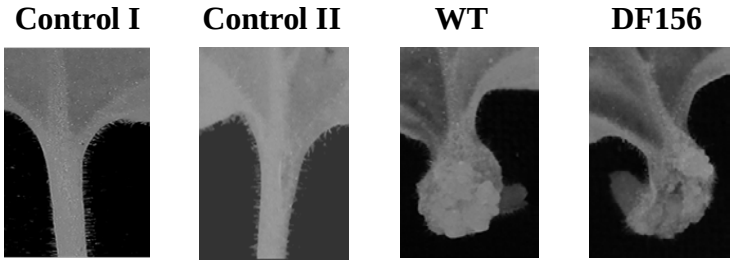

Fig. 6 Virulence assay. Tumor formation in *N. benthamiana* plants infected with the WT and DF156 (*dmeF* mutation) strains carrying the pCMA1 plasmid. Log-phase cells of *A. tumefaciens* grown in LB and then resuspended in IB 5.5 medium containing 300 μM acetosyringone (AS) were used to inoculate wounded *N. benthamiana* petioles. Control I: without infection. Control II: inoculation of wounded petioles with IB 5.5 + 300 μM AS. Fifteen petioles were inoculated for each bacterial strain, and representative petioles are shown.

3.3.6 Cobalt stress causes increased expression of iron-responsive genes. *A. tumefaciens* iron homeostasis is regulated by RirA and Irr (Hibbing & Fuqua, 2011; Rodionov et al., 2006). The promoter regions of *hmuT* (Atu2460, hemin ABC transporter substrate-binding protein), *shmR* (Atu2287, hemin receptor) and *fbpA* (Atu0407, ferric cation ABC transporter substrate-binding protein) contain the IRO motifs (RirA binding site); therefore, these genes were predicted to be regulated by $RirA_{At}$ (Rodionov et al., 2006). In contrast, *mbfA* (Atu0251, iron exporter), *hemA* (Atu2613, heme biosynthesis), *fdx* (Atu1350, ferredoxin) and *irpA* (Atu0288, iron-regulated protein A) were predicted to be regulated by Irr_{At} due to the presence of the ICE motifs (Irr binding site) in their promoters, while the *sufS2* (Atu1825, Fe-S cluster biosynthesis) and *fssA* (Atu0351, Fe-S scaffold protein) promoters contain both IRO and ICE motifs (Rodionov et al., 2006).

Cobalt toxicity in *E. coli* and *S. enterica* has been shown to disturb iron homeostasis (Ranquet et al., 2007; Thorgersen & Downs, 2007; Fantino et al., 2010). To investigate whether iron homeostasis in *A. tumefaciens* may be perturbed by stress from other metals, WT cells were exposed to a 500 μM concentration of various metals ($CoCl_2$, $CuSO_4$, $FeCl_3$, $MnCl_2$, $NiCl_2$ or $ZnCl_2$) for 15 min, and expression of the iron-responsive genes was determined using qRT-PCR. It was found that Co, but not Cu, Mn, Ni and Zn, induced the expression of iron-responsive genes, including *hmuT* (14-fold), *shmR* (30-fold), *fbpA* (5-fold), *mbfA* (35-fold), *sufS2* (7-fold) and *fssA* (4-fold) (**FIG. 7**). These genes were inducible in a concentration-dependent manner, where 500 μM $CoCl_2$ caused greater induction than 250 μM $CoCl_2$ (**FIG. 8**). In contrast, the expression of the *hemA*, *fdx* and *irpA* genes was not strikingly inducible by Co (**FIG. 7**). These results demonstrated that cobalt stress perturbs iron homeostasis in *A. tumefaciens*.

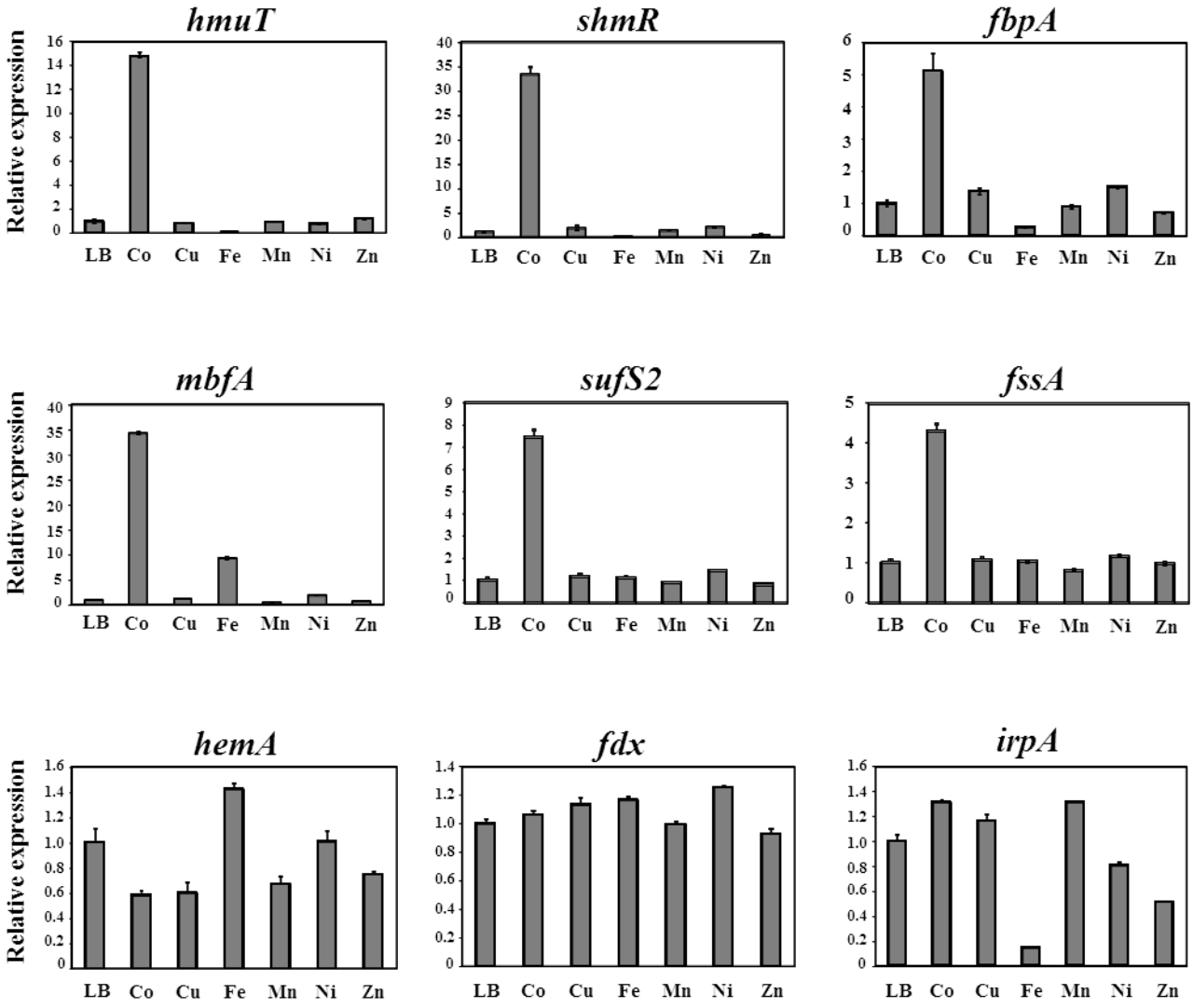

FIG. 7. qRT-PCR analysis of iron-responsive genes. Log phase cells of wild-type NTL4 grown in LB were uninduced or induced with 500 μM of $CoCl_2$, $CuSO_4$, $FeCl_3$, $MnCl_2$, $NiCl_2$ or $ZnCl_2$ for 15 min. The fold-changes in gene expression (*hmuT*, *shmR*, *fbpA*, *mbfA*, *sufS2*, *fssA*, *hemA*, *fdx* and *irpA*) are expressed relative to the untreated sample (LB, regarded as 1). The experiment was performed in biological triplicate, and the error bars indicate the standard deviations.

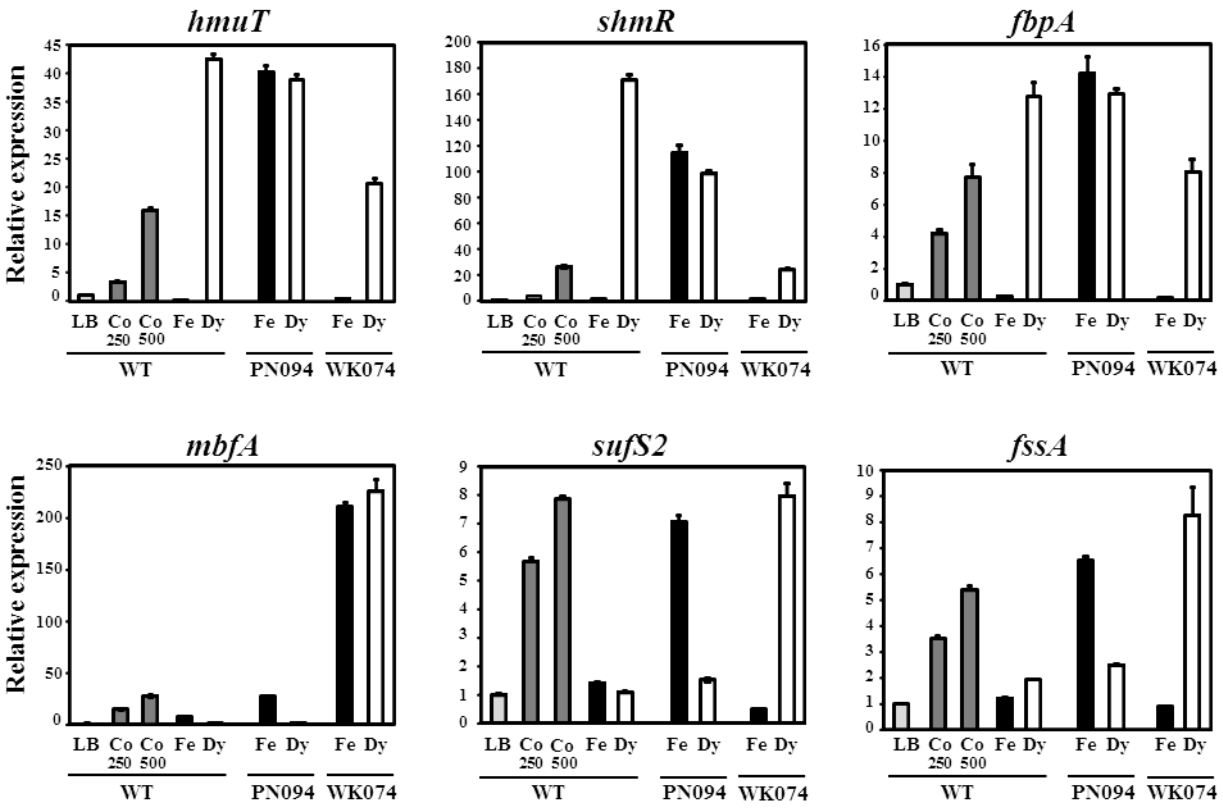

FIG. 8. Effect of cobalt stress on the expression of iron-responsive genes determined using qRT-PCR. Log-phase cells of the NTL4 (WT), PN094 (*rirA* mutation) and WK074 (*irr* mutation) strain grown in LB were either untreated or treated with $CoCl_2$ (250 and 500 μM), $FeCl_3$ (50 μM), or Dy (200 μM) for 15 min. The fold-changes in gene expression (*hmuT*, *shmR*, *fbpA*, *mbfA*, *sufS2* and *fssA*) are expressed relative to the untreated WT sample (LB, regarded as 1). The experiment was performed in biological triplicate, and the error bars indicate the standard deviations.

3.3.7 Cobalt impairs the activation of the SoxR-regulated gene *sodBII*. SoxR is a superoxide-sensing transcriptional regulator that requires 2Fe-2S for its activation function (Crack et al., 2012). *A. tumefaciens* SoxR ($SoxR_{At}$) activates s*odBII* expression as a defense response to detoxify superoxide anions (Saenkham et al., 2007). Cobalt inhibits the activity of Fe-S proteins, as shown in *E. coli* (Ranquet et al., 2007) and *S. enterica* (Thorgersen & Downs, 2007). It is possible that Fe-S clusters may be damaged during cobalt stress in *A. tumefaciens*, as many iron-responsive genes under the control of the Fe-S protein RirA were de-repressed under high cobalt conditions (**FIG. 8**). To test whether cobalt stress may also affect Fe-S dependent-$SoxR_{At}$ activity, the induction of s*odBII* by the superoxide generator menadione (MD, 500 µM) in the absence and presence of $CoCl_2$, $CuSO_4$, $FeCl_3$, $MnCl_2$, $NiCl_2$ or $ZnCl_2$ was measured via qRT-PCR using RNA isolated from the WT cells (**FIG. 9**). *sodBII* expression was inducible by ~1.4 x 10^3-fold by MD, but not by cobalt treatment (250, 500 and 750 µM of $CoCl_2$ (data not shown). The MD activation of *sodBII* was reduced by ~30%, 35% and 50% in the presence of 250, 500 and 750 µM $CoCl_2$, respectively (**FIG. 9**). These results demonstrated that Co has a negative effect on the induction of *sodBII* in response to MD exposure. In addition, Cu and Zn could also inhibit the MD activation of *sodBII*, while Fe, Mn and Ni caused a slight effect (**FIG. 9**).

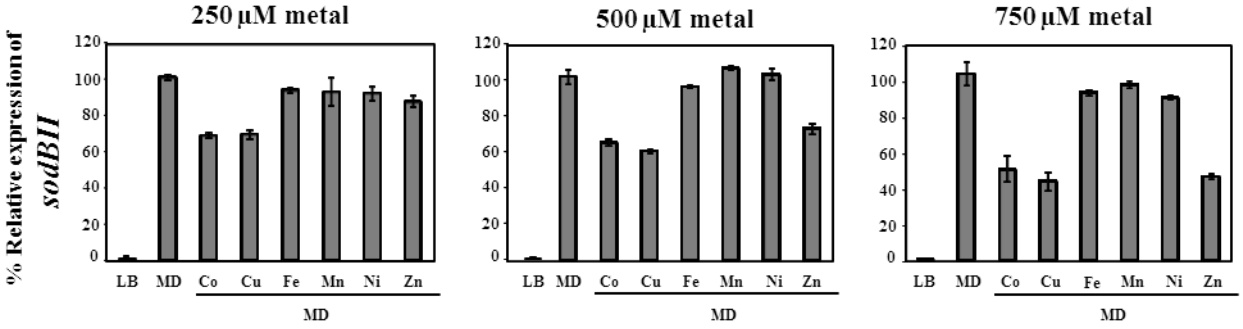

FIG. 9. qRT-PCR analysis of *sodBII* induction by menadione in the presence of various metals. Log-phase NTL4 cells grown in LB were either uninduced or induced with 500 µM menadione (MD) in the absence or presence of 200, 500, and 750 µM concentrations of various metals ($CoCl_2$, $NiCl_2$, $FeCl_3$,$CuSO_4$, $MnCl_2$ or $ZnCl_2$) for 15 min. The expression levels are presented as a percentage, relative to those in cells grown in LB induced with 500 µM MD (100%).

3.3.8 Material and Methods

Bacterial strains and growth conditions. The bacterial strains and plasmids used in the present study are shown in **Table 1**. *A. tumefaciens* and *Escherichia coli* were aerobically grown at 28 °C and 37 °C, respectively, in Luria-Bertani (LB) medium. LA refers to LB medium containing 1.5% agar. The growth conditions and antibiotic concentrations used in the present study have been previously described (Bhubhanil *et al*., 2014a).

Molecular techniques. General molecular techniques were performed using standard protocols (Sambrook *et al*., 1989). DNA sequencing was performed to confirm the sequence of the cloned DNA (Macrogen, Korea). Plasmid DNA was transferred into *A. tumefaciens* strains by electroporation (Cangelosi *et al*., 1991).

Reverse transcription PCR (RT-PCR). Total RNA was extracted from log-phase cells of wild-type NTL4 grown in LB medium and induced with 500 µM $CoCl_2$ for 15 min, and RT-PCR was performed using previously described protocols (Bhubhanil *et al*., 2014a; Ngok-ngam *et al*., 2009). Primers BT4733 (5′-AAGAGCTGGCCCAGGTGCTG-3′) and BT4734 (5′- ATATGGTGATGCTCCGCCGC-3′) were used to amplify the junction of the *dmeR* and *dmeF* genes. PCR products were visualized using gel electrophoresis on a 1.8% agarose gel with ethidium bromide staining.

Quantitative real-time PCR (qRT-PCR) analysis. RNA isolation, cDNA preparation and qRT-PCR were performed as previously described (Ngok-ngam *et al*., 2009, Bhubhanil *et al*., 2014c). The gene-specific primers for *dmeF*, *hmuT*, *shmR*, *fbpA*, *mbfA*, *hemA*, *fdx*, *irpA*, *sufS2*, *fssA* and 16S rRNA are listed in **Table S1**. The amount of a specific mRNA target was normalized to the amount of a housekeeping gene 16S rRNA. Fold changes in gene expression are relative to untreated samples from wild-type NTL4 using the $2^{-\Delta\Delta Ct}$ method (Livak & Schmittgen, 2001). The data were reported as the means of biological triplicates ± SD.

Construction of *dmeF* and *dmeR* mutant strains (DF156 and DR151). *A. tumefaciens* mutant strains were constructed using an insertional gene inactivation method (Ngok-ngam *et al*., 2009). The internal coding regions of *dmeF* [BT4569 (5′-TGCGGTAGAAAGTGGCTTGC-3′) and BT4570 (5′-TGTGCATGCGAACCGTGATC-3′), 222 bp] and *dmeR* [BT4567 (5′-ACAAGGACAAGCTGCTGACC-3′) and BT4568 (5′-ACCACGTGTTCGTGCAGATG-3′), 176 bp] were PCR amplified from genomic wild-type NTL4 with the gene-specific primers. The PCR products were cloned into pKNOCK-Km and pKNOCK-Gm, generating pKNOCKmDMEF and pKNOCKDMER, respectively. The resulting plasmids were individually electroporated into the wild-type NTL4 strain. The mutant strains, DF156 and DR151, were selected on LA + 30 µg/ml of kanamycin (Km) and LA + 60 µg/ml of gentamicin (Gm) plates, respectively.

Cloning of functional *dmeF* and *dmeR* genes for complementation. The PCR fragments containing full-length of *dmeR* [BT4618 (5′-GGTCCGAAACATTCGCGAGG-3′) and BT4619 (5′- TGGCCTGCATTGACCTACCG-3′)] and *dmeF* [BT4620 (5′-ATGACGACGACTTCCGAACC-3′) and BT4621 (5′-GTCCCATTAGGCACTTGCCG-3′)] genes were individually cloned into the SmaI site of pBBR1MCS-4 (Kovach *et al*., 1995), generating the plasmids pDmeR and pDmeF, respectively.

Construction of a *dmeRF* promoter-*lacZ* transcriptional fusion and β-galactosidase activity assay. To construct the pDmeRF-lacZ plasmid, DNA fragments (108 bp) containing the *dmeRF* promoter region were amplified from *A. tumefaciens* NTL4 genomic DNA using PCR with the primers BT5395 (5′-CATCTCGAGGGTCCGAAACATTCG-3′) and BT5396 (5′- ATCCTGCAGGACATGTGCACCTCA-3′) and then cloned into the promoter probe vector pUFR027lacZ, a derivative of pUFR027 (Cangelosi *et al*., 1990), as previously reported (Bhubhanil *et al*., 2014c). The β-galactosidase activity assay (Miller, 1972) was performed as previously described (Bhubhanil *et al*., 2014c) using log-phase cells carrying pDmeRF-lacZ grown in LB. The results are presented as specific activity, which was calculated in units per milligram of protein (U/mg protein).

Sensitivity to metals. The dilution method (Ngok-ngam *et al*., 2009) was used for the metal sensitivity test. Log-phase cells grown in LB medium were adjusted, serially diluted and spotted onto LA plates containing various concentrations of metals. The plates were subsequently incubated at 28 °C for 48 h. Each strain was examined in duplicate, and each experiment was repeated at least twice.

Inductively coupled plasma mass spectrometry. Cells were grown in LB individually supplemented with 100 μM $CoCl_2$, $CuSO_4$, $FeCl_3$, $MnCl_2$, $NiCl_2$ or $ZnCl_2$ at 28°C for 24 h. Samples were prepared and the metals were measured in parts per billion (ppb) as previously described (Bhubhanil et al., 2014a).

Virulence assay. *A. tumefaciens* strains carrying the plasmid pCMA1 were used to infect young *Nicotiana benthamiana* plants according to a previously described protocol (Kamoun et al., 2003; Bhubhanil et al., 2014b). Tumor formation was observed at 3 weeks after inoculation.

References

Alexeyev MF. 1999. The pKNOCK series of broad-host-range mobilizable suicide vectors for gene knockout and targeted DNA insertion into the chromosome of gram-negative bacteria. Biotechniques 26:824-826, 828.

Bhubhanil, S., Chamsing, J., Sittipo, P., Chaoprasid, P., Sukchawalit, R. & Mongkolsuk, S. 2014a. Roles of *Agrobacterium tumefaciens* membrane-bound ferritin (MbfA) in iron transport and resistance to iron under acidic conditions. Microbiology 160, 863-871.

Bhubhanil S, Sittipo P, Chaoprasid P, Nookabkaew S, Sukchawalit R, Mongkolsuk S. 2014b. Control of zinc homeostasis in *Agrobacterium tumefaciens* via *zur* and the zinc uptake genes *znuABC* and *zinT*. Microbiology 160:2452-2463.

Bhubhanil S, Niamyim P, Sukchawalit R, Mongkolsuk S. 2014c. Cysteine desulphurase-encoding gene *sufS2* is required for the repressor function of RirA and oxidative resistance in *Agrobacterium tumefaciens*. Microbiology 160:79-90.

Cangelosi, GA, Best EA, Martinetti G, Nester EW. 1991. Genetic analysis of *Agrobacterium*. Methods Enzymol. 204, 384-397.

Crack JC, Green J, Thomson AJ, Le Brun NE. 2012. Iron-sulfur cluster sensor-regulators. Curr Opin Chem Biol 16:35-44.

DeFeyter R, Kado CI, Gabriel DW. 1990. Small, stable shuttle vectors for use in *Xanthomonas*. Gene 88:65-72.

Fantino JR, Py B, Fontecave M, Barras F. 2010. A genetic analysis of the response of *Escherichia coli* to cobalt stress. Environ Microbiol 12:2846-2857.

Grant SG, Jessee J, Bloom FR, Hanahan D. 1990. Differential plasmid rescue from transgenic mouse DNAs into *Escherichia coli* methylation-restriction mutants. Proc. Natl. Acad. Sci. U.S.A. 87:4645-4649.

Hibbing ME, Fuqua C. 2011. Antiparallel and interlinked control of cellular iron levels by the Irr and RirA regulators of *Agrobacterium tumefaciens*. J Bacteriol 193:3461-3472.

Kamoun S, Hamada W, Huitema E. 2003. Agrosuppression: a bioassay for the hypersensitive response suited to high-throughput screening. Mol Plant Microbe Interact 16:7-13.

Kovach ME, Elzer PH, Hill DS, Robertson GT, Farris MA, Roop II RM, Peterson KM. 1995. Four new derivatives of the broad-host-range cloning vector pBBR1MCS, carrying different antibiotic-resistance cassettes. Gene 166:175-176.

Livak KJ, Schmittgen TD. 2001. Analysis of relative gene expression data using real-time quantitative PCR and the $2^{-\Delta\Delta Ct}$ Method. Methods 25:402-408.

Luo ZQ, Clemente TE, Farrand SK. 2001. Construction of a derivative of *Agrobacterium tumefaciens* C58 that does not mutate to tetracycline resistance. Mol. Plant-Microbe Interact. 14:98-103.

Metcalf WW, Jiang W, Daniels LL, Kim SK, Haldimann A, Wanner BL. 1996. Conditionally replicative and conjugative plasmids carrying *lacZ* alpha for cloning, mutagenesis, and allele replacement in bacteria. Plasmid 35:1-13.

Miller JH. 1972. *Experiments in Molecular Genetics*. Cold Spring Harbor Laboratory Press, NY.

Ngok-ngam P, Ruangkiattikul N, Mahavihakanont A, Virgem SS, Sukchawalit R, Mongkolsuk S. 2009. Roles of *Agrobacterium tumefaciens* RirA in iron regulation, oxidative stress response and virulence. J. Bacteriol. 191:2083-2090.

Ranquet C, Ollagnier-de-Choudens S, Loiseau L, Barras F, Fontecave M. 2007. Cobalt stress in *Escherichia coli*. The effect on the iron-sulfur proteins. J Biol Chem 282:30442-30451.

Rodionov DA, Gelfand MS, Todd JD, Curson AR, Johnston AW. 2006. Computational reconstruction of iron- and manganese-responsive transcriptional networks in alpha-proteobacteria. PLoS Comput Biol 2:1568-1585.

Sambrook, J., Fritsch, E. F. & Maniatis, T. 1989. *Molecular Cloning: a Laboratory Manual*, Cold Spring Harbor, NY: Cold Spring Harbor Laboratory.

Saenkham P, Eiamphungporn W, Farrand SK, Vattanaviboon P, Mongkolsuk S. 2007. Multiple superoxide dismutases in *Agrobacterium tumefaciens*: functional analysis, gene regulation, and influence on tumorigenesis. J Bacteriol 189:8807-8817.

Thorgersen MP, Downs DM. 2007. Cobalt targets multiple metabolic processes in *Salmonella enterica*. J Bacteriol 189:7774-7781.

Table 1. Bacterial strains and plasmids used in this work

Strain or plasmid	Characteristic or genotype	Reference or source
***A. tumefaciens* strains**		
NTL4	Wild-type (WT) strain, a Ti plasmid-cured derivative of strain C58	Luo, 2001
DF156	*dmeF*::pKNOCK-Km, Km^r	This study
DR151	*dmeR*::pKNOCK-Gm, Gm^r	This study
***E. coli* strains**		
BW20767	Host for plasmids pKNOCK-Gm and pKNOCK-Km	Metcalf, 1996
DH5α	Host for general DNA cloning	Grant 1990
Plasmids for gene inactivation		
pKNOCK-Gm	Suicide vector, Gm^r	Alexeyev, 1999
pKNOCK-Km	Suicide vector, Km^r	Alexeyev, 1999
pKNOCKmDMEF	Internal coding region of *dmeF* cloned into pKNOCK-Km, Km^r	This study
pKNOCKDMER	Internal coding region of *dmeR* cloned into pKNOCK-Gm, Gm^r	This study
Plasmids for complementation		
pBBR1MCS-4	Expression vector, Ap^r (pBBR)	Kovach, 1995
pDmeF	Full-length *dmeF* cloned into pBBR1MCS-4, Ap^r	This study
pDmeR	Full-length *dmeR* cloned into pBBR1MCS-4, Ap^r	This study
Promoter-lacZ fusions		
pUFR027lacZ	Promoter probe vector, Tc^r	DeFeyter, 1990
pDmeRF-lacZ	The *dmeRF* promoter fused to *lacZ* of pPR9TT, Ap^r	This study

Ap^r, ampicillin resistance; Gm^r, gentamicin resistance; Km^r, kanamycin resistance; Tc^r, tetracycline resistance

Table S1. Primers used in this study

Gene-primer name and purpose	Sequence (5'→3')
Gene inactivation	
dmeF-BT4569	TGCGGTAGAAAGTGGCTTGC
dmeF-BT4570	TGTGCATGCGAACCGTGATC
dmeR-BT4567	ACAAGGACAAGCTGCTGACC
dmeR-BT4568	ACCACGTGTTCGTGCAGATG
Complementation	
dmeR-BT4618	GGTCCGAAACATTCGCGAGG
dmeR-BT4619	TGGCCTGCATTGACCTACCG
dmeF-BT4620	ATGACGACGACTTCCGAACC
dmeF-BT4621	GTCCCATTAGGCACTTGCCG
RT-PCR	
dmeR-BT4733	AAGAGCTGGCCCAGGTGCTG
dmeF-BT4734	ATATGGTGATGCTCCGCCGC
qRT-PCR	
16S rRNA-BT1421	GAATCTACCCATCTCTGCGG
16S rRNA-BT1422	AAGGCCTTCATCACTCACGC
dmeF-BT4569	TGCGGTAGAAAGTGGCTTGC
dmeF-BT4570	TGTGCATGCGAACCGTGATC
hmuT-BT4161	GAGGCGAAACGCATCGTTGC
hmuT-BT4162	AGGATGGAGATGACATCCGC
shmR-BT4059	GGATCTCGGAAACACCACCG
shmR-BT4167	CGCACCACGTCTACAGACGA
fbpA-BT4061	TCCAGCCCCTGCTGGAATCC
fbpA-BT4062	TGGCATCGCGAAGCTCAGCG
mbfA-BT1666	AAGCTCCTGGGTGATCTGGC
mbfA-BT1667	CGCTTCAACGGTGATCCACG
hemA-BT3371	CTCGAAGCGAAGCTTAAGGC
hemA-BT3372	TGATCGTCAGACGATCCATC
fdx-BT5391	TGAGCAACGGCTCTACCGTC
fdx-BT5392	GACAGGAAAGCCGCGAAGTG
irpA-BT5393	AGCCTGGATCAAGGCACGTG
irpA-BT5394	TGGAGGCATCGACCTCTTCG
sufS2-BT3802	ACGGGTTTAACGCGTACATA
sufS2-BT2727	AGATTGGCCGCTTCGGTCGC
fssA-BT4165	CAAGGTGGTGCTGGAAAGCG
fssA-BT4166	GAAGTGCTCCATGATCGAGC
Promoter-*lacZ* fusion	
dmeRF-BT5395	CATCTCGAGGGTCCGAAACATTCG
dmeRF-BT5396	ATCCTGCAGGACATGTGCACCTCA

ภาคผนวก

ผลงานวิจัยที่ตีพิมพ์ในวารสารวิชาการระดับนานาชาติ 3 เรื่อง

1. Chaoprasid P, Nookabkaew S, **Sukchawalit R***, Mongkolsuk S. **2015.** Roles of *Agrobacterium tumefaciens* C58 ZntA and ZntB and the transcriptional regulator ZntR in controlling Cd2+/Zn2+/Co2+ resistance and the peroxide stress response. Microbiology. 160:1730-1740. (*Corresponding author)
2. Chaoprasid P, Dokpikul T, Johnrod J, Sirirakphaisarn S, Nookabkaew S, **Sukchawalit R***, Mongkolsuk S. **2016.** *Agrobacterium tumefaciens* Zur regulates the high-affinity zinc uptake system, TroCBA, and the putative metal chaperone, YciC, along with ZinT and ZnuABC for survival under zinc-limiting conditions. Appl Environ Microbiol. 82:3503-3514. (*Corresponding author)
3. Dokpikul T, Chaoprasid P, Saninjuk K, Sirirakphaisarn S, Johnrod J, Nookabkaew S, **Sukchawalit R***, Mongkolsuk S. **2016**. Regulation of the Cobalt/Nickel Efflux Operon *dmeRF* in *Agrobacterium tumefaciens* and a Link between the Iron-Sensing Regulator RirA and Cobalt/Nickel Resistance. Appl Environ Microbiol 82:4732-4742. (*Corresponding author)

Microbiology (2015), **161**, 1730–1740 **DOI** 10.1099/mic.0.000135

Roles of *Agrobacterium tumefaciens* C58 *ZntA* and *ZntB* and the transcriptional regulator *ZntR* in controlling $Cd^{2+}/Zn^{2+}/Co^{2+}$ resistance and the peroxide stress response

Paweena Chaoprasid,[1] Sumontha Nookabkaew,[2] Rojana Sukchawalit[1,3,4] and Skorn Mongkolsuk[1,4,5]

Correspondence
Rojana Sukchawalit
rojana@cri.or.th

[1]Laboratory of Biotechnology, Chulabhorn Research Institute, Lak Si, Bangkok 10210, Thailand

[2]Laboratory of Pharmacology, Chulabhorn Research Institute, Lak Si, Bangkok 10210, Thailand

[3]Applied Biological Sciences, Chulabhorn Graduate Institute, Lak Si, Bangkok 10210, Thailand

[4]Center of Excellence on Environmental Health and Toxicology (EHT), Ministry of Education, Bangkok, Thailand

[5]Department of Biotechnology, Faculty of Science, Mahidol University, Bangkok 10400, Thailand

The putative zinc exporters ZntA (a P_{1B}-type ATPase) and ZntB (2-TM-GxN family) in *Agrobacterium tumefaciens* were characterized. The expression of the *zntA* gene is inducible by $CdCl_2$, $ZnCl_2$ and $CoCl_2$, of which $CdCl_2$ is the most potent inducer, whereas *zntB* is constitutively expressed. The metal-induced expression of *zntA* is controlled by the MerR-like regulator ZntR. The *zntA* and *zntR* mutants were highly sensitive to $CdCl_2$ and $ZnCl_2$, and $CoCl_2$ sensitivity was demonstrated to a lesser extent. By contrast, the *zntB* mutant showed similar levels of metal resistance to the WT strain. Even in the *zntA* mutant background, *zntB* did not play an apparent role in metal resistance under the conditions tested. The inactivation of *zntA* increased the accumulation of intracellular cadmium and zinc, and conferred hyper-resistance to H_2O_2. Thus, the metal transporter ZntA and its regulator ZntR are important for controlling zinc homeostasis and cadmium and cobalt detoxification. The loss of either the *zntA* or *zntR* gene did not affect the virulence of *A. tumefaciens* in *Nicotiana benthamiana*.

Received 26 March 2015
Revised 27 June 2015
Accepted 10 July 2015

INTRODUCTION

Zinc plays an essential role in structural protein stabilization and as a cofactor for the catalytic activity and regulatory function of many enzymes and proteins. However, at high concentrations, zinc competes with other metal ions for active sites, generating non-functional proteins and thereby inhibiting many vital biological processes. Zinc homeostasis in bacteria is maintained through the regulation of the uptake, efflux and storage of zinc (Blencowe & Morby, 2003; Nies, 2003, 2007; Nanamiya *et al.*, 2004; Hantke, 2005; Akanuma *et al.*, 2006; Shin *et al.*, 2007; Gabriel & Helmann, 2009). Zinc uptake genes are inducible under low-zinc conditions. When zinc levels surpass cellular demand, the zinc uptake regulator (Zur) represses the zinc uptake genes, *znuABC* and *zinT*, to prevent excess zinc-mediated toxicity (Patzer & Hantke, 1998; Petrarca *et al.*, 2010). Furthermore, expression of the zinc efflux gene *zntA* is activated via the Zn^{2+}-responsive transcriptional regulator (ZntR), which maintains intracellular zinc at suitable levels in *Escherichia coli* (Brocklehurst *et al.*, 1999; Singh *et al.*, 1999). ZntA is likely not the only Zn^{2+} efflux pump in *Escherichia coli*, which also possesses *zntB*. In *Salmonella enterica* serovar Typhimurium, *zntB* is known to encode a protein belonging to the 2-TM-GxN family (Knoop *et al.*, 2005), which can mediate efflux of Zn^{2+} and Cd^{2+} ions (Worlock & Smith, 2002).

An association between zinc homeostasis and oxidative resistance has been reported (Gaballa & Helmann 2002; Yang *et al.*, 2007; Smith *et al.*, 2009; Cerasi *et al.*, 2014; Sein-Echaluce *et al.*, 2015). Zinc serves as a cofactor for oxidant-detoxifying enzymes. Zinc protects thiol groups from free radicals and inhibits free radical formation by

Abbreviations: AS, acetosyringone; Gm, gentamicin; ICP-MS, inductively coupled plasma mass spectrometer; Km, kanamycin; qRT-PCR, quantitative real-time PCR; 5′RACE, 5′ rapid amplification cDNA ends.

Seven supplementary figures and one supplementary table are available with the online Supplementary Material.

competing with redox-active metals, such as copper and iron. A role for zinc in the protection against metal-mediated oxidative damage has been demonstrated (Korbashi *et al.*, 1989; Har-el & Chevion, 1991). The deregulation of zinc transport affects the bacterial response to peroxide stress. The overexpression of Zur from cyanobacterium *Anabaena* sp. PCC 7120 confers H_2O_2 resistance (Sein-Echaluce *et al.*, 2015), while *zur* mutant strains from *Xanthomonas oryzae* pv. *oryzae*, *Corynebacterium diphtheriae* and *Anabaena* sp. PCC 7120 exhibit increased sensitivity to H_2O_2 (Yang *et al.*, 2007; Smith *et al.*, 2009; Sein-Echaluce *et al.*, 2015). In *S. enterica* serovar Typhimurium, the loss of zinc uptake genes *znuABC* and *zupT* leads to H_2O_2 hypersensitivity (Cerasi *et al.*, 2014). The increased sensitivity to H_2O_2 resulting from decreased zinc import has also been observed in a *Bacillus subtilis* strain lacking the *zosA* (*z*inc uptake under *o*xidative *s*tress) gene (Gaballa & Helmann, 2002). The expression of *zosA* is controlled by the peroxide-sensing transcriptional regulator PerR. The induction of *zosA* under H_2O_2 stress elevates zinc levels, which in turn might protect thiols from oxidation (Gaballa & Helmann, 2002). The *zosA* homologue *pmtA* (*P*erR-regulated *m*etal *t*ransporter) was identified in *Streptococcus pyogenes* (Brenot *et al.*, 2007). In contrast to *zosA*, *pmtA* might function as a zinc exporter and play a role in resistance to zinc toxicity (Brenot *et al.*, 2007). The *pmtA* mutant strain exhibits H_2O_2 hypersensitivity (Brenot *et al.*, 2007). These studies demonstrate that, in bacteria, zinc uptake and zinc export genes could play roles in H_2O_2 resistance via different mechanisms.

A. tumefaciens, a member of alphaproteobacteria, is a soil bacterium causing crown gall tumour disease in dicotyledonous plants (Zhu *et al.*, 2000). The regulation of the *A. tumefaciens* C58 zinc uptake genes *znuABC* and *zinT* via Zur has been previously reported (Bhubhanil *et al.*, 2014c). Mutation of the *A. tumefaciens zur* gene increased the expression of *znuABC* and *zinT* and increased the accumulation of intracellular zinc (Bhubhanil *et al.*, 2014c). Herein, we aimed to assess the physiological roles of the genes annotated *zntR* (Atu0888), *zntA* (Atu0843) and *zntB* (Atu0731), which may be involved in controlling zinc efflux in *A. tumefaciens* C58 (Wood *et al.*, 2001). ZntA is important for *A. tumefaciens*' survival under high-zinc conditions, whereas ZntB plays no role in zinc resistance under the conditions tested. The control of zinc levels and H_2O_2 stress resistance through Zur via zinc uptake and ZntR via zinc efflux was also investigated.

METHODS

Bacterial strains and growth conditions. The bacterial strains and plasmids used in the present study are shown in Table 1. *A. tumefaciens* and *E. coli* were aerobically grown at 28 and 37 °C, respectively, in Luria–Bertani (LB) medium. LA refers to LB medium containing 1.5 % agar. The growth conditions and antibiotic concentrations used in the present study have been previously described (Bhubhanil *et al.*, 2014a). Minimal AB medium [containing (l^{-1}): K_2HPO_4, 3 g; NaH_2PO_4, 1.15 g; NH_4Cl, 1 g; $MgSO_4.7H_2O$, 0.3 g; KCl, 0.15 g; $CaCl_2$, 0.01 g; $FeSO_4.7H_2O$, 2.5 mg; glucose, 0.45 %] and induction broth, pH 5.5 (IB 5.5), were prepared as previously reported (Bhubhanil *et al.*, 2014a; Cangelosi *et al.*, 1991).

Molecular techniques. General molecular techniques were performed using standard protocols (Sambrook *et al.*, 1989). The primers are listed in Table S1, available in the online Supplementary Material. DNA sequencing was performed to confirm the sequence of the cloned DNA (Macrogen). Plasmid DNA was transferred into *A. tumefaciens* strains by electroporation (Angelosi *et al.*, 1991).

Construction of *zntR*, *zntA*, *zntB* and double-mutant strains. The mutant strains were generated using a single homologous recombination method (Ngok-Ngam *et al.*, 2009). The *A. tumefaciens* *zntR* (Atu0888), *zntA* (Atu0843) and *zntB* (Atu0731) genes were individually disrupted. Primer pairs for gene inactivation (Table S1) were used to amplify the internal coding regions of *zntR*, *zntA* and *zntB*, and the PCR products were cloned into pKNOCK-Km, generating pKNOCKmZNTR, pKNOCKmZNTA and pKNOCKmZNTB, respectively. The plasmids were electroporated into the WT strain, and the *zntR* (ZR1423), *zntA* (ZA141) and *zntB* (ZB141) mutant strains were selected on LA containing 30 μg ml^{-1} kanamycin (Km).

To generate the ZAB141 strain (disruption of both *zntA* and *zntB* genes), the PCR fragment corresponding to the internal coding region of *zntB* was cloned into pKNOCK-Gm, generating the plasmid pKNOCKZNTB. The plasmid was electroporated into the mutant ZA141 strain, and the mutant ZAB141 was selected on LA containing 60 μg ml^{-1} gentamicin (Gm) and 30 μg ml^{-1} Km.

To generate the ZRA15 strain (disruption of both *zntR* and *zntA* genes), the PCR fragment corresponding to the internal coding region of *zntA* was cloned into pKNOCK-Gm, generating the plasmid pKNOCKZNTA. The plasmid was electroporated into the mutant ZR1423 strain, and the mutant ZRA15 strain was selected on LA containing 60 μg ml^{-1} Gm and 30 μg ml^{-1} Km. All the mutant strains were confirmed through Southern blot analysis.

Construction of plasmids expressing functional *zntR*, *zntA* and *zntB* genes. DNA fragments of full-length *zntR*, *zntA* and *zntB* were PCR amplified using genomic WT DNA as a template, gene-specific primer pairs for complementation (Table S1) and *Pfu* DNA polymerase (Fermentas). The PCR products were cloned into *Sma*I-digested pBBR1MCS-4 (Kovach *et al.*, 1995), generating the plasmids pZNTR, pZNTA and pZNTB, respectively.

Quantitative real-time PCR (qRT-PCR) analysis. qRT-PCR was performed as previously described (Bhubhanil *et al.*, 2014b). Exponential-phase cells grown in LB were either untreated or treated with various metals for 15 min prior to harvest. The metal salts $CdCl_2$, $CoCl_2$, $CuSO_4$, $FeCl_3$, $MgCl_2$, $MnCl_2$, $NiCl_2$ and $ZnCl_2$ were used at a final concentration of 100, 250, 500 or 750 μM. The gene-specific primers for *zntA*, *zntB* and 16S rRNA are listed in Table S1. The relative gene expression was determined using the $2^{-\Delta\Delta CT}$ method. The fold-changes in gene expression are expressed relative to the untreated control as previously described (Livak & Schmittgen, 2001). The data are reported as the means of biological triplicates ± SD.

Determination of the transcriptional start site for *zntA* using 5′ rapid amplification cDNA ends (5′RACE). The transcriptional start site of *zntA* was determined using RNA samples isolated from WT exponential-phase cells grown in LB and treated with 750 μM $ZnCl_2$ for 15 min, followed by 5′RACE (Roche), according to the manufacturer's instructions. Specific primers SP1 and SP2 correspond to BT4122 and BT4822, respectively.

Table 1. Strains and plasmids used in this study

Strain or plasmid	Relevant characteristics	Reference or source
A. tumefaciens		
NTL4	WT, a Ti plasmid-cured derivative of strain C58	Luo *et al.* (2001)
SPP12	*zur* : : pKNOCK-Gm, Gm^r	Bhubhanil *et al.* (2014c)
ZA141	*zntA* : : pKNOCK-Km, Km^r	This study
ZB141	*zntB* : : pKNOCK-Km, Km^r	This study
ZAB141	*zntA* : : pKNOCK-Km, Km^r and *zntB* : : pKNOCK-Gm, Gm^r	This study
ZR1423	*zntR* : : pKNOCK-Km, Km^r	This study
ZRA15	*zntR* : : pKNOCK-Km, Km^r and *zntA* : : pKNOCK-Gm, Gm^r	This study
Escherichia coli		
DH5α	Host for general DNA cloning	Grant *et al.* (1990)
BW20767	Host for plasmids pKNOCK-Gm and pKNOCK-Km	Metcalf *et al.* (1996)
Plasmids for gene inactivation		
pKNOCK-Gm	Suicide vector, Gm^r	Alexeyev (1999)
pKNOCK-Km	Suicide vector, Km^r	Alexeyev (1999)
pKNOCKmZNTA	Internal coding region of *zntA* cloned into pKNOCK-Km, Km^r	This study
pKNOCKmZNTB	Internal coding region of *zntB* cloned into pKNOCK-Km, Km^r	This study
pKNOCKmZNTR	Internal coding region of *zntR* cloned into pKNOCK-Km, Km^r	This study
pKNOCKZNTA	Internal coding region of *zntA* cloned into pKNOCK-Gm, Gm^r	This study
pKNOCKZNTB	Internal coding region of *zntB* cloned into pKNOCK-Gm, Gm^r	This study
Plasmids for complementation		
pBBR1MCS-4	Expression vector, Ap^r (pBBR)	Kovach *et al.* (1995)
pZNTA	Full-length *zntA* cloned into pBBR1MCS-4, Ap^r	This study
pZNTB	Full-length *zntB* cloned into pBBR1MCS-4, Ap^r	This study
pZNTR	Full-length *zntR* cloned into pBBR1MCS-4, Ap^r	This study
Plasmid for the virulence assay		
pCMA1	pTiC58*traM* : : *nptII*, Km^r	Hwang *et al.* (1995)

Ap^r, ampicillin resistance; Gm^r, gentamicin resistance; Km^r, kanamycin resistance.

Sensitivity to metals. The dilution method (Ngok-Ngam *et al.*, 2009) was used for the metal sensitivity test. Exponential-phase cells grown in LB medium were adjusted, serially diluted and spotted onto plates containing LA, LA + $CdCl_2$ (25, 50, 350, 400 and 450 μM), LA + $CoCl_2$ (0.75, 1 and 1.25 mM) and LA + $ZnCl_2$ (350, 400 and 450 μM). The plates were subsequently incubated at 28 °C for 48 h. Each strain was examined in duplicate, and each experiment was repeated at least twice.

Measurement of the total cellular metal content. Cells were grown in LB individually supplemented with 10 μM $CdCl_2$ and 50 μM $CoCl_2$, $CuSO_4$, $FeCl_3$, $MnCl_2$, $NiCl_2$ or $ZnCl_2$ at 28 °C for 24 h. The cells were washed three times with 50 mM potassium phosphate buffer, pH 7.0 (KPB), and 10 mM EDTA. The cells were subsequently washed twice with 50 mM KPB and resuspended in KPB to achieve OD_{600} 1. The cell suspension (2.5 ml) was used for sample preparation, and the metals were measured using an inductively coupled plasma mass spectrometer (ICP-MS), as previously described (Bhubhanil *et al.*, 2014a). The data were reported as the means of biological triplicates ± SD.

Sensitivity to H_2O_2 and diamide. Exponential-phase cells grown in LB medium were adjusted, serial-diluted and spotted onto plates containing LA or LA + 275 μM H_2O_2 in the absence or presence of 50 μM $ZnCl_2$ and LA + diamide (600, 700 and 800 μM). The plates were incubated at 28 °C for 48 h. Each strain was examined in duplicate, and each experiment was repeated at least twice.

Catalase activity assay. Exponential-phase cells grown in LB medium were either left untreated or treated with 500 μM H_2O_2 for 30 min. Crude bacterial lysates were subsequently prepared, and catalase activity was determined based on the degradation of H_2O_2 at a wavelength of 240 nm using a previously described protocol (Beers & Sizer, 1952; Kitphati *et al.*, 2007). One unit (U) of catalase was defined as the amount of enzyme capable of catalysing the turnover of 1 μmol H_2O_2 min^{-1} under the assay conditions. Specific activity was calculated in U (mg protein)$^{-1}$. The data are reported as the means of biological triplicates ± SD.

Virulence assay. *A. tumefaciens* strains carrying the plasmid pCMA1 were used to infect young *Nicotiana benthamiana* plants according to a previously described protocol (Kamoun *et al.*, 2003; Bhubhanil *et al.*, 2014c). Exponential-phase cells grown in LB were washed and grown in an IB 5.5 medium containing 300 μM acetosyringone (AS) for another 20 min. A 5 μl aliquot of the cell suspension (OD_{600} 1 in IB 5.5 + 300 μM AS) was used to inoculate a wounded *N. benthamiana* petiole. Fifteen petioles were tested for each bacterial strain. Tumour formation was observed at 4 weeks after inoculation.

RESULTS

zntR mediates the induction of *zntA* in response to cadmium, zinc and cobalt

The expression of the putative zinc exporter genes *zntA* and *zntB* in response to zinc levels was determined using

quantitative real-time PCR (qRT-PCR) analysis. In the WT strain, the expression of *zntA*, but not *zntB*, was increased after treatments with 100, 500 and 750 μM $ZnCl_2$ (Fig. 1a). The zinc-mediated induction of *zntA* was abolished in the *zntR* mutant strain (ZR1423), suggesting that *zntR* activates *zntA* (Fig. 1a). The loss of zinc-induced *zntA* expression was able to be restored in the complemented strain (ZR1423/pZNTR) (Fig. S1a). Next, the metal-specific response of *zntA* was determined using WT cells grown in LB individually supplemented with 250 μM $CdCl_2$, $CoCl_2$, $CuSO_4$, $FeCl_3$, $MgCl_2$, $MnCl_2$, $NiCl_2$, $PbSO_4$ or $ZnCl_2$. The results shown in Fig. 1b suggest that Cd was the best inducer (~100-fold), followed by Zn (~14-fold) and Co (~8-fold), while other metals induced less than 3-fold *zntA* expression (Ni and Pb) or had no effect (Cu, Fe, Mg and Mn). The induction of *zntA* through Cd and Co was also abolished in the ZR1423 strain (data not shown). The expression of *zntB* was not affected by the *zntR* mutation (Fig. S1a), and *zntB* expression was not strikingly changed upon treatment with zinc (Fig. 1a) or other metals (Fig. S1b).

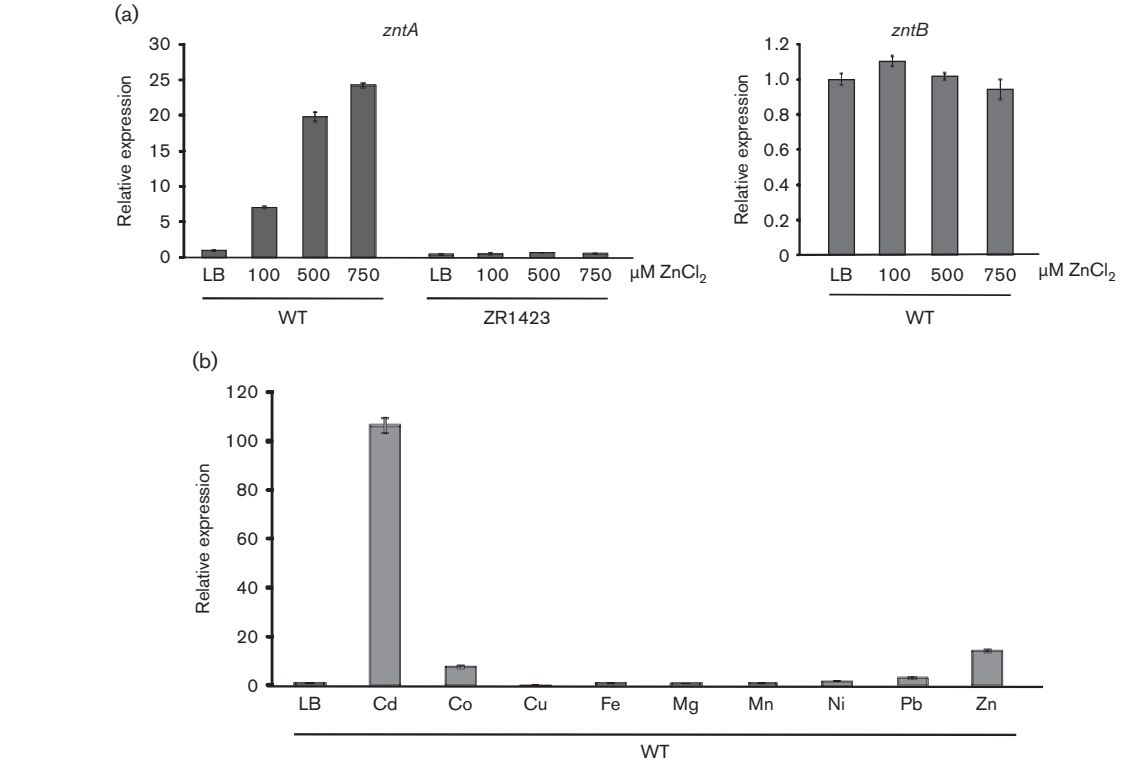

Fig. 1. (a) Transcription analyses of *zntA* and *zntB* in response to increased zinc levels using qRT-PCR. WT and *zntR* mutant (ZR1423) cells were grown to exponential phase in LB medium supplemented with 100, 500 and 750 μM $ZnCl_2$ for 15 min. The expression of the target genes was normalized to 16S rRNA, and the fold-changes in gene expression were assessed relative to WT cells grown in LB (regarded as 1). The experiment was performed in biological triplicate, and the error bars indicate SD. (b) qRT-PCR analysis of *zntA* expression in response to various metals. WT cells were grown in LB medium to exponential phase and individually supplemented with 250 μM $CdCl_2$, $CoCl_2$, $CuSO_4$, $FeCl_3$, $MgCl_2$, $MnCl_2$, $NiCl_2$, $PbNO_3$ or $ZnCl_2$ for 15 min. The fold-changes in gene expression were assessed relative to cells grown in LB (regarded as 1). (c) Features of the *A. tumefaciens zntA* promoter. The ATG start codons for *zntA* and Atu0844 are indicated in bold. The transcriptional start site +1 of *zntA*, determined through 5′RACE, is indicated with an asterisk, and the corresponding guanine (G) is indicated in bold. The predicted −35 and −10 sequences are shown in bold. The dyad sequence has 6 bp of perfect symmetry (arrows) separated by 3 bp, indicated with a grey box. The putative ribosome-binding site (RBS) is also indicated.

The *A. tumefaciens* zntA promoter ($PzntA_{At}$)

To identify the promoter region of $zntA_{At}$, we used 5′RACE to determine the transcriptional start site of $zntA_{At}$, and the −35 and −10 sequences were predicted using BPROM (www.softberry.com). The features of $PzntA_{At}$ are shown in Fig. 1c. The 5′RACE results indicated that the $zntA_{At}$ transcript starts at the G residue located 24 bp upstream of the ATG start codon. The predicted −10 sequence (CAGATT) and −35 sequence (TTGAAG) share 3/6 and 4/6 bp identity, respectively, with the consensus *E. coli* −10 sequence (TATAAT) and −35 sequence (TTGACA). The spacing between the predicted −10 and −35 boxes was 19 bp, compared with the 16–18 bp spacing of the consensus *E. coli* σ^{70} promoter sequences (Harley & Reynolds, 1987). The dyad-symmetrical DNA sequence (the 6-3-6 bp inverted repeat, CTCTAG-TTG-CTAGAG) identified within the 19 bp spacer of $PzntA_{At}$ could be a potential binding site for the *zntA* regulator ZntR.

ZntR and ZntA are required for resistance to cadmium, zinc and cobalt

Next, the *zntR* (ZR1423) and *zntA* (ZA141) mutant strains were generated, and the metal sensitivity was determined (Fig. 2). The results showed that the ZR1423 strain was ~100-fold more sensitive to 50 μM $CdCl_2$ and 450 μM $ZnCl_2$ than WT (Fig. 2). The loss of *zntA* severely affected cell tolerance to cadmium and zinc. The ZA141 strain was ~10^4-fold more sensitive to 450 μM $ZnCl_2$ than WT, while a low concentration (50 μM) of $CdCl_2$ completely inhibited the growth of ZA141 (Fig. 2). Furthermore, the strains ZR1423 and ZA141 also exhibited ~10-fold more sensitivity to $CoCl_2$ than WT (Fig. 2). The sensitive phenotypes of the *zntR* (ZR1423/pBBR) and *zntA* (ZA141/pBBR) mutant strains to $CdCl_2$, $ZnCl_2$ and $CoCl_2$ could be reversed in the complemented strains (ZR1423/pZNTR and ZA141/pZNTA) (Fig. S2). However, the resistance to other metal salts ($CuSO_4$, $FeCl_3$, $MgCl_2$, $MnCl_2$, $NiCl_2$ and $PbSO_4$) was similar in WT and the mutants ZR1423 and ZA141 (data not shown). These results demonstrated that *A. tumefaciens zntR* and *zntA* are important for the detoxification of cadmium, zinc and cobalt. In addition, strain ZRA15 (*zntR* and *zntA* mutations) did not show increased metal sensitivity when compared with ZA141 (*zntA* mutation) (Fig. S2), suggesting that the phenotype of ZRA15 was likely due to the loss of *zntA*. This notion was supported by the fact that the metal-sensitive phenotype of ZRA15 could be completely reversed by complementation with *zntA* carried on the plasmid pZNTA (Fig. S2).

ZntB plays no role in zinc resistance under the conditions tested

It has been reported that *S. enterica* serovar Typhimurium ZntB mediates the efflux of Zn^{2+} and Cd^{2+}, and the *zntB* mutant shows increased sensitivity to zinc and cadmium (Worlock & Smith, 2002). The single inactivation of *A. tumefaciens zntB* (ZB141) had no effect on cell tolerance to cadmium, zinc, cobalt (Fig. 2) and other metal salts ($CuSO_4$, $FeCl_3$, $MgCl_2$, $MnCl_2$, $NiCl_2$ and $PbSO_4$) (data not shown). The metal sensitivity was also tested in the double-mutation strain (ZAB141) and the WT strain expressing multiple copies of *zntB* (WT/pZNTB). Mutations at *zntB* and *zntA* (ZAB141) showed no additional effect on the sensitivity to cadmium, zinc and cobalt compared with the single *zntA* mutation (ZA141) (Fig. 2). Moreover, the WT/pZNTB strain showed resistance to cadmium, zinc and cobalt similar to the WT strain carrying the empty vector (data not shown). Under the conditions tested, *A. tumefaciens zntB* did not show an apparent role for metal resistance.

The *zntA* mutant showed a striking increase in the accumulation of cadmium and zinc

ICP-MS analysis was performed to determine the metal content in the WT and mutant strains (Fig. 3). The cells were grown in LB medium individually supplemented with 50 μM $CoCl_2$, $CuSO_4$, $FeCl_3$, $MnCl_2$, $NiCl_2$ or $ZnCl_2$. However, $CdCl_2$ was used at 10 μM owing to the Cd-hypersensitivity of the mutant strains (ZR1423, ZA141 and ZAB141; Fig. 2). The *zur* (zinc uptake regulator) mutant strain (SPP12) (Bhubhanil *et al.*, 2014c) was used as a control, which showed the increased accumulation of zinc (~ 5-fold; Fig. 3). The inactivation of *zntR* (ZR1423) led to the increased accumulation of Cd (~1.5-fold), while the levels of other metals were similar to those in WT (Fig. 3). The loss of *zntA* increased the accumulation of Cd (~4-fold), Zn (~2-fold) and Mn (~1.2-fold) compared with WT, and the WT showed higher levels of Co (~1.6-fold) and Fe (~1.2-fold) than the *zntA* mutant (ZA141) (Fig. 3). The *zntB* mutation had a lesser effect on the metal content than the *zntA* mutation, as only the Cu and Mn contents in the *zntB* mutant (ZB141) were slightly changed relative to WT (Fig. 3). In addition, the accumulation of Ni in all of the mutants and WT was similar. The striking increase in the accumulation of Cd and Zn in the *zntA* mutant suggests that ZntA is an exporter of Cd and Zn ions.

Roles of zinc uptake and export systems in H_2O_2 resistance

Zinc-mediated protection against H_2O_2 stress has been reported in *B. subtilis* (Gaballa & Helmann, 2002) and *S. enterica* (Cerasi *et al.*, 2014). Thus, to examine whether the disruption of the zinc exporter or deregulation of zinc uptake in *A. tumefaciens* affected the ability of cells to survive under H_2O_2 stress, the H_2O_2 sensitivity test was performed. The ZR1423, ZA141 and SPP12 strains displayed more tolerance to H_2O_2 than WT (LA + H_2O_2 and LA + H_2O_2 + $ZnCl_2$; Fig. 4a). Furthermore, the survival of *A. tumefaciens* cells under H_2O_2 stress was increased in the presence of $ZnCl_2$. As hyper-resistance to H_2O_2 in these mutants could also reflect increased catalase levels, the catalase activity assay was performed. However, as shown in Fig. S3a, the catalase levels in the mutant strains were not elevated compared

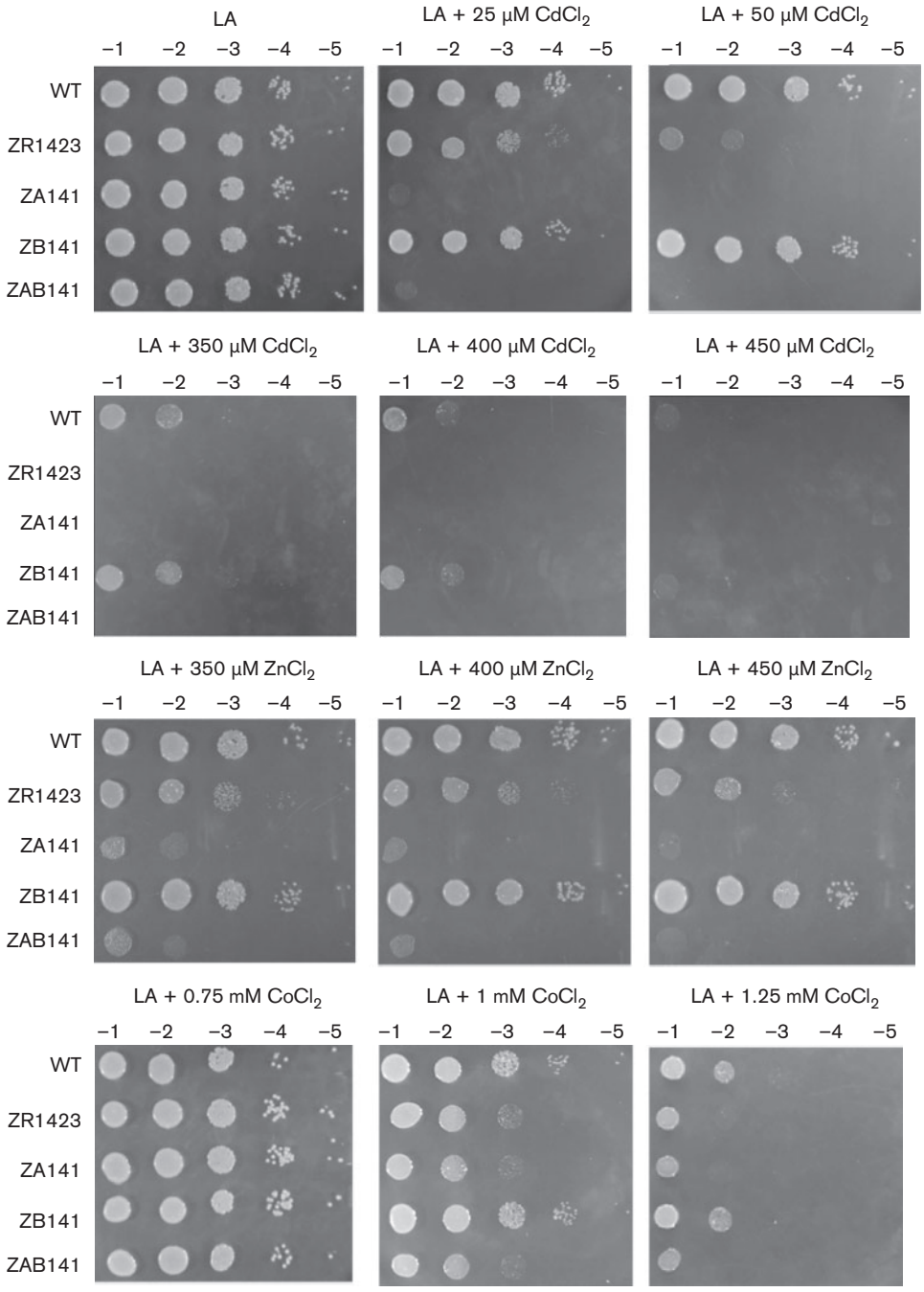

Fig. 2. Sensitivity to metals. WT, ZR1423 (*zntR* mutation), ZA141 (*zntA* mutation), ZB141 (*zntB* mutation) and ZAB141 (*zntA* and *zntB* mutations) exponential-phase cells grown in LB medium were adjusted, serially diluted and spotted onto plates containing LA, LA + $CdCl_2$ (25, 50, 350, 400 and 450 μM), LA + $ZnCl_2$ (350, 400 and 450 μM) and LA + $CoCl_2$ (0.75, 1 and 1.25 mM). The 10-fold serial dilutions are indicated, and the plates were incubated at 28 °C for 48 h.

with WT. It was possible that increased intracellular zinc levels might influence the H_2O_2 resistance observed in the mutant strains. To determine whether zinc plays a protective role against H_2O_2 stress in *A. tumefaciens* through the protection of protein thiols from oxidation, sensitivity to the thiol-oxidizing agent diamide was examined. The results showed that WT and the mutant strains showed similar levels of diamide resistance (Fig. S3b). Therefore, the mechanism for enhanced H_2O_2 resistance in the *A. tumefaciens* mutants (ZR1423, ZA141 and SPP12) remains unknown.

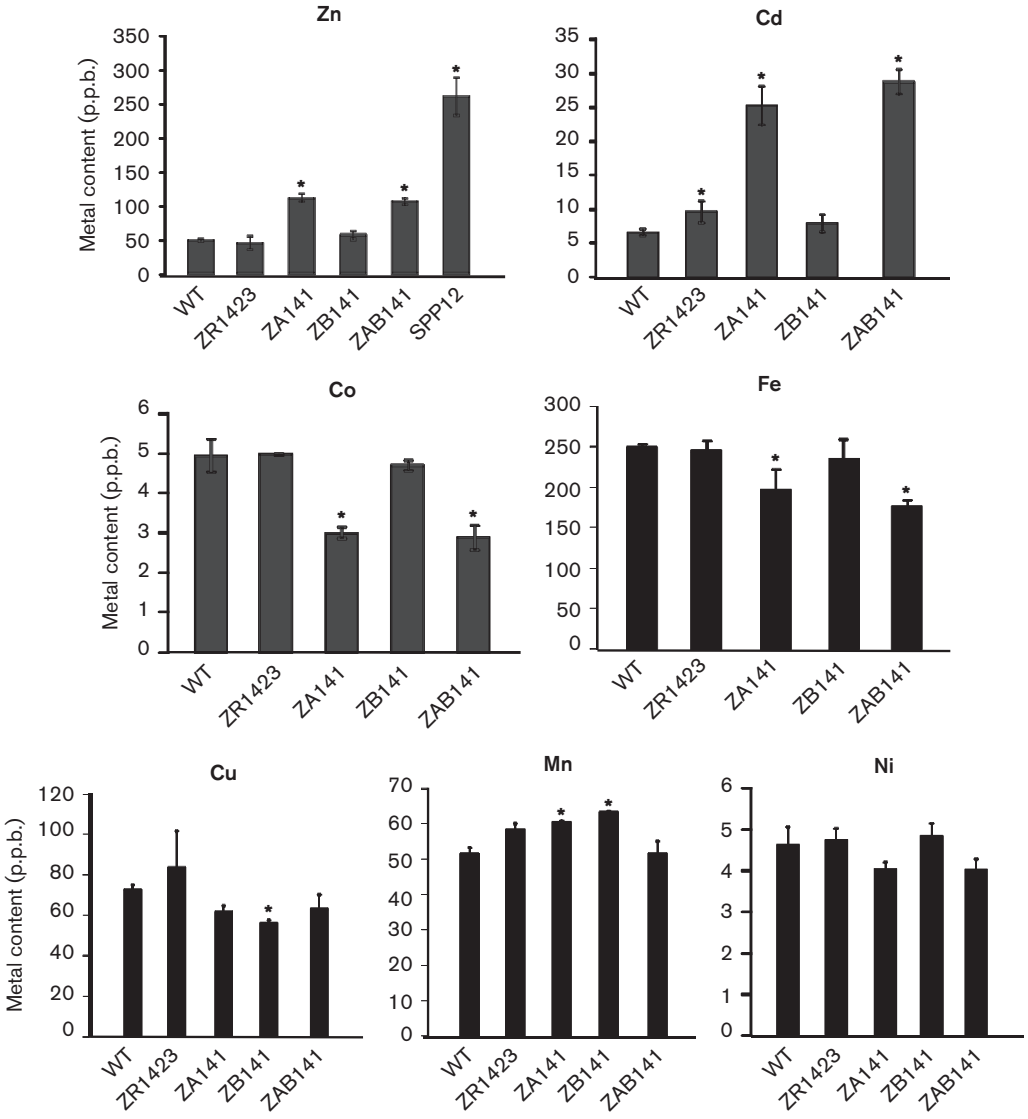

Fig. 3. Determination of metal contents using ICP-MS. WT, ZR1423 (*zntR* mutation), ZA141 (*zntA* mutation), ZB141 (*zntB* mutation) ZAB141, (*zntA* and *zntB* mutations) and SPP12 (*zur* mutation) cells were grown in LB medium individually supplemented with 10 μM $CdCl_2$ and 50 μM $CoCl_2$, $CuSO_4$, $FeCl_3$, $MnCl_2$, $NiCl_2$ or $ZnCl_2$ at 28 °C for 24 h. The total metal contents were measured using ICP-MS. The results are shown as the means of biological triplicate samples, and the error bars indicate SD. The bars marked with an asterisk are significantly different from WT ($P<0.05$ in an unpaired Student's *t*-test). p.p.b., Parts per billion.

The inactivation of either *zntR* or *zntA* did not affect the virulence of *A. tumefaciens*

A. tumefaciens causes crown gall disease through the insertion of T-DNA from the tumour-inducing (Ti) plasmid into the plant genome (Zhu *et al.*, 2000). The virulence of the mutant strains (ZR1423 and ZA141) compared with WT was examined after infecting *N. benthamiana* petioles. The results showed that tumour formation on *N. benthamiana* petioles infected with the mutant strains and WT was similar (Fig. 4b). These results suggested that *zntR* and *zntA* are not important for *A. tumefaciens* virulence in infecting the *N. benthamiana* host plant.

DISCUSSION

It has been reported that ZntA (a P_{1B}-type ATPase) and ZntB (a transporter belonging to the 2-TM-GxN family) are zinc exporters (Knoop *et al.*, 2005; Smith *et al.*, 2014). In addition to Zn^{2+}, *E. coli* ZntA ($ZntA_{Ec}$) extrudes Cd^{2+}, Co^{2+} and Pb^{2+} (Beard *et al.*, 1997; Rensing *et al.*, 1997, 1998; Binet & Poole, 2000), *Staphylococcus aureus* ZntA ($ZntA_{Sa}$) exports Co^{2+} (Xiong & Jayaswal, 1998), and *S. enterica* ZntB ($ZntB_{St}$) mediates the efflux of Cd^{2+} (Worlock & Smith, 2002). The genomic context of *A. tumefaciens zntR*, *zntA* and *zntB* is shown in Fig. S4. The expression of $zntA_{At}$

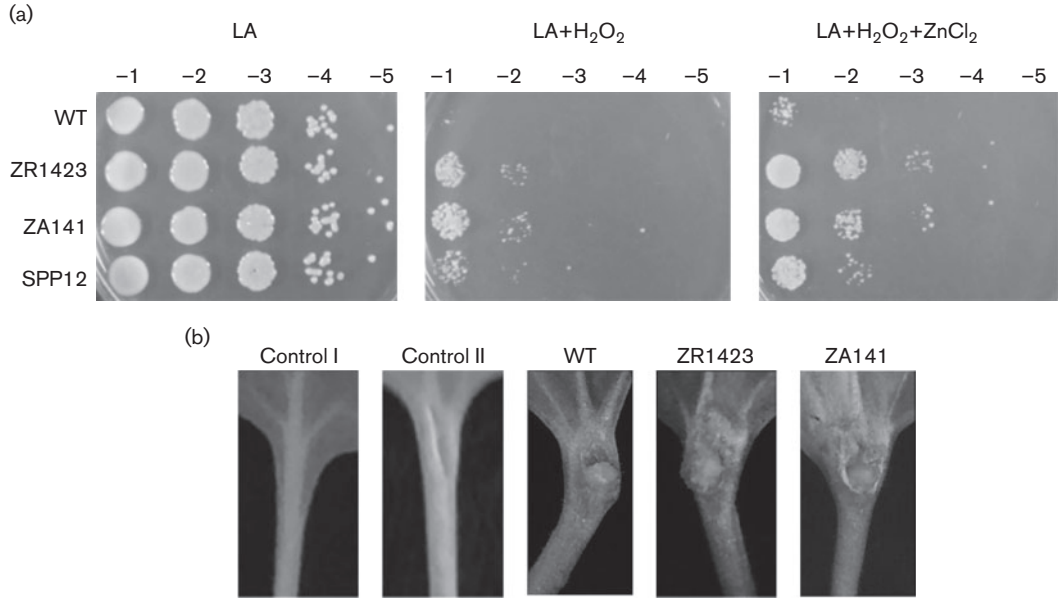

Fig. 4. (a) Sensitivity to H_2O_2. WT, ZA141 (*zntA* mutation), ZR1423 (*zntR* mutation) and SPP12 (*zur* mutation) cells grown in LB medium were adjusted, serially diluted and spotted onto plates containing LA, LA + 275 μM H_2O_2 and LA + 275 μM H_2O_2 + 50 μM $ZnCl_2$. Tenfold serial dilutions are indicated, and the plates were incubated at 28 °C for 48 h. (b) Virulence assay using young *N. benthamiana* plants. *A. tumefaciens* strains carrying the plasmid pCMA1 were grown in IB 5.5 medium containing 300 μM AS and used to inoculate wounded *N. benthamiana* petioles. Fifteen petioles were tested for each bacterial strain. Tumour formation was observed at 4 weeks after inoculation. Representative petioles are shown. Control I: without inoculation. Control II: inoculation of wounded petiole with IB 5.5 + 300 μM AS.

was inducible with the following order of effectiveness: $CdCl_2$ > $ZnCl_2$ > $CoCl_2$ (Fig. 1b). The *A. tumefaciens zntA* mutant was slightly sensitive to $CoCl_2$ but highly sensitive to $CdCl_2$ and $ZnCl_2$ (Fig. 2), suggesting that $ZntA_{At}$ might be involved in the export of these metals. The ICP-MS analysis showed that the *A. tumefaciens zntA* mutant apparently accumulated Cd^{2+} and Zn^{2+}, but not Co^{2+}, to levels higher than WT (Fig. 3), further suggesting that $ZntA_{At}$ plays a role in exporting Cd^{2+} and Zn^{2+}, rather than Co^{2+}. In contrast to $ZntA_{At}$, $ZntB_{At}$ did not show an apparent role for metal resistance under the conditions tested using various strains, including the single $zntB_{At}$ mutation (Fig. 2) and the expression of multiple copies of $zntB_{At}$ from a plasmid in the WT background (data not shown). Furthermore, inactivation of $zntB_{At}$ in the $zntA_{At}$ mutant background (ZAB141) showed levels of metal resistance similar to the $zntA_{At}$ mutant (ZA141) (Fig. 2).

The CorA protein, a member of the 2-TM-GxN family, facilitates Mg^{2+} uptake (Smith & Maguire, 1998; Knoop *et al.*, 2005) and mediates Co^{2+} and Ni^{2+} uptake (Snavely *et al.*, 1989). Although *S. enterica* serovar Typhimurium ZntB ($ZntB_{St}$) is a distant CorA homologue (Knoop *et al.*, 2005) (Fig. S5), this protein does not transport Mg^{2+} (Worlock & Smith, 2002). Sensitivity to magnesium, cobalt and nickel was examined to determine whether $zntB_{At}$ is involved in the transport of these metals. However, WT and the $zntB_{At}$ mutant strain showed similar resistance to magnesium, cobalt and nickel (data not shown). *A. tumefaciens* contains a gene annotated *corA* (Atu0710) (Fig. S5); however the gene function has not been investigated. The signature motifs of CorA (YGMNFxxMPEL) and ZntB (GxxG[I/V]NxGGxP) contribute differently to metal selectivity (Knoop *et al.*, 2005). $ZntB_{At}$ contains the GxxGMNxDExP motif, which differs from the highly conserved G[I/V]N and GG dipeptide, resulting in the classification of $ZntB_{At}$ in a different subclass from $ZntB_{St}$, which contains the GxxGVNxGGxP motif (Knoop *et al.*, 2005) (Fig. S5). The $zntB_{At}$ gene is flanked upstream by *mmgC* (Atu0732), encoding an acyl-CoA-dehydrogenase (Fig. S4). Downstream of $zntB_{At}$ is a gene (Atu0730) encoding a lectin-like protein (Fig. S4). $ZntB_{At}$ shares 17 % amino acid identity with $ZntB_{St}$ (Fig. S5). The C94 and C307 residues in the $ZntB_{St}$ protein may be involved in Zn^{2+} transport (Wan *et al.*, 2011). In $ZntB_{At}$, the residues corresponding to C94 and C307 in $ZntB_{St}$ are replaced with D94 and S311, respectively (Fig. S5). The signature motif sequence and corresponding metal-specific-binding residues in $ZntB_{At}$ are different from those in $ZntB_{St}$, implying that $ZntB_{At}$ might serve a different function, which remains elusive. The expression of $zntB_{At}$ in response to metals was not dramatically changed (Fig. S1b) compared with $zntA_{At}$ expression (Fig. 1b). It is possible that $ZntB_{At}$ could be a metal transporter with broad specificity. However, ICP-MS analysis revealed that the $zntB_{At}$ mutation showed only a minor effect on the accumulation of metals in the cells grown in LB

supplemented with metals (Fig. 3). In addition, the lack of a phenotype in the *A. tumefaciens zntB* mutant might reflect the functional redundancy of *zntB* with *zntA* and other putative cation diffusion facilitator genes, such as Atu0891, Atu0991 and Atu2274, that have not yet been characterized (Cubillas *et al.*, 2013). $ZntB_{At}$ is a homologue of the metal importer CorA (Smith & Maguire, 1998; Knoop *et al.*, 2005). We could not rule out the possibility that $ZntB_{At}$ may function as a metal importer. To test this idea, ICP-MS analysis was performed using cells grown in LB and minimal AB medium (Fig. S6). However, the results showed that the Cu content in the *zntB* mutant (ZB141) changed only slightly relative to WT when cells were grown in LB (Fig. S6). It is possible that the function of $ZntB_{At}$ may be masked by functional redundancy with other metal transporters, and thus was not revealed under the test conditions.

In *E. coli* and *S. aureus*, *zntA* is under the control of ZntR, but acts through different mechanisms to activate *zntA* expression in response to increased zinc levels (Brocklehurst *et al.*, 1999; Singh *et al.*, 1999). *E. coli* ZntR ($ZntR_{Ec}$) is a transcriptional activator belonging to the MerR family, while *S. aureus* ZntR ($ZntR_{Sa}$) is a transcriptional repressor belonging to the ArsR/SmtB family. $ZntR_{Sa}$ binds to the imperfect 9-2-9 bp inverted repeat (ATATGAACA-AA-TATTCATAT) in the $zntA_{Sa}$ promoter region, and this interaction is inhibited in the presence of Zn^{2+} (Singh *et al.*, 1999). Apo-$ZntR_{Ec}$ binds to the perfect 11-11 bp inverted repeat (ACTCTGGAGTC-GACTCCA-GAGT) in the $zntA_{Ec}$ promoter region (Brocklehurst *et al.*, 1999). $ZntR_{Ec}$ acts as an activator upon binding to Zn^{2+}, which mediates $zntA_{Ec}$ transcription via a MerR-like DNA distortion mechanism (Outten *et al.*, 1999). Similar to *E. coli*, metal-induced $zntA_{At}$ expression is mediated by the activation of $zntR_{At}$ (Fig. 1a). The $zntA_{At}$ promoter contains a 19 bp spacer between the −35 and −10 sequences (Fig. 1c) compared with the *E. coli* σ^{70} consensus promoter sequences, which are spaced 16–18 bp apart (Harley & Reynolds, 1987). The 19 bp extended spacer is a characteristic of the metal-ion-responsive MerR family promoters, including the Tn*501 mer* (Lund *et al.*, 1986), *E. coli zntA* (Brocklehurst *et al.*, 1999), *E. coli copA* (Stoyanov *et al.*, 2001) and *Cupriavidus metallidurans pbrA* (Hobman *et al.*, 2012) promoters. It has been shown that the 19 bp spacer between −35 and −10 sequences is essential for both normally weak levels of activity and the induction of the *mer* (mercury resistance) promoter through MerR (Parkhill & Brown, 1990). MerR mediates both the repression and activation of *mer* through MerR bending and Hg-MerR untwisting of the spacer region (Ansari *et al.*, 1995). The expression of the copper exporter *copA* and the lead exporter *pbrA* is regulated by the MerR family transcriptional activators CueR and PbrR, respectively. MerR (7-4-7 bp, TCCGTAC-ATGA-GTACGGA), CueR (7-7-7 bp, ACCTTCC-CCTTGCT-GGAAGGT) and PbrR (7-1-7 bp, CTATAGT-A-ACTAGAG) bind to different dyad symmetrical DNA sequences within the 19 bp spacer sequence in the respective regulated promoters (Lund *et al.*, 1986; Stoyanov *et al.*, 2001; Hobman *et al.*, 2012). In contrast to the *E. coli zntA* promoter (11-11 bp inverted repeat), the *A. tumefaciens zntA* promoter contains a 6-3-6 bp inverted repeat (CTCTAG-TTG-CTAGAG) within the 19 bp spacer (Fig. 1c). $ZntR_{At}$ shares 34 % amino acid identity with $ZntR_{Ec}$ (Fig. S7). It has been shown that cysteine (C79, C114, C115, C124 and C141) and histidine (H29, H53, H76, H77 and H119) residues are important for the $ZntR_{Ec}$-mediated regulation of *zntA* expression (Khan *et al.*, 2002). Mutations at these residues induce changes in metal-ion preference, sensitivity and induction magnitude. The H29, H53 and H119 residues corresponding, respectively, to E29, H53 and H116 in $ZntR_{At}$ are likely involved in either zinc ligation or DNA-bend modulation (Khan *et al.*, 2002). C79, C114 and C124, corresponding to C78, C113 and C121, respectively, in $ZntR_{At}$ are conserved metal-binding residues belonging to the MerR family (Fig. S7). The presence of a characteristic 19 bp spacer in the $zntA_{At}$ promoter (Fig. 1c) and the conserved residues in the $ZntR_{At}$ protein (Fig. S7) suggest that $ZntR_{At}$ might activate $zntA_{At}$ transcription through a mechanism similar to that of $ZntR_{Ec}$ and the MerR family regulators (Ansari *et al.*, 1995; Outten *et al.*, 1999; Stoyanov *et al.*, 2001; Hobman *et al.*, 2012).

The loss of $zntR_{At}$ (ZR1423) increased the sensitivity to $CdCl_2$, $ZnCl_2$ and $CoCl_2$ compared with WT (Fig. 2). Compared with the $zntA_{At}$ mutant (ZA141), the $zntR_{At}$ mutant (ZR1423) showed similar levels of $CoCl_2$ tolerance, but higher levels of resistance to $CdCl_2$ and $ZnCl_2$. This finding might reflect the fact that $zntA_{At}$ activation is impaired in the ZR1423 strain. As $zntA_{At}$ might play a major role in the efflux of cadmium and zinc, the complete loss of $zntA_{At}$ (ZA141) showed a more severe effect on metal resistance. This notion was supported by evidence that the $zntA_{At}$ mutant accumulated higher levels of Cd^{2+} and Zn^{2+} than the $zntR_{At}$ mutant (Fig. 3). Interestingly, the $zntA_{At}$ mutant was more sensitive to $CoCl_2$ (Fig. 2) but had reduced intracellular Co^{2+} (Fig. 3) relative to WT. Therefore, the cobalt hypersensitive phenotype of the $zntA_{At}$ mutant was not due to the increased levels of intracellular Co^{2+}. The cobalt hypersensitivity might be an indirect effect resulting from a disruption of metal homeostasis affecting metals that are not specific substrates for $ZntA_{At}$.

The zinc content in the zur_{At} mutant was approximately 5-fold higher than that in the WT (Fig. 3), consistent with the previous report. However, the zur_{At} mutant showed levels of zinc resistance similar to WT (0.5–4 mM $ZnCl_2$) (Bhubhanil *et al.*, 2014c). In contrast, compared with WT, the $zntA_{At}$ mutant possessed an approximately 2-fold higher zinc content (Fig. 3) and showed high sensitivity to zinc (0.35–0.45 mM $ZnCl_2$) (Fig. 2). Unlike the $zntA_{At}$ mutant, it is likely that zinc is kept safely in the zur_{At} mutant and does not damage the cell.

The disruption of either zinc uptake or zinc export affects intracellular zinc levels and might be involved in peroxide resistance (Gaballa & Helmann, 2002; Brenot *et al.*, 2007;

Yang *et al.*, 2007; Smith *et al.*, 2009; Cerasi *et al.*, 2014; Sein-Echaluce *et al.*, 2015). Increased zinc levels could protect some bacteria from H_2O_2 killing (Gaballa & Helmann, 2002; Cerasi *et al.*, 2014). However, in other bacteria, the upregulation of zinc uptake or reduction of zinc export could lead to increased sensitivity to H_2O_2 killing (Brenot *et al.*, 2007; Yang *et al.*, 2007; Smith *et al.*, 2009; Sein-Echaluce *et al.*, 2015). Either increased zinc uptake (SPP12) or reduced zinc export (ZA141) increased intracellular zinc (Fig. 3) and enhanced H_2O_2 resistance (Fig. 4a). Zinc might confer protection against H_2O_2 stress in *Agr. tumefaciens*, although the exact mechanism remains unknown. Oxidative burst is an initial plant defence mechanism (Wojtaszek, 1997; Fones & Preston, 2013). The inactivation of the zinc exporter provided a benefit that would help *A. tumefaciens* to cope with H_2O_2 stress (Fig. 4a); thus, it was not surprising that *A. tumefaciens* virulence was fully retained in the zinc-exporter-defective mutants (ZR1423 and ZA141, Fig. 4b).

In conclusion, the *A. tumefaciens zntA* gene is an important metal exporter for the detoxification of cadmium, zinc and cobalt. The regulation of zinc homeostasis by uptake systems via Zur and the exporter ZntA via ZntR plays a role in the ability of *A. tumefaciens* to survive H_2O_2 stress.

ACKNOWLEDGEMENTS

The authors thank S. K. Farrand for the pCMA1 plasmid and P. Srifah Huehne and K. Bhinija for technical assistance with the virulence assay. The authors also thank P. Sittipo and S. Bhubhanil for assistance with the experiments. This work was financially supported by a grant from the Chulabhorn Research Institute and the Thailand Research Fund (no. RSA5880010) to R. S.

REFERENCES

Akanuma, G., Nanamiya, H., Natori, Y., Nomura, N. & Kawamura, F. (2006). Liberation of zinc-containing L31 (RpmE) from ribosomes by its paralogous gene product, YtiA, in *Bacillus subtilis*. *J Bacteriol* **188**, 2715–2720.

Alexeyev, M. F. (1999). The pKNOCK series of broad-host-range mobilizable suicide vectors for gene knockout and targeted DNA insertion into the chromosome of Gram-negative bacteria. *Biotechniques* **26**, 824–826, 828.

Angelosi, G. A., Abest, E., Martinetti, G. & Nester, E. W. (1991). Genetic analysis of *Agrobacterium*. *Methods Enzymol* **204**, 384–397.

Ansari, A. Z., Bradner, J. E. & O'Halloran, T. V. (1995). DNA-bend modulation in a repressor-to-activator switching mechanism. *Nature* **374**, 370–375.

Beard, S. J., Hashim, R., Membrillo-Hernández, J., Hughes, M. N. & Poole, R. K. (1997). Zinc(II) tolerance in *Escherichia coli* K-12: evidence that the *zntA* gene (*o732*) encodes a cation transport ATPase. *Mol Microbiol* **25**, 883–891.

Beers, R. F. Jr & Sizer, I. W. (1952). A spectrophotometric method for measuring the breakdown of hydrogen peroxide by catalase. *J Biol Chem* **195**, 133–140.

Bhubhanil, S., Chamsing, J., Sittipo, P., Chaoprasid, P., Sukchawalit, R. & Mongkolsuk, S. (2014a). Roles of *Agrobacterium tumefaciens* membrane-bound ferritin (MbfA) in iron transport and resistance to iron under acidic conditions. *Microbiology* **160**, 863–871.

Bhubhanil, S., Niamyim, P., Sukchawalit, R. & Mongkolsuk, S. (2014b). Cysteine desulphurase-encoding gene *sufS2* is required for the repressor function of RirA and oxidative resistance in *Agrobacterium tumefaciens*. *Microbiology* **160**, 79–90.

Bhubhanil, S., Sittipo, P., Chaoprasid, P., Nookabkaew, S., Sukchawalit, R. & Mongkolsuk, S. (2014c). Control of zinc homeostasis in *Agrobacterium tumefaciens* via *zur* and the zinc uptake genes *znuABC* and *zinT*. *Microbiology* **160**, 2452–2463.

Binet, M. R. & Poole, R. K. (2000). Cd(II), Pb(II) and Zn(II) ions regulate expression of the metal-transporting P-type ATPase ZntA in *Escherichia coli*. *FEBS Lett* **473**, 67–70.

Blencowe, D. K. & Morby, A. P. (2003). Zn(II) metabolism in prokaryotes. *FEMS Microbiol Rev* **27**, 291–311.

Brenot, A., Weston, B. F. & Caparon, M. G. (2007). A PerR-regulated metal transporter (PmtA) is an interface between oxidative stress and metal homeostasis in *Streptococcus pyogenes*. *Mol Microbiol* **63**, 1185–1196.

Brocklehurst, K. R., Hobman, J. L., Lawley, B., Blank, L., Marshall, S. J., Brown, N. L. & Morby, A. P. (1999). ZntR is a Zn(II)-responsive MerR-like transcriptional regulator of *zntA* in *Escherichia coli*. *Mol Microbiol* **31**, 893–902.

Cerasi, M., Liu, J. Z., Ammendola, S., Poe, A. J., Petrarca, P., Pesciaroli, M., Pasquali, P., Raffatellu, M. & Battistoni, A. (2014). The ZupT transporter plays an important role in zinc homeostasis and contributes to *Salmonella enterica* virulence. *Metallomics* **6**, 845–853.

Cubillas, C., Vinuesa, P., Tabche, M. L. & García-de los Santos, A. (2013). Phylogenomic analysis of cation siffusion facilitator proteins uncovers Ni^{2+}/Co^{2+} transporters. *Metallomics* **5**, 1634–1643.

Fones, H. & Preston, G. M. (2013). The impact of transition metals on bacterial plant disease. *FEMS Microbiol Rev* **37**, 495–519.

Gaballa, A. & Helmann, J. D. (2002). A peroxide-induced zinc uptake system plays an important role in protection against oxidative stress in *Bacillus subtilis*. *Mol Microbiol* **45**, 997–1005.

Gabriel, S. E. & Helmann, J. D. (2009). Contributions of Zur-controlled ribosomal proteins to growth under zinc starvation conditions. *J Bacteriol* **191**, 6116–6122.

Grant, S. G., Jessee, J., Bloom, F. R. & Hanahan, D. (1990). Differential plasmid rescue from transgenic mouse DNAs into Escherichia coli methylation-restriction mutants. *Proc Natl Acad Sci U S A* **87**, 4645–4649.

Hantke, K. (2005). Bacterial zinc uptake and regulators. *Curr Opin Microbiol* **8**, 196–202.

Harel, R. & Chevion, M. (1991). Zinc(II) protects against metal-mediated free radical induced damage: studies on single and double-strand DNA breakage. *Free Radic Res Commun* **13**, 509–515.

Harley, C. B. & Reynolds, R. P. (1987). Analysis of *E. coli* promoter sequences. *Nucleic Acids Res* **15**, 2343–2361.

Hobman, J. L., Julian, D. J. & Brown, N. L. (2012). Cysteine coordination of Pb(II) is involved in the PbrR-dependent activation of the lead-resistance promoter, P*pbrA*, from *Cupriavidus metal-lidurans* CH34. *BMC Microbiol* **12**, 109.

Hwang, I., Cook, D. M. & Farrand, S. K. (1995). A new regulatory element modulates homoserine lactone-mediated autoinduction of Ti plasmid conjugal transfer. *J Bacteriol* **177**, 449–458.

Kamoun, S., Hamada, W. & Huitema, E. (2003). Agrosuppression: a bioassay for the hypersensitive response suited to high-throughput screening. *Mol Plant Microbe Interact* **16**, 7–13.

Khan, S., Brocklehurst, K. R., Jones, G. W. & Morby, A. P. (2002). The functional analysis of directed amino-acid alterations in ZntR from *Escherichia coli*. *Biochem Biophys Res Commun* **299**, 438–445.

Kitphati, W., Ngok-Ngam, P., Suwanmaneerat, S., Sukchawalit, R. & Mongkolsuk, S. (2007). *Agrobacterium tumefaciens fur* has important

physiological roles in iron and manganese homeostasis, the oxidative stress response, and full virulence. *Appl Environ Microbiol* **73**, 4760–4768.

Knoop, V., Groth-Malonek, M., Gebert, M., Eifler, K. & Weyand, K. (2005). Transport of magnesium and other divalent cations: evolution of the 2-TM-GxN proteins in the MIT superfamily. *Mol Genet Genomics* **274**, 205–216.

Korbashi, P., Katzhendler, J., Saltman, P. & Chevion, M. (1989). Zinc protects *Escherichia coli* against copper-mediated paraquat-induced damage. *J Biol Chem* **264**, 8479–8482.

Kovach, M. E., Elzer, P. H., Hill, D. S., Robertson, G. T., Farris, M. A., Roop, R. M. II & Peterson, K. M. (1995). Four new derivatives of the broad-host-range cloning vector pBBR1MCS, carrying different antibiotic-resistance cassettes. *Gene* **166**, 175–176.

Livak, K. J. & Schmittgen, T. D. (2001). Analysis of relative gene expression data using real-time quantitative PCR and the $2^{-\Delta\Delta CT}$ method. *Methods* **25**, 402–408.

Lund, P. A., Ford, S. J. & Brown, N. L. (1986). Transcriptional regulation of the mercury-resistance genes of transposon Tn*501*. *J Gen Microbiol* **132**, 465–480.

Luo, Z. Q., Clemente, T. E. & Farrand, S. K. (2001). Construction of a derivative of *Agrobacterium tumefaciens* C58 that does not mutate to tetracycline resistance. *Mol Plant Microbe Interact* **14**, 98–103.

Metcalf, W. W., Jiang, W., Daniels, L. L., Kim, S. K., Haldimann, A. & Wanner, B. L. (1996). Conditionally replicative and conjugative plasmids carrying *lacZ* for cloning, mutagenesis, and allele replacement in bacteria. *Plasmid* **35**, 1–13.

Nanamiya, H., Akanuma, G., Natori, Y., Murayama, R., Kosono, S., Kudo, T., Kobayashi, K., Ogasawara, N., Park, S. M. & other authors (2004). Zinc is a key factor in controlling alternation of two types of L31 protein in the *Bacillus subtilis* ribosome. *Mol Microbiol* **52**, 273–283.

Ngok-Ngam, P., Ruangkiattikul, N., Mahavihakanont, A., Virgem, S. S., Sukchawalit, R. & Mongkolsuk, S. (2009). Roles of *Agrobacterium tumefaciens* RirA in iron regulation, oxidative stress response, and virulence. *J Bacteriol* **191**, 2083–2090.

Nies, D. H. (2003). Efflux-mediated heavy metal resistance in prokaryotes. *FEMS Microbiol Rev* **27**, 313–339.

Nies, D. H. (2007). Biochemistry. How cells control zinc homeostasis. *Science* **317**, 1695–1696.

Outten, C. E., Outten, F. W. & O'Halloran, T. V. (1999). DNA distortion mechanism for transcriptional activation by ZntR, a Zn(II)-responsive MerR homologue in *Escherichia coli*. *J Biol Chem* **274**, 37517–37524.

Parkhill, J. & Brown, N. L. (1990). Site-specific insertion and deletion mutants in the *mer* promoter-operator region of Tn*501*; the nineteen base-pair spacer is essential for normal induction of the promoter by MerR. *Nucleic Acids Res* **18**, 5157–5162.

Patzer, S. I. & Hantke, K. (1998). The ZnuABC high-affinity zinc uptake system and its regulator Zur in *Escherichia coli*. *Mol Microbiol* **28**, 1199–1210.

Petrarca, P., Ammendola, S., Pasquali, P. & Battistoni, A. (2010). The Zur-regulated ZinT protein is an auxiliary component of the high-affinity ZnuABC zinc transporter that facilitates metal recruitment during severe zinc shortage. *J Bacteriol* **192**, 1553–1564.

Rensing, C., Mitra, B. & Rosen, B. P. (1997). The *zntA* gene of *Escherichia coli* encodes a Zn(II)-translocating P-type ATPase. *Proc Natl Acad Sci U S A* **94**, 14326–14331.

Rensing, C., Sun, Y., Mitra, B. & Rosen, B. P. (1998). Pb(II)-translocating P-type ATPases. *J Biol Chem* **273**, 32614–32617.

Sambrook, J., Fritsch, E. F. & Maniatis, T. (1989). *Molecular Cloning: a Laboratory Manual*, 2nd edn. Cold Spring Harbor, NY: Cold Spring Harbor Laboratory.

Sein-Echaluce, V. C., González, A., Napolitano, M., Luque, I., Barja, F., Peleato, M. L. & Fillat, M. F. (2015). Zur (FurB) is a key factor in the control of the oxidative stress response in *Anabaena* sp *PCC 7120*. *Environ Microbiol* **17**, 2006–2017.

Shin, J. H., Oh, S. Y., Kim, S. J. & Roe, J. H. (2007). The zinc-responsive regulator Zur controls a zinc uptake system and some ribosomal proteins in *Streptomyces coelicolor* A3(2). *J Bacteriol* **189**, 4070–4077.

Singh, V. K., Xiong, A., Usgaard, T. R., Chakrabarti, S., Deora, R., Misra, T. K. & Jayaswal, R. K. (1999). ZntR is an autoregulatory protein and negatively regulates the chromosomal zinc resistance operon *znt* of *Staphylococcus aureus*. *Mol Microbiol* **33**, 200–207.

Smith, R. L. & Maguire, M. E. (1998). Microbial magnesium transport: unusual transporters searching for identity. *Mol Microbiol* **28**, 217–226.

Smith, K. F., Bibb, L. A., Schmitt, M. P. & Oram, D. M. (2009). Regulation and activity of a zinc uptake regulator, Zur, in *Corynebacterium diphtheriae*. *J Bacteriol* **191**, 1595–1603.

Smith, A. T., Smith, K. P. & Rosenzweig, A. C. (2014). Diversity of the metal-transporting P1B-type ATPases. *J Biol Inorg Chem* **19**, 947–960.

Snavely, M. D., Florer, J. B., Miller, C. G. & Maguire, M. E. (1989). Magnesium transport in *Salmonella typhimurium*: $28Mg^{2+}$ transport by the CorA, MgtA, and MgtB systems. *J Bacteriol* **171**, 4761–4766.

Stoyanov, J. V., Hobman, J. L. & Brown, N. L. (2001). CueR (YbbI) of *Escherichia coli* is a MerR family regulator controlling expression of the copper exporter CopA. *Mol Microbiol* **39**, 502–512.

Wan, Q., Ahmad, M. F., Fairman, J., Gorzelle, B., de la Fuente, M., Dealwis, C. & Maguire, M. E. (2011). X-ray crystallography and isothermal titration calorimetry studies of the *Salmonella* zinc transporter ZntB. *Structure* **19**, 700–710.

Wojtaszek, P. (1997). Oxidative burst: an early plant response to pathogen infection. *Biochem J* **322**, 681–692.

Wood, D. W., Setubal, J. C., Kaul, R., Monks, D. E., Kitajima, J. P., Okura, V. K., Zhou, Y., Chen, L., Wood, G. E. & other authors (2001). The genome of the natural genetic engineer *Agrobacterium tumefaciens* C58. *Science* **294**, 2317–2323.

Worlock, A. J. & Smith, R. L. (2002). ZntB is a novel Zn^{2+} transporter in *Salmonella enterica* serovar Typhimurium. *J Bacteriol* **184**, 4369– 4373.

Xiong, A. & Jayaswal, R. K. (1998). Molecular characterization of a chromosomal determinant conferring resistance to zinc and cobalt ions in *Staphylococcus aureus*. *J Bacteriol* **180**, 4024–4029.

Yang, W., Liu, Y., Chen, L., Gao, T., Hu, B., Zhang, D. & Liu, F. (2007). Zinc uptake regulator (*zur*) gene involved in zinc homeostasis and virulence of *Xanthomonas oryzae* pv. *oryzae* in rice. *Curr Microbiol* **54**, 307–314.

Zhu, J., Oger, P. M., Schrammeijer, B., Hooykaas, P. J., Farrand, S. K. & Winans, S. C. (2000). The bases of crown gall tumorigenesis. *J Bacteriol* **182**, 3885–3895.

Edited by: G. Thomas

AMERICAN SOCIETY FOR MICROBIOLOGY | Applied and Environmental Microbiology

Agrobacterium tumefaciens Zur Regulates the High-Affinity Zinc Uptake System TroCBA and the Putative Metal Chaperone YciC, along with ZinT and ZnuABC, for Survival under Zinc-Limiting Conditions

Paweena Chaoprasid,[a] Thanittra Dokpikul,[b] Jaruwan Johnrod,[c] Sirin Sirirakphaisarn,[c] Sumontha Nookabkaew,[d] Rojana Sukchawalit,[a,c,e] Skorn Mongkolsuk[a,e,f]

Laboratory of Biotechnology, Chulabhorn Research Institute, Lak Si, Bangkok, Thailand[a]; Environmental Toxicology, Chulabhorn Graduate Institute, Lak Si, Bangkok, Thailand[b]; Applied Biological Sciences, Chulabhorn Graduate Institute, Lak Si, Bangkok, Thailand[c]; Laboratory of Pharmacology, Chulabhorn Research Institute, Lak Si, Bangkok, Thailand[d]; Center of Excellence on Environmental Health and Toxicology (EHT), Ministry of Education, Bangkok, Thailand[e]; Department of Biotechnology, Faculty of Science, Mahidol University, Bangkok, Thailand[f]

ABSTRACT

***Agrobacterium tumefaciens* has a cluster of genes (Atu3178, Atu3179, and Atu3180) encoding an ABC-type transporter, here named *troA*, *troB*, and *troC*, respectively, which is shown here to be a zinc-specific uptake system. Reverse transcription (RT)-PCR analysis confirmed that *troA*, *troB*, and *troC* are cotranscribed, with *troC* as the first gene of the operon. The *yciC* (Atu3181) gene is transcribed in the opposite orientation to that of the *troCBA* operon and belongs to a metal-binding GTPase family. Expression of *troCBA* and *yciC* was inducible under zinc-limiting conditions and was controlled by the zinc uptake regulator, Zur. Compared to the wild type, the mutant strain lacking *troC* was hypersensitive to a metal chelator, EDTA, and the phenotype could be rescued by the addition of zinc, while the strain with a single *yciC* mutation showed no phenotype. However, *yciC* was important for survival under zinc limitation when either *troC* or *zinT* was inactivated. The periplasmic zinc-binding protein, ZinT, could not function when TroC was inactivated, suggesting that ZinT may interact with TroCBA in zinc uptake. Unlike many other bacteria, the ABC-type transporter ZnuABC was not the major zinc uptake system in *A. tumefaciens*. However, the important role of *A. tumefaciens* ZnuABC was revealed when TroCBA was impaired. The strain containing double mutations in the *znuA* and *troC* genes exhibited a growth defect in minimal medium. *A. tumefaciens* requires cooperation of zinc uptake systems and zinc chaperones, including TroCBA, ZnuABC, ZinT, and YciC, for survival under a wide range of zinc-limiting conditions.**

IMPORTANCE

Both host and pathogen battle over access to essential metals, including zinc. In low-zinc environments, physiological responses that make it possible to acquire enough zinc are important for bacterial survival and could determine the outcome of host-pathogen interactions. *A. tumefaciens* was found to operate a novel pathway for zinc uptake in which ZinT functions in concert with the high-affinity zinc importer TroCBA.

Zinc is an essential metal for bacteria because it is required for the functions of many enzymes and proteins (1, 2). However, zinc overload is toxic to cells (3–7). Bacteria have mechanisms to maintain zinc homeostasis via the coordinated response of genes involved in zinc uptake, efflux, and storage (8–13). The zinc uptake regulator Zur is a transcriptional regulator belonging to the Fur family and functions as a repressor of zinc uptake genes, including *znuABC* and *zinT* (10). To prevent excessive amounts of zinc in cells under high-zinc conditions, Zur uses Zn^{2+} as its cofactor to bind to a conserved AT-rich sequence, called the Zur box (14), found in the promoter region of the zinc uptake genes, leading to inhibition of gene expression (15–17). ZnuA is a periplasmic protein that binds zinc and transfers it to the membrane permease ZnuB and the ATPase ZnuC (15). The ZinT protein is a periplasmic zinc-binding protein (18–21) that has been shown to directly interact with and assist ZnuABC in transporting zinc in *Salmonella enterica* (22, 23).

Agrobacterium tumefaciens is an alphaproteobacterium that causes crown gall tumor in plants (24). Negative regulation of zinc uptake genes, such as *znuABC* and *zinT*, by *A. tumefaciens* Zur (Zur_{At}) has been reported previously (25). Expression of *A. tumefaciens znuABC* and *zinT* was inducible with zinc depletion and was repressed in response to increased zinc concentrations (25). Loss of Zur_{At} led to derepression of the *znuABC* and *zinT* genes and increased accumulation of intracellular zinc content (25). The roles of the periplasmic zinc-binding proteins *A. tumefaciens* ZnuA and ZinT ($ZnuA_{At}$ and $ZinT_{At}$, respectively) have been in-

Received 28 January 2016 **Accepted** 25 March 2016

Accepted manuscript posted online 8 April 2016

Citation Chaoprasid P, Dokpikul T, Johnrod J, Sirirakphaisarn S, Nookabkaew S, Sukchawalit R, Mongkolsuk S. 2016. *Agrobacterium tumefaciens* Zur regulates the high-affinity zinc uptake system TroCBA and the putative metal chaperone YciC, along with ZinT and ZnuABC, for survival under zinc-limiting conditions. Appl Environ Microbiol 82:3503–3514. doi:10.1128/AEM.00299-16.

Editor: A. M. Spormann, Stanford University

Address correspondence to Rojana Sukchawalit, rojana@cri.or.th.

P.C. and T.D. contributed equally to this article.

Supplemental material for this article may be found at http://dx.doi.org/10.1128/AEM.00299-16.

vestigated. It was found that $ZinT_{At}$ played an important role in *A. tumefaciens* survival under severe zinc shortage, whereas $ZnuA_{At}$ did not show an apparent role under the tested conditions (25). Disruption of both $znuA_{At}$ and $zinT_{At}$ slightly affected the total cellular zinc content (25), implying the existence of other, unidentified zinc uptake genes in *A. tumefaciens*.

The *A. tumefaciens* C58 genome contains a cluster of genes consisting of Atu3178, Atu3179, and Atu3180 that are annotated as a putative zinc/manganese ABC transport system (http://www.genome.jp/kegg-bin/show_organism?org=atu). Atu3178 encodes a periplasmic substrate-binding protein belonging to the TroA (transport-related operon) superfamily. Atu3179 encodes a permease, and Atu3180 encodes an ATP-binding protein. Here, we have named these genes *troA*, *troB*, and *troC* (the first gene of the operon), respectively. Atu3181 is a gene that has a transcription orientation opposite to that of the *troCBA* operon and encodes a putative metal chaperone, YciC, belonging to the COG0523 family of GTPases (26). In *Bacillus subtilis*, YciC was proposed to be a zinc chaperone that participates in an unidentified low-affinity zinc transport pathway (27, 28). *B. subtilis yciC* is regulated by Zur (28). The *A. tumefaciens troCBA* operon and *yciC* were predicted to be controlled by Zur due to the presence of a Zur box in their promoter regions (26). However, their physiological functions and metal regulation have not been experimentally verified.

The role of TroABCD in zinc transport was first reported in *Treponema pallidum* (29, 30). TroA is a substrate-binding protein, and TroB is an ATPase, while TroC and TroD form a heterodimeric cytoplasmic membrane permease. *T. pallidum* has the ZnuABC and TroABCD systems for zinc uptake (30). While the *T. pallidum* ZnuABC transporter is specific to zinc, *T. pallidum* TroABCD can transport zinc, manganese, and iron (29, 30). *T. pallidum troABCD* was shown to be negatively regulated by a zinc-responsive transcriptional regulator, TroR, a DtxR-like repressor (29). However, a later study showed that *T. pallidum* TroR is a manganese-dependent rather than a zinc-dependent regulator (31). Unlike many other bacteria, *T. pallidum* does not contain Zur, and the regulator of *T. pallidum znuABC* has not been reported.

Both ZnuA and TroA are substrate-binding proteins that belong to the cluster A-1 family (32). While ZnuA has been shown to respond specifically to zinc, the metal selectivity of TroA proteins and regulation of *tro* operons are different among bacteria (29, 33–36). *Streptococcus suis* TroA is involved in the uptake of manganese, not zinc (36), even though it can bind both Mn^{2+} and Zn^{2+} with high affinity (35). A gene encoding a protein that has high similarity to the manganese-responsive transcriptional regulator ScaR, located directly downstream of the *S. suis troA* gene, may be involved in the manganese regulation of the *troA* gene (36). *Treponema denticola troABCD* is negatively regulated by Mn^{2+} and Fe^{2+} via TroR (33). In contrast, *Corynebacterium diphtheriae troA* is under the control of Zur in a zinc-dependent manner (34).

Here, the physiological functions of the *A. tumefaciens troCBA* operon and *yciC* are characterized. The metal regulation of *A. tumefaciens troCBA* and *yciC* was investigated, and their regulator was identified. Important roles for *A. tumefaciens* TroCBA and YciC in zinc acquisition under zinc-limiting conditions were demonstrated. *A. tumefaciens* ZinT may interact with the TroCBA system. In addition, a role for *A. tumefaciens* ZnuA under zinc starvation conditions was revealed when the TroCBA system was disrupted. Our findings provide a step toward understanding how *A. tumefaciens* controls zinc homeostasis.

MATERIALS AND METHODS

Bacterial strains and growth conditions. The bacterial strains and plasmids used in this study are shown in Table 1. The growth conditions, media, and antibiotic concentrations that were used for *A. tumefaciens* and *E. coli* were reported previously (25, 44).

Molecular techniques. General molecular techniques were performed according to standard protocols (46). The nucleotide sequence of the cloned DNA fragment was confirmed by DNA sequencing (Macrogen). Plasmids were transferred into *A. tumefaciens* by electroporation (47). All the *A. tumefaciens* mutant strains were confirmed by Southern blotting.

Construction of the *A. tumefaciens troC* mutant and *yciC* mutant strains. The *A. tumefaciens troC* and *yciC* mutant strains were constructed using a single homologous-recombination method as described previously (48). The internal coding regions of *troC* (BT3751 [5′-TGAAACC GCTCGGCGGTGAG-3′] and BT3752 [5′-CTGCGCATCCTGCAACAT GG-3′]; 293 bp) and *yciC* (BT5027 [5′-GTGATGGCGACAACCGCACC-3′] and BT5028 [5′-GCCCTGGCGAAATCGAAGCG-3′]; 223 bp) were amplified by PCR using the specific primers indicated. The PCR products were cloned into the unique SmaI sites of pKNOCK-Gm and pKNOCK-Km, respectively (40). The resulting plasmids, pKNOCKTROC and pKNOCKmYCIC, were electroporated into wild-type (WT) NTL4 (a Ti plasmid-cured derivative of strain C58 with an internal deletion of the *tetA-tetR* locus) (37). The *troC* mutant (TC142) and *yciC* mutant (YC154) were selected on Luria-Bertani (LB) agar plates containing 60 μg/ml gentamicin (Gm) and 30 μg/ml kanamycin (Km), respectively.

Construction of the double-mutant (TCYC15, ZAYC15, ZTYC15, and ZURYC15) strains. The plasmid pKNOCKmZNUA (25) was electroporated into the TC142 strain, generating the TCZA15 strain (with disruptions of both the *troC* and *znuA* genes), which was selected on LB agar (LA) plates containing 60 μg/ml Gm and 30 μg/ml Km. The plasmid pKNOCKmZINT was constructed by PCR amplification of the internal coding region of *zinT* (238 bp) using primers BT3747 (5′-TGACGGA CTGGGAAGGCGAC-3′) and BT3748 (5′-ATCTCCTGGCCGTCGCT GAC-3′), which was then cloned into SmaI-digested pKNOCK-Km (40). The plasmid pKNOCKmZINT was electroporated into the TC142 strain, generating the TCZT14 strain (*troC* and *zinT* mutations). The plasmid pKNOCKmYCIC was electroporated into TC142, PS132 (25), PC135 (25), and SPP12 (25) to generate the double-mutant strains TCYC15 (*troC* and *yciC* mutations), ZAYC15 (*znuA* and *yciC* mutations), ZTYC15 (*zinT* and *yciC* mutations), and ZURYC15 (*zur* and *yciC* mutations), respectively.

Construction of plasmids expressing functional *troC*, *troCBA*, and *yciC* for complementation. DNA fragments of full-length *troC* (BT3809 [5′-ATGAACGATCCGTGCCTCAC-3′] and BT3810 [5′-AAATCAGCC ATGGGCATTCG-3′]; 837 bp), *troCBA* (BT3809 and BT4627 [5′-GAAA CTGTGCGTTTTACTGG-3′]; 2,747 bp), and *yciC* (BT5033 [5′-ATGAA AAAACTCCCTGTCAC-3′] and BT5034 [5′-AATCAGGCCGCCTGTC TATC-3′]; 1,205 bp) were amplified by PCR using *Pfu* DNA polymerase (Fermentas) and the specific primers. The PCR products were cloned into SmaI-digested pBBR1MCS-4 (41), generating pTROC, pTROCBA, and pYCIC, respectively.

RT-PCR. Total RNA was extracted from cells grown in LB at 28°C for 4 h and then treated with 1 mM EDTA for 15 min using a modified hot-phenol method (49). Reverse transcription (RT)-PCR was performed as previously described (49). Primer sets were used for amplifying the junction of *troC-troB* (BT4265 [5′-AGGCGCGTCATTTCCACGAG-3′] and BT4266 [5′-TGAGGCTCATGCGCCGCAAC-3′]; 280 bp) and *troB-troA* (BT4267 [5′-GCATGGTCTCCTGCTTTGCC-3′] and BT4268 [5′-CGATGATCGAGAAGCTGGCC-3′]; 310 bp). The PCR products were visualized using gel electrophoresis on a 1.8% agarose gel with ethidium bromide staining.

TABLE 1 Strains and plasmids used in this study

Strain or plasmid	Relevant characteristics[a]	Reference or source
Agrobacterium tumefaciens		
NTL4	WT strain: a Ti plasmid-cured derivative of strain C58	37
PC135	*zinT*::pKNOCK-Gm (*zinT*::Gm); Gm^r	25
PS132	*znuA*::pKNOCK-Gm (*znuA*::Gm); Gm^r	25
SPP12	*zur*::pKNOCK-Gm (*zur*::Gm); Gm^r	25
TC142	*troC*::pKNOCK-Gm (*troC*::Gm); Gm^r	This study
TCZA15	*troC*::pKNOCK-Gm and *znuA*::pKNOCK-Km (*troC*::Gm *znuA*::Km); Gm^r and Km^r	This study
TCZT14	*troC*::pKNOCK-Gm and *zinT*::pKNOCK-Km (*troC*::Gm *zinT*::Km); Gm^r Km^r	This study
TCYC15	*troC*::pKNOCK-Gm and *yciC*::pKNOCK-Km (*troC*::Gm *yciC*::Km); Gm^r Km^r	This study
YC154	*yciC*::pKNOCK-Km (*yciC*::Km); Km^r	This study
ZAYC15	*znuA*::pKNOCK-Gm and *yciC*::pKNOCK-Km (*znuA*::Gm *yciC*::Km); Gm^r Km^r	This study
ZTYC15	*zinT*::pKNOCK-Gm and *yciC*::pKNOCK-Km (*zinT*::Gm *yciC*::Km); Gm^r Km^r	This study
ZURYC15	*zur*::pKNOCK-Gm and *yciC*::pKNOCK-Km (*zur*::Gm *yciC*::Km); Gm^r Km^r	This study
Escherichia coli		
DH5α	Host for general DNA cloning	38
BW20767	Host for plasmid pKNOCK-Gm and pKNOCK-Km	39
Plasmids for gene inactivation		
pKNOCK-Gm	Suicide vector; Gm^r	40
pKNOCK-Km	Suicide vector; Km^r	40
pKNOCKTROC	Internal coding region of *troC* cloned into pKNOCK-Gm; Gm^r	This study
pKNOCKmYCIC	Internal coding region of *yciC* cloned into pKNOCK-Km; Km^r	This study
pKNOCKmZINT	Internal coding region of *zinT* cloned into pKNOCK-Km; Km^r	This study
pKNOCKmZNUA	Internal coding region of *znuA* cloned into pKNOCK-Km; Km^r	25
Plasmids for complementation		
pBBR1MCS-4	Expression vector; Ap^r (pBBR)	41
pTROC	Full-length *troB* cloned into pBBR1MCS-4; Ap^r	This study
pTROCBA	Full-length *troCBA* operon cloned into pBBR1MCS-4; Ap^r	This study
pYCIC	Full-length *yciC* cloned into pBBR1MCS-4; Ap^r	This study
pZINT	Full-length *zinT* cloned into pBBR1MCS-4; Ap^r	25
pZNUA	Full-length *znuA* cloned into pBBR1MCS-4; Ap^r	25
pZUR	Full-length *zur* cloned into pBBR1MCS-4; Ap^r	25
Promoter-*lacZ* transcriptional fusions		
pUFR027lacZ	Promoter probe vector; Tc^r	42
p027troC-lacZ	266-bp DNA fragment containing *troC* promoter fused to *lacZ* of pUFR027lacZ	This study
p027yciC-lacZ	274-bp DNA fragment containing *yciC* promoter fused to *lacZ* of pUFR027lacZ	This study
YciC-LacZ and YciC-PhoA translational fusions		
pPR9TT	Reporter vector, LacZ as a reporter; Ap^r	43
pYCLacZ	YciC amino acid residues 1–400 fused to LacZ of pPR9TT; Ap^r	This study
p'PhoA	5′-truncated *phoA* gene lacking its signal peptide sequence cloned into pBBR; Ap^r	44
pYCPhoA	YciC amino acid residues 1–400 fused to PhoA of p′PhoA; Ap^r	This study
Plasmid for tumor assay		
pCMA1	pTiC58*traM*::*nptII*; Km^r	45

[a] Ap^r, ampicillin resistance; Gm^r, gentamicin resistance; Km^r, kanamycin resistance; Tc^r, tetracycline resistance.

qRT-PCR analysis. Quantitative real-time (qRT)-PCR was performed as previously described (50). Log-phase cells grown in LB were not treated or were treated with metal and a metal chelator for 15 min prior to harvest. The metals $CdCl_2$, $CoCl_2$, $CuSO_4$, $FeCl_3$, $MgCl_2$, $MnCl_2$, $NiCl_2$, and $ZnCl_2$ were used at a final concentration of 0.45 mM. The metal chelator used was EDTA (1 mM). Gene-specific primers for *troC* (BT3751 [5′-TGAAACCGCTCGGCGGTGAG-3′] and BT3752 [5′-CTGCGCATC CTGCAACATGG-3′]; 293 bp), *yciC* (BT5027 [5′-GTGATGGCGACAA CCGCACC-3′] and BT5028 [5′-GCCCTGGCGAAATCGAAGCG-3′]; 223 bp), and the 16S rRNA gene (BT1421 [5′-GAATCTACCCATCTCT GCGG-3′] and BT1422 [5′-AAGGCCTTCATCACTCACGC-3′]; 280 bp) were used.

The amount of a specific mRNA target was normalized to the amount of a housekeeping gene 16S rRNA. Fold changes in gene expression are relative to untreated samples from wild-type NTL4 using the $2^{-\Delta\Delta Ct}$ method (51). The data are reported as the means of biological triplicates and standard deviations (SD).

Determination of the transcriptional start site for *troC* and *yciC* using 5′ RACE. RNA samples were isolated from wild-type NTL4 log-phase cells grown in LB and treated with 1 mM EDTA for 15 min. 5′ Rapid

amplification cDNA ends (RACE) (Roche) was performed according to the manufacturer's instructions. The specific primers SP1 and SP2 for *troC* are BT3752 (5′-CTGCGCATCCTGCAACATGG-3′) and BT3758 (5′-TAGCGCCATCCAGATGATGC-3′), respectively. The specific primers SP1 and SP2 for *yciC* are BT5028 (5′-GCCCTGGCGAAATCGAAGCG-3′) and BT5042 (5′-CGAGGATGTGGTTGAGAAGG-3′), respectively.

Construction of promoter-*lacZ* transcriptional fusions. DNA fragments containing the promoter region of *troC* (BT3757 [5′-TATGTGCGACATGTCAACGG-3′] and BT3758 [5′-TAGCGCCATCCAGATGATGC-3′]; 269 bp) and *yciC* (BT5041 [5′-TTAGAGTGGCGCGCTGTTGG-3′] and BT5042 [5′-CGAGGATGTGGTTGAGAAGG-3′]; 274 bp) were amplified from *A. tumefaciens* NTL4 genomic DNA using PCR. The PCR products were cloned into a unique HindIII site (and end-gap filled with Klenow enzyme) of the promoter probe vector pUFR027lacZ, a derivative of pUFR027 (42), to generate the plasmids p027troC-lacZ and p027yciC-lacZ, respectively.

β-Galactosidase activity assay. β-Galactosidase (β-Gal) activity was measured as described by Miller (52). Log-phase cells grown in LB were not treated or were treated with 1 mM EDTA for 1 h. The cells were then harvested. Crude bacterial cell lysates were prepared as previously described (48). Protein concentrations were determined using the Bradford Bio-Rad protein assay. Specific activity was calculated in units per milligram of protein. Data are reported as the means of biological triplicates ± SD.

EDTA sensitivity test. Log-phase cells grown in LB were adjusted, serially diluted, and spotted onto plates containing AB medium (47) and AB plus EDTA (0.3, 0.6, 0.9, 1, 1.1, 1.2, 1.3, 1.4, and 1.5 mM) according to a protocol previously described (25). In some experiments, AB plates containing 1.2 mM EDTA were individually supplemented with 50 μM $ZnCl_2$, $CdCl_2$, $CoCl_2$, $CuSO_4$, $FeCl_3$, $MgCl_2$, $MnCl_2$, or $NiCl_2$. The plates were then incubated at 28°C for 48 h. Each strain was tested in duplicate, and the experiment was repeated at least twice.

Construction of *yciC-lacZ* and *yciC-phoA* translational fusions. Primers BT5041 (5′-TTAGAGTGGCGCGCTGTTGG-3′) and BT5309 (5′-GCCGCCTGTCTATCCCAGT-3′) were used to amplify the *yciC* promoter region and sequences encoding the entire 400 amino acids of YciC. The DNA fragments were cloned into the SmaI sites of the plasmid vectors pPR9TT (43) and p′PhoA (44) to generate plasmids pYCLacZ and pYCPhoA, respectively. The β-galactosidase and alkaline phosphatase activities were assayed as previously described (44), using wild-type NTL4 carrying plasmids pYCLacZ and pYCPhoA, which express the hybrid proteins YciC-LacZ and YciC-PhoA, respectively.

Measurement of total cellular zinc content. Zinc ions were measured in parts per billion using an inductively coupled plasma mass spectrometer (ICP-MS), as previously described (44). Samples were prepared from cells grown in LB plus 0.5 mM EDTA at 28°C for 24 h. The data are reported as the means of biological triplicates and SD.

Virulence assay. *A. tumefaciens* strains carrying plasmid pCMA1 were used to infect young *Nicotiana benthamiana* plants as previously described (25). Cells grown in LB plus 0.5 mM EDTA at 28°C for 24 h were washed and resuspended in induction broth (47), pH 5.5 (IB 5.5), plus 300 μM acetosyringone (AS). The cells were incubated at 28°C with shaking for 20 min, harvested, and adjusted to an optical density at 600 nm (OD_{600}) of 0.1 in IB 5.5 plus 300 μM AS. A 5-μl aliquot of the cell suspension was inoculated into a wounded *N. benthamiana* petiole. Each bacterial strain was used to infect 15 petioles. Tumor formation at 4 weeks after infection was assessed.

RESULTS

The *A. tumefaciens troCBA* operon and *yciC* are negatively regulated by Zur. *A. tumefaciens* genome sequence analysis (53) revealed that the gene arrangement in the *tro* operon starts with *troC* (Atu3180), followed by *troB* (Atu3179) and *troA* (Atu3178) (Fig. 1A), and these genes may be cotranscribed. RT-PCR analysis was performed, confirming that *troC*, *troB*, and *troA* are cotranscribed (see Fig. S1 in the supplemental material). The *A. tumefaciens troCBA* operon and *yciC* are divergently oriented. The translational start codons of *troC* and *yciC* are separated by 300 bp (Fig. 1B). The transcriptional start sites of *troC* (at the A residue) and of *yciC* (at the A residue) were determined by 5′ RACE, and the −10 and −35 sequences were predicted using BPROM (Softberry) (Fig. 1B). A Zur-binding site (5′-TTAATGTTATTTCATTAC-3′; underlined nucleotides are the center of symmetry for the inverted palindrome) was identified previously in the intergenic region between *A. tumefaciens troCBA* and *yciC* (26) and overlaps the predicted −35 site of *troC* (Fig. 1B). Furthermore, we identified another Zur-binding site (5′-GTAATGTTATTACGTTAC-3′) that overlaps the predicted −10 site of *yciC* (Fig. 1B). An alignment of *A. tumefaciens* Zur boxes found in the Zur-regulated genes is shown in Fig. 1C.

To assess the promoter activity of *troC* and *yciC*, the DNA fragments upstream of the translational start codon, predicted −10 and −35 sequences, and a potential Zur-binding site for the *troC* promoter or for the *yciC* promoter were fused to a promoterless *lacZ* reporter gene (transcriptional fusions) (plasmids p027troC-lacZ and p027yciC-lacZ, respectively) (Fig. 1D), and β-Gal activity was measured. In wild-type NTL4 (the WT), β-Gal activities from both *troC-lacZ* and *yciC-lacZ* fusions were increased when cells were treated with EDTA (WT/pBBR) (Fig. 1E). β-Gal in the *zur* mutant strain, SPP12, was constitutively expressed at high levels under all the tested conditions (*zur*::Gm/pBBR) (Fig. 1E); however, expression of the *zur* gene from a multicopy plasmid, pZUR, could suppress this phenotype (*zur*::Gm/pZUR) (Fig. 1E).

The *A. tumefaciens troCBA* operon and *yciC* are inducible with zinc depletion. Expression of the *troC* and *yciC* genes was determined using qRT-PCR. As expected for genes involved in metal acquisition, expression of the *troC* and *yciC* genes in the WT was inducible (~10^3-fold) by the metal chelator EDTA compared to untreated cells. Both genes were constitutively expressed at high levels in the *zur* mutant but were suppressed when complemented with pZUR (Fig. 2A). These results further supported the view that *A. tumefaciens* Zur negatively regulates *troCBA* and *yciC*. To investigate the metal-specific responses of *troC* and *yciC*, repression of the EDTA-induced expression by various metals was determined. In the wild type, Zn^{2+} was the most potent metal ion that could repress the EDTA-induced expression of *troC* and *yciC* (Fig. 2B) compared to other metals, including cadmium, cobalt, copper, iron, magnesium, manganese, and nickel. These results demonstrated that the *A. tumefaciens troCBA* operon and *yciC* are inducible, specifically by zinc depletion, which supports the view that *A. tumefaciens* TroCBA and YciC are involved in zinc acquisition.

The *troC* mutant is hypersensitive to EDTA treatment, and inactivation of *yciC* further increases the sensitivity; however, the TroCBA transporter can function independently of YciC. *A. tumefaciens* mutant strains were constructed to assess the physiological functions of *troC* (TC142) and *yciC* (YC154). Growth was determined under metal limitation in the presence of EDTA (1, 1.1, 1.2, 1.3, 1.4, and 1.5 mM [see Fig. S2 in the supplemental material]). Inactivation of *troC*, but not *yciC*, caused cells to become hypersensitive to EDTA. Consistent with a previous report (25), the *znuA* mutant (PS132) showed no phenotype, while the *zinT* mutant (PC135) was hypersensitive to EDTA (Fig. 3A). Similar to the *zinT* mutant, the *troC* mutant was ~10^2-fold more

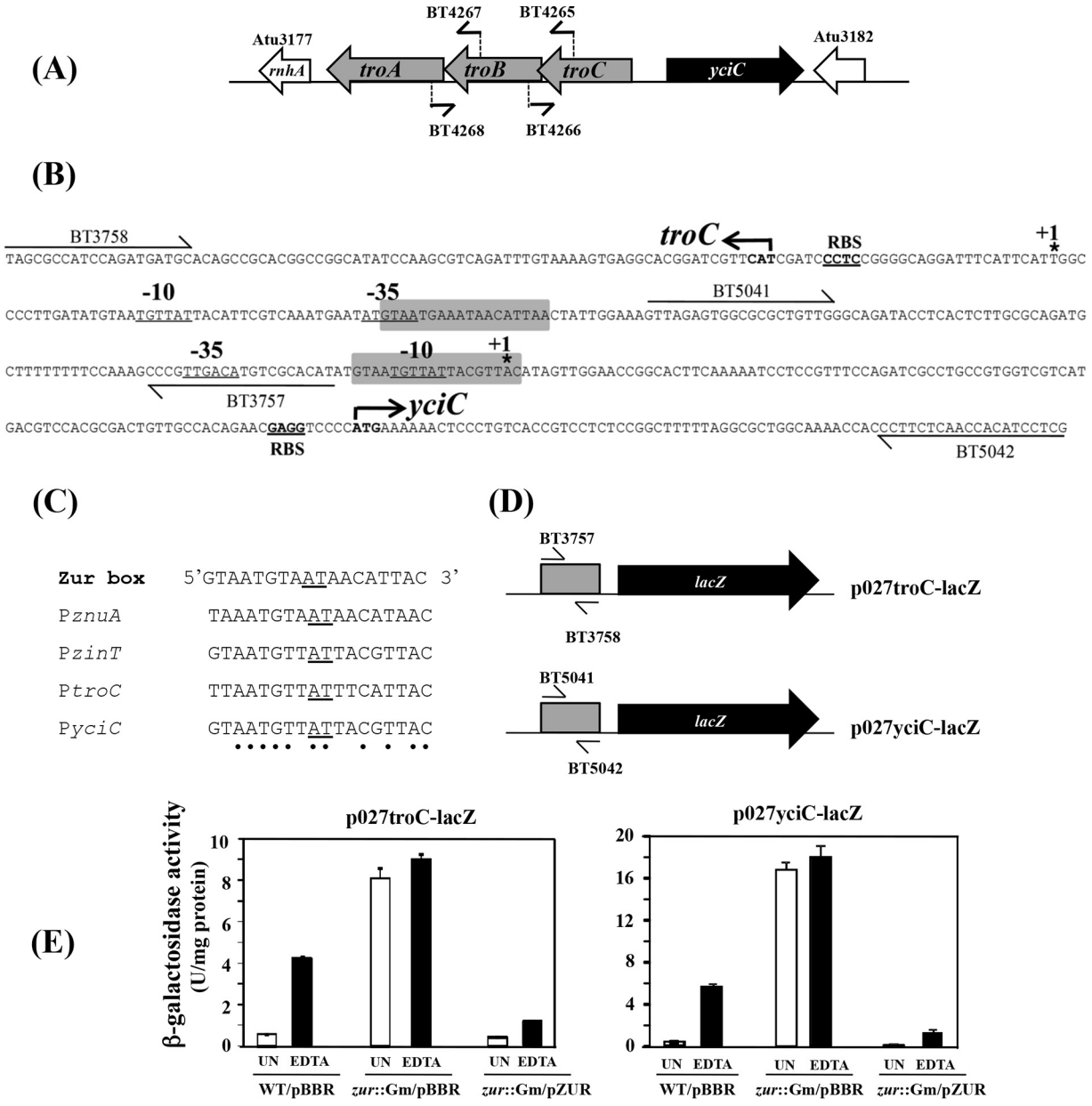

FIG 1 (A) Genomic context of the *A. tumefaciens troCBA* operon and *yciC*. The *rnhA* (Atu3177) gene encoding RNase H is located downstream of the *troCBA* operon. The Atu3182 gene encoding a hypothetical protein with unknown function is located downstream of the *yciC* gene. The primer sets used to amplify the junctions between *troC* and *troB* (BT4265 and BT4266) and between *troB* and *troA* (BT4267 and BT4268) with RT-PCR analysis are indicated. (B) *troC* and *yciC* promoters. The ATG start codons for *troC* and *yciC* are shown in boldface with bent arrows. The transcriptional +1 start site of *troC* and *yciC* was determined using 5′ RACE and is indicated by asterisks. The predicted −10 and −35 sequences are underlined. The Zur-binding sites are shaded. The putative ribosome-binding sites (RBS) are underlined. (C) Conserved Zur-binding site (Zur box) for *A. tumefaciens* (14). The sequences of Zur boxes found in the promoter regions of *A. tumefaciens znuA*, *zinT*, *troC*, and *yciC* (P*znuA*, P*zinT*, P*troC*, and P*yciC*, respectively) are shown. The conserved residues in all the Zur boxes are marked with dots. (D) Schematic representation of the promoter-*lacZ* fusions (not drawn to scale) from plasmids p027troC-lacZ and p027yciC-lacZ. (E) β-Galactosidase activity assay. Wild-type NTL4 (WT/pBBR), the *zur* mutant strain SPP12 (*zur*::Gm/pBBR), and the complemented strain (*zur*::Gm/pZUR) contain either p027troC-lacZ or p027yciC-lacZ. pBBR is a plasmid vector, while pZur contains a functional *zur* gene. Cells were grown in LB for 4 h and then were left untreated (UN) or treated with 1 mM EDTA for 1 h. The results are the means and SD of triplicate samples.

sensitive to 1.2 mM EDTA than the WT (Fig. 3A) and could be fully rescued by the addition of 50 μM $ZnCl_2$ (Fig. 3A, 1.2 mM EDTA plus Zn) but not by other metals (see Fig. S3A in the supplemental material).

The EDTA-sensitive phenotype of the *troC* mutant (TC142) could not be reversed by the plasmid pTROC (see Fig. S3B in the supplemental material), suggesting that the *troC* gene knockout by insertional inactivation used to generate the TC142 strain may have a polar effect on other downstream genes in the *troCBA* operon. This notion was supported by the observation that the plasmid pTROCBA could fully restore the growth of the *troC* mutant (Fig. 3B; see Fig. S3B in the supplemental material).

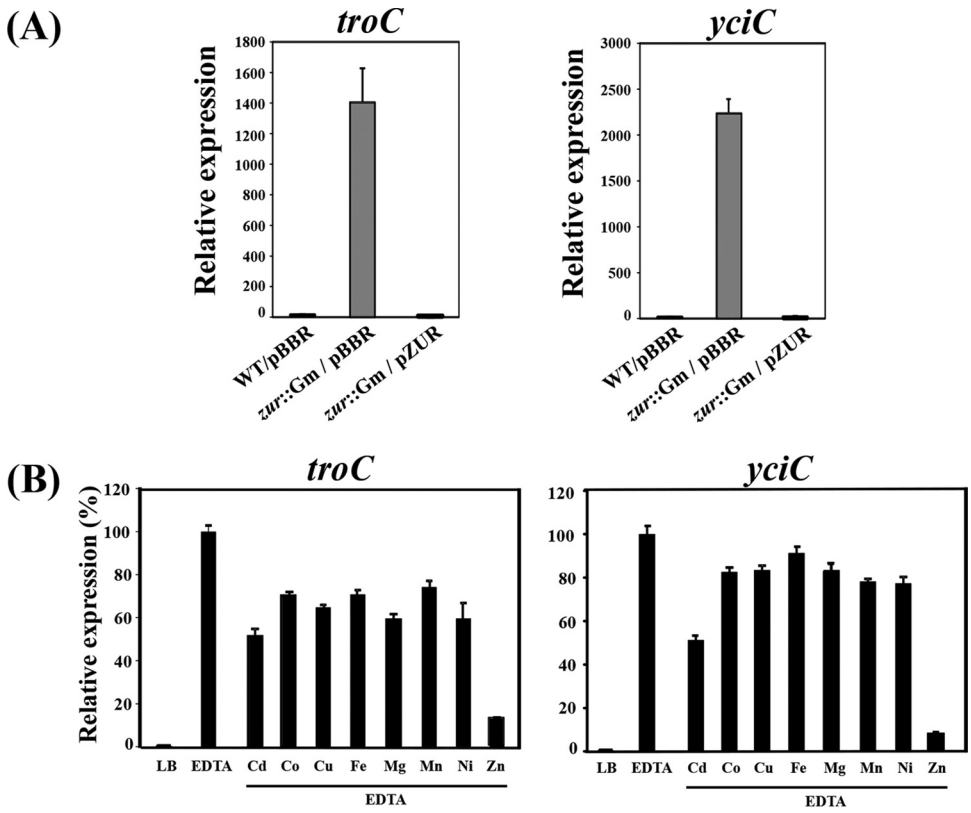

FIG 2 (A) Expression analysis of *troC* and *yciC* using qRT-PCR. (A) RNA samples were isolated from log-phase cells of the wild type (WT/pBBR), the *zur* mutant (*zur*::Gm/pBBR), and the complemented strain (*zur*::Gm/pZUR) grown in LB medium. pBBR is the plasmid vector. pZUR is the plasmid containing a functional *zur* gene. The expression of the target genes was normalized to that of 16S rRNA, and the fold changes in gene expression in *zur*::Gm/pBBR and *zur*::Gm/pZUR are relative to those in WT/pBBR (regarded as 1). The experiment was performed in biological triplicate, and the error bars indicate the standard deviations. (B) Induction of *troC* and *yciC* is specific to zinc limitation. Shown is qRT-PCR analysis of *troC* and *yciC* expression. Wild-type NTL4 cells were grown in LB medium and under metal-limiting conditions (LB plus 1 mM EDTA). Metals ($CdCl_2$, $CoCl_2$, $CuSO_4$, $FeCl_3$, $MnCl_2$, $NiCl_2$, and $ZnCl_2$) were supplemented at a final concentration of 0.45 mM. The expression levels are presented as percentages and are relative to those in cells grown in LB plus 1 mM EDTA (100%).

Although the *yciC* mutant strain showed no phenotype (Fig. 3A; see Fig. S2 and S4 in the supplemental material), the inactivation of *yciC* further increased the sensitivity of the *troC* mutant to EDTA (Fig. 3B). Growth of the *troC* mutant strain TC142 (*troC*::Gm/pBBR) on the AB plate containing 0.6 mM EDTA was similar to that of the WT (WT/pBBR), while the TCYC15 strain lacking both *troC* and *yciC* (*troC*::Gm *yciC*::Km/pBBR) was ~10^3-fold more sensitive to 0.6 mM EDTA than the WT (Fig. 3B). Expressing the functional *yciC* gene from the plasmid pYCIC could restore the growth defect of TCYC15 (*troC* and *yciC* mutations) to levels similar to that of TC142 (*troC* mutation) and the WT at 0.6 mM EDTA, but not at higher levels of EDTA (0.9 and 1.2 mM) (*troC*::Gm *yciC*::Km/pYCIC) (Fig. 3B). In contrast, at 0.6, 0.9, and 1.2 mM EDTA, the EDTA-hypersensitive phenotype of TCYC15 could be fully reversed to WT by complementation with pTROCBA (*troC*::Gm *yciC*::Km/pTROCBA) (Fig. 3B), demonstrating that *A. tumefaciens* requires the TroCBA transporter to survive under severe metal-limiting conditions and that TroCBA can function even in the absence of YciC.

The important role of ZnuA is revealed when TroCBA is disrupted. Inactivation of either *znuA* or *znuAB* had no detectable effect on the growth of *A. tumefaciens* on the AB plate containing 1.4 mM EDTA compared to the WT (see Fig. S2 in the supplemental material) (25). However, disruption of *znuA* in combination with *troC* (TCZA15) led to a growth defect of *A. tumefaciens* in a minimal AB medium and hypersensitivity to EDTA (*troC*::Gm *znuA*::Km) (Fig. 4). The growth defect of TCZA15 could be rescued by zinc supplementation (1.2 mM EDTA plus Zn) (Fig. 4). Furthermore, the EDTA sensitivity of TCZA15 (*troC* and *znuA* mutations) could be reversed to that of TC142 (*troC* mutation) by complementation with the plasmid pZNUA (*troC*::Gm *znuA*::Km/pZNUA) (Fig. 5A), but not by the plasmid pZINT or pTROA. Although TCZA15 showed a growth defect on the AB plate (a minimal medium), it could grow on the LA plate (a rich medium) similarly to the WT (*troC*::Gm *znuA*::Km/pBBR) (Fig. 5A). These results demonstrated the role of *A. tumefaciens* ZnuA (a periplasmic zinc-binding protein) in zinc acquisition under zinc limitation and that *A. tumefaciens* ZnuA function could not be substituted for by other periplasmic zinc-binding proteins, such as ZinT and TroA.

ZinT may interact with TroCBA. It has been reported previously that *A. tumefaciens* ZinT functions independently of ZnuABC (25). The inactivation of *zinT* caused a reduction in the total zinc content and hypersensitivity to EDTA (25). To test the possibility of interaction between *A. tumefaciens* ZinT (a periplasmic protein) and TroCBA in zinc transport, a strain (TCZT14) containing mutations in *troC* and *zinT* was generated, and its sensitivity to EDTA was determined. The TC142 (*troC* mutation) and

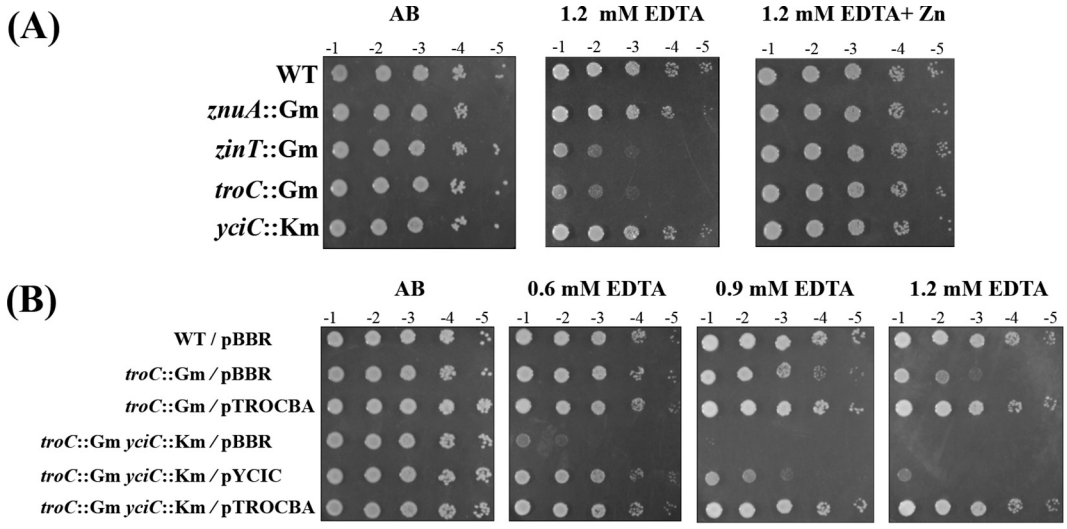

FIG 3 Effects of a single mutation (A) and double mutations (B) in the *troC* and *yciC* genes on the sensitivity of *A. tumefaciens* to EDTA. (A) The strains are wild-type NTL4 (WT), PS132 (*znuA*::Gm), PC135 (*zinT*::Gm), TC142 (*troC*::Gm), and YC154 (*yciC*::Km). (B) The WT, TC142 (*troC*::Gm), and TCYC15 (*troC*::Gm *yciC*::Km) strains carry the plasmid vector (pBBR). The mutant strains were complemented with functional *troCBA* or *yciC* from the multicopy plasmids pTROCBA and pYciC, respectively. Cells were adjusted, serially diluted, and spotted onto plates containing AB and AB plus EDTA (0.6, 0.9, and 1.2 mM) with or without 50 μM $ZnCl_2$. Tenfold serial dilutions are indicated. The plates were incubated at 28°C for 48 h.

TCZT14 (*troC* and *zinT* mutations) strains were ~10^2-fold and ~10^3-fold, respectively, more sensitive to 1.2 mM EDTA than the WT (Fig. 4). Moreover, the EDTA-hypersensitive phenotype of TCZT14 (*troC* and *zinT* mutations) could not be reversed to that of TC142 (*troC* mutation) by complementation with the plasmid pZINT (Fig. 5B), but the EDTA-hypersensitive phenotype of PC135 (*zinT* mutation) could be fully restored by pZINT (Fig. 5B). The results suggested that TroCBA is required for the function of *A. tumefaciens* ZinT.

Loss of the zinc chaperones ZinT and YciC causes a severe EDTA-mediated growth defect. Double mutations in *zinT* and *yciC* (ZTYC15) led to hypersensitivity to EDTA, and this EDTA-dependent growth defect could be detected at 0.3 mM EDTA (~10^3-fold more sensitive than the wild type) (Fig. 4). At 0.3 and 0.6 mM EDTA, the growth defect of ZTYC15 could be fully restored to PC135 (*zinT* mutation) by complementation with the plasmid pZINT or pYCIC (Fig. 5C). At 1.2 mM EDTA, complementation with either pZINT or pYCIC did not rescue ZTYC15 (Fig. 5C), but addition of zinc did (1.2 mM EDTA plus Zn) (Fig. 4). These results demonstrated that *A. tumefaciens* requires both zinc chaperones, ZinT and YciC, to cope with severe zinc-limiting conditions.

$YciC_{At}$ is a cytoplasmic protein. *B. subtilis* YciC ($YciC_{Bs}$) is a membrane protein (27). Unlike $YciC_{Bs}$, *A. tumefaciens* YciC ($YciC_{At}$) is likely to reside in the cytoplasm. The hydropathy of $YciC_{At}$ was determined using the Kyte-Doolittle hydropathy plot (54). The hydropathy plot and other programs, including HMMTOP (55) and Phobius (56), predicted that there would be no transmembrane segment in the $YciC_{At}$ protein. To determine the localization of $YciC_{At}$, the entire 400 amino acids of $YciC_{At}$ was fused to PhoA (alkaline phosphatase) and LacZ (β-galactosidase) to generate $YciC_{At}$-PhoA and $YciC_{At}$-LacZ fusions using a previously described protocol (44). The alkaline phosphatase and β-galactosidase activities of the hybrid proteins could be used as indicators for the periplasmic and cytoplasmic locations, respectively, of the target protein fusion sites (57, 58). The $YciC_{At}$-PhoA fusion displayed low levels of alkaline phosphatase activity (~0.22 U), while the $YciC_{At}$-LacZ fusion exhibited high levels of β-galactosidase activity (~240 U) compared to the negative-control vectors, p′PhoA (~0.04 U) and pPR9TT (~8 U), which showed low ac-

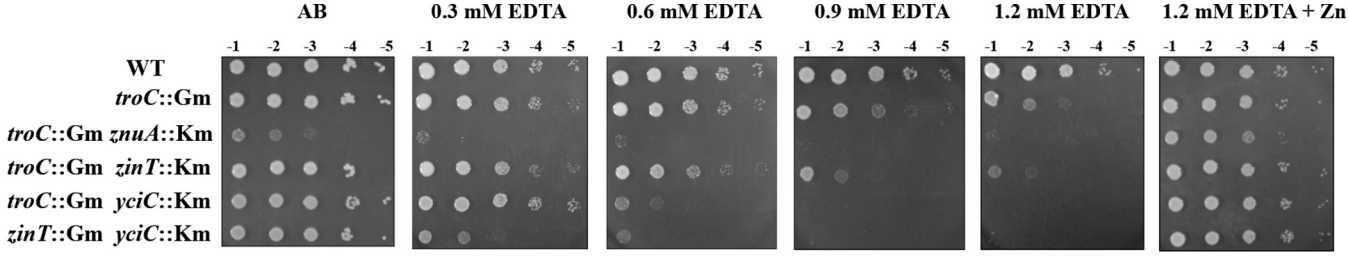

FIG 4 EDTA-sensitive phenotypes of strains containing double mutations of genes encoding zinc uptake proteins and zinc chaperones. The EDTA sensitivities of TCZA15 (*troC*::Gm *znuA*::Km), TCZT14 (*troC*::Gm *zinT*::Km), TCYC15 (*troC*::Gm *yciC*::Km), and ZTYC15 (*zinT*::Gm *yciC*::Km) were compared to that of wild-type NTL4 (WT) and TC142 (*troC*::Gm). Sensitivity to EDTA on plates containing AB and AB plus EDTA (0.3, 0.6, 0.9, and 1.2 mM) with or without 50 μM $ZnCl_2$ was assessed as described for Fig. 3.

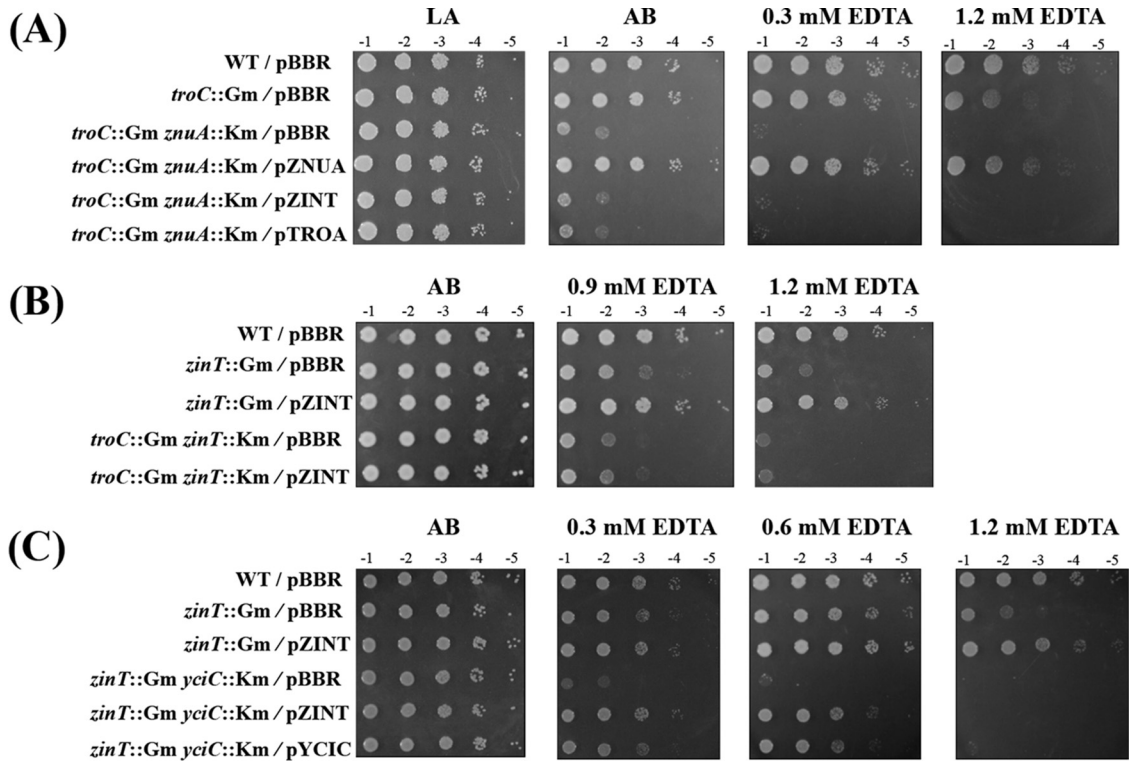

FIG 5 (A) ZnuA under metal limitation conditions could not be replaced by the periplasmic zinc-binding proteins ZinT and TroA. The TCZA15 (*troC*::Gm *znuA*::Km) strain was complemented with functional *znuA*, *zinT*, or *troA* from the plasmids pZNUA, pZINT, and pTROA, respectively. The cells were tested on plates containing LA (rich medium) and AB (minimal medium). Sensitivity to EDTA on AB plates containing EDTA (0.3, 0.6, 0.9, and 1.2 mM) was assessed as described for Fig. 3. (B) ZinT could not function when TroCBA was inactivated. The PC135 (*zinT*::Gm) and TCZT14 (*troC*::Gm *zinT*::Km) strains were complemented with functional *zinT* from the plasmid pZINT. (C) Important role of zinc chaperones ZinT and YciC. The ZTYC15 (*zinT*::Gm *yciC*::Km) strain was complemented with functional *zinT* or *yciC* from the plasmids pZINT and pYCIC, respectively.

tivity of alkaline phosphatase and β-galactosidase, respectively. The results suggest that the $YciC_{At}$ protein is a cytoplasmic protein.

$YciC_{At}$ may possibly catalyze GTP hydrolysis to drive the $TroCBA_{At}$ transporter. However, $YciC_{At}$ is not essential for the $TroCBA_{At}$ transporter (Fig. 3B). Another possible function of $YciC_{At}$ is as a zinc chaperone that may transfer zinc ions to the zinc sensor Zur_{At}. To test this idea, expression of the *znuA*, *zinT*, and *troC* genes in the *yciC*::Km strain was determined by qRT-PCR. Similarly to the WT, EDTA induction and zinc repression of *znuA*, *zinT*, and *troC* were observed in the *yciC*::Km strain (data not shown). Therefore, $YciC_{At}$ is unlikely to function in zinc loading to Zur_{At} for mediating repression of the Zur_{At} regulon.

Decreased zinc levels in the EDTA-hypersensitive mutants. Total zinc content in the mutant strains compared to the WT was determined using ICP-MS (Fig. 6A). Because the *troC znuA* double-mutant strain has a growth defect in the minimal AB medium (Fig. 4), ICP-MS was performed using cells grown in LB (rich medium) for 24 h; however, the zinc levels in the mutant strains were not dramatically different from those in the WT (data not shown). When cells were grown in LB plus 0.5 mM EDTA for 24 h, all the EDTA-hypersensitive mutants showed an obvious reduction in zinc content compared to the WT (Fig. 6A). It should be noted that 0.5 mM EDTA in LB did not inhibit the growth of the WT and all the tested mutant strains (data not shown). The lowest levels of intracellular zinc were detected in the *troC*::Gm *znuA*::Km strain (*troC*::Gm *yciC*::Km and *troC*::Gm *zinT*::Km strains < *troC*::Gm and *zinT*::Gm *yciC*::Km strains < *zinT*::Gm strain) (Fig. 6A). The WT and the *yciC*::Km and *znuA*::Gm *yciC*::Km mutant strains showed similar levels of EDTA sensitivity (see Fig. S4 in the supplemental material) and intracellular zinc levels (Fig. 6A).

Virulence assay. *N. benthamiana* plants were infected with the WT and the mutant strains carrying pCMA1 (a tumor-inducing plasmid). The mutant strains TC142 (*troC* mutation), TCYC15 (*troC* and *yciC* mutations), TCZT14 (*troC* and *zinT* mutations), and ZTYC15 (*zinT* and *yciC* mutations) were tested. All *A. tumefaciens* strains grown in LB for 24 h caused similar tumor formation on infected plants (data not shown). Next, the *A. tumefaciens* strains were grown under metal limitation in LB plus 0.5 mM EDTA for 24 h and used to infect plants. However, TC142, TCYC15, TCZT14, and ZTYC15 all caused tumors on the infected plants and were similar to the WT (Fig. 6B). Unfortunately, several attempts were made, but we could not select the TCZA15 (*troC* and *znuA* mutations) strain carrying pCMA1; thus, we were unable to determine the virulence of TCZA15.

DISCUSSION

The high-affinity zinc importer ZnuABC is found widely in many bacteria. Rarely, some bacteria have a second high-affinity zinc uptake system in addition to ZnuABC, such as *T. pallidum* TroABCD ($TroABCD_{Tp}$) (29, 30) and *Haemophilus influenzae*

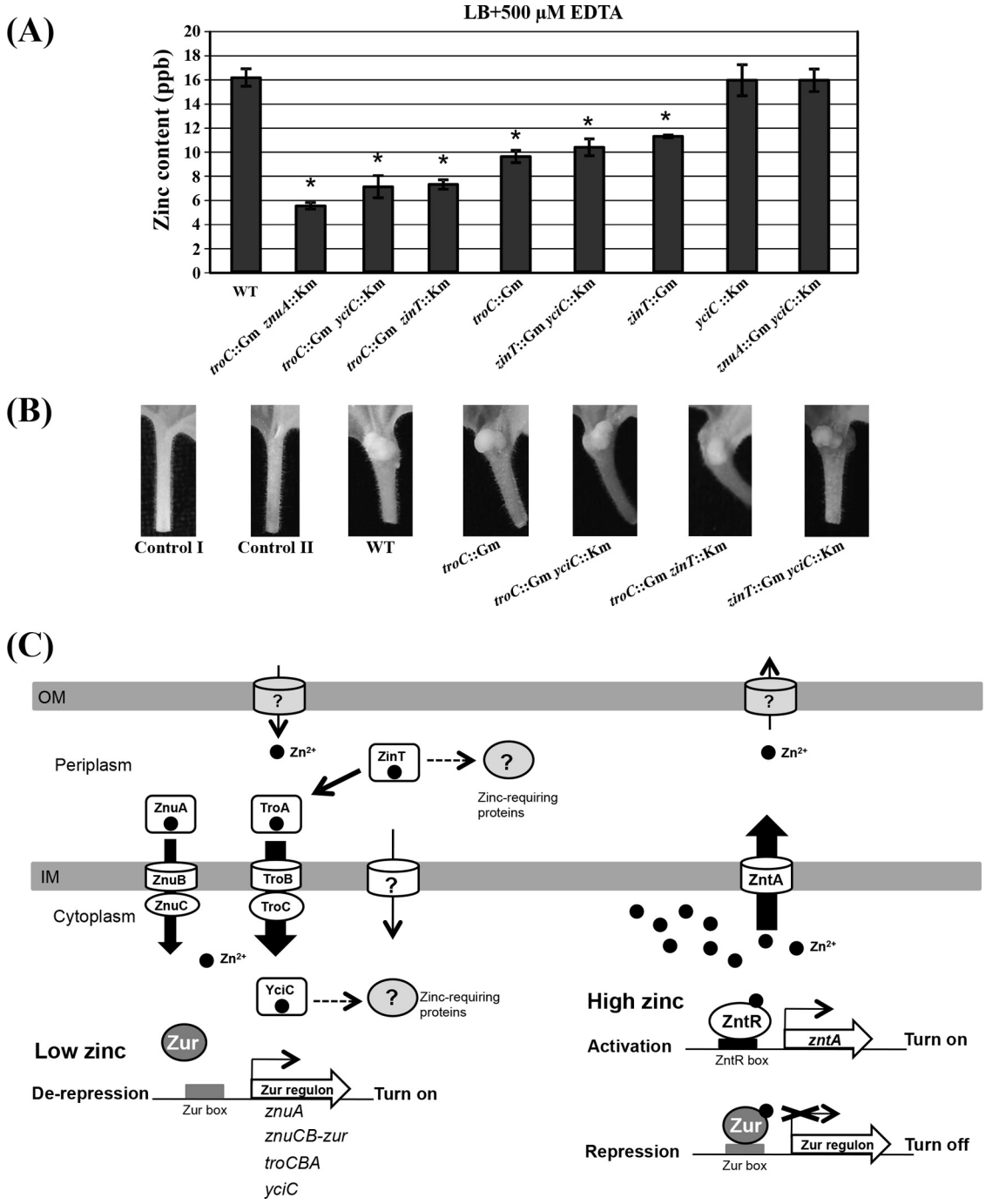

FIG 6 (A) Intracellular zinc content was determined using ICP-MS. The WT and the mutant strains TCZA15 (*troC*::Gm *znuA*::Km), TCYC15 (*troC*::Gm *yciC*::Km), TCZT15 (*troC*::Gm *zinT*::Km), TC142 (*troC*::Gm), ZTYC15 (*zinT*::Gm *yciC*::Km), PC135 (*zinT*::Gm), YC154 (*yciC*::Km), and ZAYC15 (*znuA*::Gm *yciC*::Km) were grown in LB plus 0.5 mM EDTA for 24 h. The results are shown as the means of samples in triplicate, and the error bars indicate the standard deviations. The bars marked with asterisks are significantly different from the WT ($P < 0.05$ in an unpaired Student's *t* test). (B) Virulence assay. Shown is tumor formation on the petioles of *N. benthamiana* plants infected with the WT and the mutant strains TC142 (*troC*::Gm), TCYC15 (*troC*::Gm *yciC*::Km), TCZT15 (*troC*::Gm *zinT*::Km), and ZTYC15 (*zinT*::Gm *yciC*::Km) grown in IB 5.5 medium containing 300 μM AS. Control I, without inoculation; control II, inoculation of the wounded petiole with IB 5.5 plus 300 μM AS. (C) Proposed model of zinc homeostasis. *A. tumefaciens* contains two zinc sensors, Zur and ZntR, which control zinc homeostasis. Zur is the transcriptional repressor of zinc acquisition genes, including *znuA*, *znuBC*, *zinT*, *troCBA*, and *yciC*. ZntR is a transcriptional activator of a zinc efflux gene, *zntA*. Under low-zinc conditions, Zur is in the apo form and dissociates from DNA to trigger expression of the Zur regulon. The TroABC system is the major zinc uptake system (thick solid arrow) compared to ZnuABC. ZinT functions in association with TroCBA. ZinT and YciC may function as zinc chaperones that supply Zn^{2+} (black dots) to zinc-requiring proteins in the periplasm and cytoplasm, respectively. When the intracellular zinc levels are high, the complexes ZntR-Zn^{2+} and Zur-Zn^{2+} are formed, which in turn activates zinc efflux by ZntA and represses zinc uptake systems, respectively. The outer membrane (OM) channels for zinc import and zinc extrusion have not been identified. Zinc ions may also be transported into the cytoplasm via unknown inner membrane (IM) transporters. ?, unknown; dashed arrows, possible mechanisms.

ZevAB (59). *Listeria monocytogenes* contains two zinc permease systems, ZurAM and ZinABC, which are regulated by Zur (60). The presence of two high-affinity zinc uptake systems helps these bacteria to survive in diverse zinc-limiting environments and during infection. In addition to ZnuABC, *A. tumefaciens* has a cluster of genes (Atu3178, Atu3179, and Atu3180) encoding an ABC-type transporter. The Atu3178 gene encodes a protein belonging to the TroA superfamily that has amino acid identity to $TroA_{Tp}$ (28%), ZinA (26%), and *A. tumefaciens* ZnuA (25%). Therefore, we named Atu3178, Atu3179, and Atu3180 *troA*, *troB*, and *troC*, respectively. In other bacteria, *tro* operons are involved in metal uptake and can transport either zinc or manganese and possibly iron (29, 33–36). The *A. tumefaciens troCBA* operon ($troCBA_{At}$) was shown here to respond specifically to zinc limitation.

To survive under a wide range of zinc-deficient conditions, *A. tumefaciens* requires the cooperation of Zur-regulated zinc acquisition systems, including two ABC-type zinc importers, $TroCBA_{At}$ and $ZnuABC_{At}$, and two zinc chaperones, $ZinT_{At}$ and $YciC_{At}$. Zinc uptake in *A. tumefaciens* differs from the systems in many other bacteria in that $TroCBA_{At}$ is the major zinc importer while $ZnuABC_{At}$ plays a lesser role. $ZnuABC_{At}$ is very important for supporting growth under zinc limitation in the absence of $TroCBA_{At}$. This indicates that $ZnuABC_{At}$ may function as a backup system for high-affinity zinc uptake. It is also possible that the two transporters function optimally under different conditions, such as different pHs. Consequently, $TroCBA_{At}$ may play a dominant role in zinc uptake under laboratory test conditions and $ZnuABC_{At}$ may play a more crucial role under other, as yet unidentified conditions. The severe growth defect of the *troC*::Gm *znuA*::Km strain could be rescued by supplementation with zinc, suggesting that zinc can be taken up through additional low-affinity zinc transporters.

ZinT proteins in *Escherichia coli* O157 (20) and *S. enterica* (22, 23) ($ZinT_{Ec}$ and $ZinT_{Se}$, respectively) are accessory components of the ZnuABC transporters that enhance the ability of cells to recruit zinc under severe zinc shortage. In contrast to $ZinT_{Ec}$ and $ZinT_{Se}$, $ZinT_{At}$ plays a critical role for survival under zinc depletion and can function in the absence of $ZnuABC_{At}$ (25). It was found that $ZinT_{At}$ may interact with $TroCBA_{At}$. It is likely that $ZinT_{At}$ is an additional component of the $TroCBA_{At}$ transporter, and it may help increase the rate of zinc delivery to $TroCBA_{At}$ when *A. tumefaciens* faces severe zinc deprivation. $ZinT_{At}$ may also supply zinc ions to other periplasmic zinc-requiring proteins.

The members of the COG0523 subfamily of G3E-GTPases have been reported to function as metal insertases by using GTP hydrolysis to drive the incorporation of a metal cofactor into the catalytic site of the target enzyme and/or as metal chaperones to allocate a metal cofactor to the target zinc-requiring proteins (26). *B. subtilis* YciC ($YciC_{Bs}$) belongs to a subgroup, Zur-regulated COG0523 proteins. $YciC_{Bs}$ is a membrane protein, and it was proposed to be a component of a low-affinity zinc transporter and possibly a zinc chaperone (27, 28). Unlike $YciC_{Bs}$, $YciC_{At}$ is a cytoplasmic protein. Inactivation of $yciC_{At}$ in combination with the mutation of a gene encoding the major zinc importer, $troC_{At}$, or the periplasmic zinc chaperone, $zinT_{At}$, caused a growth defect on LA plates containing EDTA. When *A. tumefaciens* encounters conditions of severe zinc shortage, even if the high-affinity zinc uptake $TroCBA_{At}$ and $ZnuABC_{At}$ systems are still functioning, it may need $ZinT_{At}$ and $YciC_{At}$ to effectively shuttle zinc ions to essential zinc-dependent proteins whose functions are required to cope with low-zinc stress.

Zinc uptake systems are known to be important for virulence in many bacteria (59, 60). However, in virulence assays using *N. benthamiana* as the host plant, growth either in LB (a zinc-replete condition) or in LB plus 0.5 mM EDTA (a zinc-depleted condition) had no effect on the virulence of *A. tumefaciens* mutant strains lacking zinc uptake genes compared to the wild type. Zinc availability at the infection site may differ between different types of plants, and this may alter the sensitivity of the assay in different host plants.

A model of zinc homeostasis in *A. tumefaciens* is proposed in Fig. 6C. Intracellular zinc levels are sensed by two transcriptional regulators, Zur and ZntR (25, 61). Zur is a repressor in the Fur family, whereas ZntR is an activator belonging to the MerR family. Under low-zinc conditions, Zur is in the apo form, which in turn triggers the expression of zinc acquisition genes, including *znuABC*, *troCBA*, *zinT*, and *yciC*. The TroCBA transporter plays a dominant role in zinc uptake compared to the ZnuABC system. ZinT may help enhance the efficiency of zinc recruitment to the TroCBA transporter. When TroCBA is impaired, the ZnuABC system plays an essential role in zinc uptake to support bacterial growth. It is likely that zinc can also be transported into the cytoplasm by an unidentified low-affinity zinc importer(s). The ZinT and YciC proteins may act as metallochaperones to allocate zinc to their target zinc-dependent proteins in the periplasm and cytoplasm, respectively. When intracellular zinc is overloaded, the complexes of Zn^{2+} with the zinc sensors, Zur-Zn^{2+} and ZntR-Zn^{2+}, are formed. The Zur-Zn^{2+} complex represses the zinc uptake genes, whereas the ZntR-Zn^{2+} complex activates the zinc efflux gene, *zntA*. Consequently, the high-affinity zinc uptake systems, TroCBA and ZnuABC, are shut down, and excess zinc can be pumped out of the cytoplasm by a P_{1B}-type ATPase, ZntA. However, the outer-membrane channels for zinc import and zinc extrusion in *A. tumefaciens* remain to be identified.

A. tumefaciens was shown here to operate a novel pathway for zinc uptake in which $ZinT_{At}$ is part of a high-affinity zinc importer, $TroCBA_{At}$. Whether $ZinT_{At}$ interacts with $TroA_{At}$ or directly interacts with the inner-membrane permease, $TroB_{At}$, during the process of zinc transport awaits further study. High-affinity zinc uptake systems, such as $TroCBA_{At}$ and $ZnuABC_{At}$, are necessary for *A. tumefaciens* to survive under low-zinc stress, but zinc allocation to zinc-dependent proteins facilitated by the zinc chaperones $ZinT_{At}$ and $YciC_{At}$ is also essential. Nevertheless, the exact molecular mechanisms of $ZinT_{At}$ and $YciC_{At}$, as well as their target proteins, have yet to be elucidated.

ACKNOWLEDGMENTS

We thank S. K. Farrand for the plasmid pCMA1. We also thank P. Srifah Huehne and K. Bhinija for technical assistance with the virulence assay.

This work was supported by the Chulabhorn Research Institute and Thailand Research Fund grant RSA5880010.

REFERENCES

1. **Vallee BL, Falchuk KH.** 1993. The biochemical basis of zinc physiology. Physiol Rev **73**:79–118.
2. **Andreini C, Bertini I, Cavallaro G, Holliday GL, Thornton JM.** 2008. Metal ions in biological catalysis: from enzyme databases to general principles. J Biol Inorg Chem **13**:1205–1218. http://dx.doi.org/10.1007/s00775-008-0404-5.
3. **Kasahara M, Anraku Y.** 1974. Succinate- and NADH oxidase systems of

Escherichia coli membrane vesicles. Mechanism of selective inhibition of the systems by zinc ions. J Biochem **76:**967–976.
4. **Singh AP, Bragg PD.** 1974. Inhibition of energization of *Salmonella typhimurium* membrane by zinc ions. FEBS Lett **40:**200–202. http://dx.doi.org/10.1016/0014-5793(74)80927-0.
5. **Beard SJ, Hughes MN, Poole RK.** 1995. Inhibition of the cytochrome bd-terminated NADH oxidase system in *Escherichia coli* K-12 by divalent metal cations. FEMS Microbiol Lett **131:**205–210. http://dx.doi.org/10.1111/j.1574-6968.1995.tb07778.x.
6. **Aagaard A, Brzezinski P.** 2001. Zinc ions inhibit oxidation of cytochrome c oxidase by oxygen. FEBS Lett **494:**157–160. http://dx.doi.org/10.1016/S0014-5793(01)02299-2.
7. **Xu FF, Imlay JA.** 2012. Silver(I), mercury(II), cadmium(II), and zinc(II) target exposed enzymic iron-sulfur clusters when they toxify *Escherichia coli*. Appl Environ Microbiol **78:**3614–3621. http://dx.doi.org/10.1128/AEM.07368-11.
8. **Blencowe DK, Morby AP.** 2003. Zn(II) metabolism in prokaryotes. FEMS Microbiol Rev **27:**291–311. http://dx.doi.org/10.1016/S0168-6445(03)00041-X.
9. **Nies DH.** 2003. Efflux-mediated heavy metal resistance in prokaryotes. FEMS Microbiol Rev **27:**313–339. http://dx.doi.org/10.1016/S0168-6445(03)00048-2.
10. **Hantke K.** 2005. Bacterial zinc uptake and regulators. Curr Opin Microbiol **8:**196–202. http://dx.doi.org/10.1016/j.mib.2005.02.001.
11. **Nies DH.** 2007. Biochemistry. How cells control zinc homeostasis. Science **317:**1695–1696.
12. **Shin JH, Oh SY, Kim SJ, Roe JH.** 2007. The zinc-responsive regulator Zur controls a zinc uptake system and some ribosomal proteins in *Streptomyces coelicolor* A3(2). J Bacteriol **189:**4070–4077. http://dx.doi.org/10.1128/JB.01851-06.
13. **Gabriel SE, Helmann JD.** 2009. Contributions of Zur-controlled ribosomal proteins to growth under zinc starvation conditions. J Bacteriol **191:**6116–6122. http://dx.doi.org/10.1128/JB.00802-09.
14. **Panina EM, Mironov AA, Gelfand MS.** 2003. Comparative genomics of bacterial zinc regulons: enhanced ion transport, pathogenesis, and rearrangement of ribosomal proteins. Proc Natl Acad Sci U S A **100:**9912–9917. http://dx.doi.org/10.1073/pnas.1733691100.
15. **Patzer SI, Hantke K.** 1998. The ZnuABC high-affinity zinc uptake system and its regulator Zur in *Escherichia coli*. Mol Microbiol **28:**1199–1210. http://dx.doi.org/10.1046/j.1365-2958.1998.00883.x.
16. **Patzer SI, Hantke K.** 2000. The zinc-responsive regulator Zur and its control of the *znu* gene cluster encoding the ZnuABC zinc uptake system in *Escherichia coli*. J Biol Chem **275:**24321–24332. http://dx.doi.org/10.1074/jbc.M001775200.
17. **Outten CE, O'Halloran TV.** 2001. Femtomolar sensitivity of metalloregulatory proteins controlling zinc homeostasis. Science **292:**2488–2492. http://dx.doi.org/10.1126/science.1060331.
18. **Kershaw CJ, Brown NL, Hobman JL.** 2007. Zinc dependence of *zinT* (*yodA*) mutants and binding of zinc, cadmium and mercury by ZinT. Biochem Biophys Res Commun **364:**66–71. http://dx.doi.org/10.1016/j.bbrc.2007.09.094.
19. **Graham AI, Hunt S, Stokes SL, Bramall N, Bunch J, Cox AG, McLeod CW, Poole RK.** 2009. Severe zinc depletion *of Escherichia coli*: roles for high affinity zinc binding by ZinT, zinc transport and zinc-independent proteins. J Biol Chem **284:**18377–18389. http://dx.doi.org/10.1074/jbc.M109.001503.
20. **Gabbianelli R, Scotti R, Ammendola S, Petrarca P, Nicolini L, Battistoni A.** 2011. Role of ZnuABC and ZinT in *Escherichia coli* O157:H7 zinc acquisition and interaction with epithelial cells. BMC Microbiol **11:**36. http://dx.doi.org/10.1186/1471-2180-11-36.
21. **Lim J, Lee KM, Kim SH, Kim Y, Kim SH, Park W, Park S.** 2011. YkgM and ZinT proteins are required for maintaining intracellular zinc concentration and producing curli in enterohemorrhagic Escherichia coli (EHEC) O157:H7 under zinc deficient conditions. Int J Food Microbiol **149:**159–170. http://dx.doi.org/10.1016/j.ijfoodmicro.2011.06.017.
22. **Petrarca P, Ammendola S, Pasquali P, Battistoni A.** 2010. The Zur-regulated ZinT protein is an auxiliary component of the high-affinity ZnuABC zinc transporter that facilitates metal recruitment during severe zinc shortage. J Bacteriol **192:**1553–1564. http://dx.doi.org/10.1128/JB.01310-09.
23. **Ilari A, Alaleona F, Tria G, Petrarca P, Battistoni A, Zamparelli C, Verzili D, Falconi M, Chiancone E.** 2014. The *Salmonella enterica* ZinT structure, zinc affinity and interaction with the high-affinity uptake protein ZnuA provide insight into the management of periplasmic zinc. Biochim Biophys Acta **1840:**535–544. http://dx.doi.org/10.1016/j.bbagen.2013.10.010.
24. **Ziemienowicz A.** 2001. Odyssey of *Agrobacterium* T-DNA. Acta Biochim Pol **48:**623–635.
25. **Bhubhanil S, Sittipo P, Chaoprasid P, Nookabkaew S, Sukchawalit R, Mongkolsuk S.** 2014. Control of zinc homeostasis in *Agrobacterium tumefaciens* via *zur* and the zinc uptake genes *znuABC* and *zinT*. Microbiology **160:**2452–2463. http://dx.doi.org/10.1099/mic.0.082446-0.
26. **Haas CE, Rodionov DA, Kropat J, Malasarn D, Merchant SS, de Crécy-Lagard V.** 2009. A subset of the diverse COG0523 family of putative metal chaperones is linked to zinc homeostasis in all kingdoms of life. BMC Genomics **10:**470. http://dx.doi.org/10.1186/1471-2164-10-470.
27. **Gaballa A, Helmann JD.** 1998. Identification of a zinc-specific metalloregulatory protein, Zur, controlling zinc transport operons in *Bacillus subtilis*. J Bacteriol **180:**5815–5821.
28. **Gabriel SE, Miyagi F, Gaballa A, Helmann JD.** 2008. Regulation of the *Bacillus subtilis yciC* gene and insights into the DNA-binding specificity of the zinc-sensing metalloregulator Zur. J Bacteriol **190:**3482–3488. http://dx.doi.org/10.1128/JB.01978-07.
29. **Hazlett KR, Rusnak F, Kehres DG, Bearden SW, La Vake CJ, La Vake ME, Maguire ME, Perry RD, Radolf JD.** 2003. The *Treponema pallidum tro* operon encodes a multiple metal transporter, a zinc-dependent transcriptional repressor, and a semi-autonomously expressed phosphoglycerate mutase. J Biol Chem **278:**20687–20694. http://dx.doi.org/10.1074/jbc.M300781200.
30. **Desrosiers DC, Sun YC, Zaidi AA, Eggers CH, Cox DL, Radolf JD.** 2007. The general transition metal (Tro) and Zn^{2+} (Znu) transporters in *Treponema pallidum*: analysis of metal specificities and expression profiles. Mol Microbiol **65:**137–152. http://dx.doi.org/10.1111/j.1365-2958.2007.05771.x.
31. **Liu Y, Li W, Wei Y, Jiang Y, Tan X.** 2013. Efficient preparation and metal specificity of the regulatory protein TroR from the human pathogen *Treponema pallidum*. Metallomics **5:**1448–1457. http://dx.doi.org/10.1039/c3mt00163f.
32. **Berntsson RP, Smits SH, Schmitt L, Slotboom DJ, Poolman B.** 2010. A structural classification of substrate-binding proteins. FEBS Lett **584:**2606–2617. http://dx.doi.org/10.1016/j.febslet.2010.04.043.
33. **Brett PJ, Burtnick MN, Fenno JC, Gherardini FC.** 2008. *Treponema denticola* TroR is a manganese- and iron-dependent transcriptional repressor. Mol Microbiol **70:**396–409. http://dx.doi.org/10.1111/j.1365-2958.2008.06418.x.
34. **Smith KF, Bibb LA, Schmitt MP, Oram DM.** 2009. Regulation and activity of a zinc uptake regulator, Zur, in *Corynebacterium diphtheriae*. J Bacteriol **191:**1595–1603. http://dx.doi.org/10.1128/JB.01392-08.
35. **Zheng B, Zhang Q, Gao J, Han H, Li M, Zhang J, Qi J, Yan J, Gao GF.** 2011. Insight into the interaction of metal ions with TroA from *Streptococcus suis*. PLoS One **6:**e19510. http://dx.doi.org/10.1371/journal.pone.0019510.
36. **Wichgers Schreur PJ, Rebel JM, Smits MA, van Putten JP, Smith HE.** 2011. TroA of *Streptococcus suis* is required for manganese acquisition and full virulence. J Bacteriol **193:**5073–5080. http://dx.doi.org/10.1128/JB.05305-11.
37. **Luo ZQ, Clemente TE, Farrand SK.** 2001. Construction of a derivative of *Agrobacterium tumefaciens* C58 that does not mutate to tetracycline resistance. Mol Plant Microbe Interact **14:**98–103. http://dx.doi.org/10.1094/MPMI.2001.14.1.98.
38. **Grant SG, Jessee J, Bloom FR, Hanahan D.** 1990. Differential plasmid rescue from transgenic mouse DNAs into *Escherichia coli* methylation-restriction mutants. Proc Natl Acad Sci U S A **87:**4645–4649. http://dx.doi.org/10.1073/pnas.87.12.4645.
39. **Metcalf WW, Jiang W, Daniels LL, Kim SK, Haldimann A, Wanner BL.** 1996. Conditionally replicative and conjugative plasmids carrying *lacZ* alpha for cloning, mutagenesis, and allele replacement in bacteria. Plasmid **35:**1–13. http://dx.doi.org/10.1006/plas.1996.0001.
40. **Alexeyev MF.** 1999. The pKNOCK series of broad-host-range mobilizable suicide vectors for gene knockout and targeted DNA insertion into the chromosome of gram-negative bacteria. Biotechniques **26:**824–826, 828.
41. **Kovach ME, Elzer PH, Hill DS, Robertson GT, Farris MA, Roop RM II, Peterson KM.** 1995. Four new derivatives of the broad-host-range cloning vector pBBR1MCS, carrying different antibiotic-resistance cassettes. Gene **166:**175–176. http://dx.doi.org/10.1016/0378-1119(95)00584-1.
42. **DeFeyter R, Kado CI, Gabriel DW.** 1990. Small, stable shuttle vectors

for use in *Xanthomonas*. Gene **88:**65–72. http://dx.doi.org/10.1016/0378-1119(90)90060-5.
43. **Santos PM, Di Bartolo I, Blatny JM, Zennar E, Valla S.** 2001. New broad-host-range promoter probe vectors based on the plasmid RK2 replicon. FEMS Microbiol Lett **195:**91–96. http://dx.doi.org/10.1111/j.1574-6968.2001.tb10503.x.
44. **Bhubhanil S, Chamsing J, Sittipo P, Chaoprasid P, Sukchawalit R, Mongkolsuk S.** 2014. Roles of *Agrobacterium tumefaciens* membrane-bound ferritin (MbfA) in iron transport and resistance to iron under acidic conditions. Microbiology **160:**863–871. http://dx.doi.org/10.1099/mic.0.076802-0.
45. **Hwang I, Cook DM, Farrand SK.** 1995. A new regulatory element modulates homoserine lactone-mediated autoinduction of Ti plasmid conjugal transfer. J Bacteriol **177:**449–458.
46. **Sambrook J, Fritsch EF, Maniatis T.** 1989. Molecular cloning: a laboratory manual. Cold Spring Harbor Laboratory Press, Cold Spring Harbor, NY.
47. **Cangelosi GA, Best EA, Martinetti G, Nester EW.** 1991. Genetic analysis of *Agrobacterium*. Methods Enzymol **204:**384–397. http://dx.doi.org/10.1016/0076-6879(91)04020-O.
48. **Kitphati W, Ngok-Ngam P, Suwanmaneerat S, Sukchawalit R, Mongkolsuk S.** 2007. *Agrobacterium tumefaciens fur* has important physiological roles in iron and manganese homeostasis, the oxidative stress response, and full virulence. Appl Environ Microbiol **73:**4760–4768. http://dx.doi.org/10.1128/AEM.00531-07.
49. **Ngok-Ngam, P, Ruangkiattikul N, Mahavihakanont A, Virgem SS, Sukchawalit R, Mongkolsuk, S.** 2009. Roles of *Agrobacterium tumefaciens* RirA in iron regulation, oxidative stress response and virulence. J Bacteriol **191:**2083–2090. http://dx.doi.org/10.1128/JB.01380-08.
50. **Bhubhanil S, Niamyim P, Sukchawalit R, Mongkolsuk S.** 2014. Cysteine desulphurase-encoding gene *sufS2* is required for the repressor function of RirA and oxidative resistance in *Agrobacterium tumefaciens*. Microbiology **160:**79–90. http://dx.doi.org/10.1099/mic.0.068643-0.
51. **Livak KJ, Schmittgen TD.** 2001. Analysis of relative gene expression data using real-time quantitative PCR and the $2^{-\Delta\Delta Ct}$ method. Methods **25:**402–408. http://dx.doi.org/10.1006/meth.2001.1262.
52. **Miller JH.** 1972. Experiments in molecular genetics. Cold Spring Harbor Laboratory Press, Cold Spring Harbor, NY.
53. **Wood DW, Setubal JC, Kaul R, Monks DE, Kitajima JP, Okura VK, Zhou Y, Chen L, Wood GE, Almeida NF, Jr, Woo L, Chen Y, Paulsen IT, Eisen JA, Karp PD, Bovee D, Sr, Chapman P, Clendenning J, Deatherage G, Gillet W, Grant C, Kutyavin T, Levy R, Li MJ, McClelland E, Palmieri A, Raymond C, Rouse G, Saenphimmachak C, Wu Z, Romero P, Gordon D, Zhang S, Yoo H, Tao Y, Biddle P, Jung M, Krespan W, Perry M, Gordon-Kamm B, Liao L, Kim S, Hendrick C, Zhao ZY, Dolan M, Chumley F, Tingey SV, Tomb JF, Gordon MP, Olson MV, Nester EW.** 2001. The genome of the natural genetic engineer *Agrobacterium tumefaciens* C58. Science **294:**2317–2323. http://dx.doi.org/10.1126/science.1066804.
54. **Kyte J, Doolittle R.** 1982. A simple method for displaying the hydropathic character of a protein. J Mol Biol **157:**105–132. http://dx.doi.org/10.1016/0022-2836(82)90515-0.
55. **Tusnady GE, Simon I.** 2001. The HMMTOP transmembrane topology prediction server. Bioinformatics **17:**849–850. http://dx.doi.org/10.1093/bioinformatics/17.9.849.
56. **Käll L, Krogh A, Sonnhammer EL.** 2004. A combined transmembrane topology and signal peptide prediction method. J Mol Biol **338:**1027–1036. http://dx.doi.org/10.1016/j.jmb.2004.03.016.
57. **Manoil C, Beckwith J.** 1986. A genetic approach to analyzing membrane protein topology. Science **233:**1403–1408. http://dx.doi.org/10.1126/science.3529391.
58. **Manoil C.** 1990. Analysis of protein localization by use of gene fusions with complementary properties. J Bacteriol **172:**1035–1042.
59. **Rosadini CV, Gawronski JD, Raimunda D, Argüello JM, Akerley BJ.** 2011. A novel zinc binding system, ZevAB, is critical for survival of nontypeable *Haemophilus influenzae* in a murine lung infection model. Infect Immun **79:**3366–3376. http://dx.doi.org/10.1128/IAI.05135-11.
60. **Corbett D, Wang J, Schuler S, Lopez-Castejon G, Glenn S, Brough D, Andrew PW, Cavet JS, Roberts IS.** 2012. Two zinc uptake systems contribute to the full virulence of *Listeria monocytogenes* during growth *in vitro* and *in vivo*. Infect Immun **80:**14–21. http://dx.doi.org/10.1128/IAI.05904-11.
61. **Chaoprasid P, Nookabkaew S, Sukchawalit R, Mongkolsuk S.** 2015. Roles of *Agrobacterium tumefaciens* C58 ZntA and ZntB and the transcriptional regulator ZntR in controlling $Cd2^{+}$/$Zn2^{+}$/$Co2^{+}$ resistance and the peroxide stress response. Microbiology **161:**1730–1740. http://dx.doi.org/10.1099/mic.0.000135.

AMERICAN SOCIETY FOR MICROBIOLOGY | Applied and Environmental Microbiology

Regulation of the Cobalt/Nickel Efflux Operon *dmeRF* in *Agrobacterium tumefaciens* and a Link between the Iron-Sensing Regulator RirA and Cobalt/Nickel Resistance

Thanittra Dokpikul,[a] Paweena Chaoprasid,[b] Kritsakorn Saninjuk,[c] Sirin Sirirakphaisarn,[d] Jaruwan Johnrod,[d] Sumontha Nookabkaew,[e] Rojana Sukchawalit,[b,d,f] Skorn Mongkolsuk[b,c,f]

Environmental Toxicology, Chulabhorn Graduate Institute, Lak Si, Bangkok, Thailand[a]; Laboratory of Biotechnology, Chulabhorn Research Institute, Lak Si, Bangkok, Thailand[b]; Department of Biotechnology, Faculty of Science, Mahidol University, Bangkok, Thailand[c]; Applied Biological Sciences, Chulabhorn Graduate Institute, Lak Si, Bangkok, Thailand[d]; Laboratory of Pharmacology, Chulabhorn Research Institute, Lak Si, Bangkok, Thailand[e]; Center of Excellence on Environmental Health and Toxicology (EHT), Ministry of Education, Bangkok, Thailand[f]

ABSTRACT

The *Agrobacterium tumefaciens* C58 genome harbors an operon containing the *dmeR* (Atu0890) and *dmeF* (Atu0891) genes, which encode a transcriptional regulatory protein belonging to the RcnR/CsoR family and a metal efflux protein belonging to the cation diffusion facilitator (CDF) family, respectively. The *dmeRF* operon is specifically induced by cobalt and nickel, with cobalt being the more potent inducer. Promoter-*lacZ* transcriptional fusion, an electrophoretic mobility shift assay, and DNase I footprinting assays revealed that DmeR represses *dmeRF* transcription through direct binding to the promoter region upstream of *dmeR*. A strain lacking *dmeF* showed increased accumulation of intracellular cobalt and nickel and exhibited hypersensitivity to these metals; however, this strain displayed full virulence, comparable to that of the wild-type strain, when infecting a *Nicotiana benthamiana* plant model under the tested conditions. Cobalt, but not nickel, increased the expression of many iron-responsive genes and reduced the induction of the SoxR-regulated gene *sodBII*. Furthermore, control of iron homeostasis via RirA is important for the ability of *A. tumefaciens* to cope with cobalt and nickel toxicity.

IMPORTANCE

The molecular mechanism of the regulation of *dmeRF* transcription by DmeR was demonstrated. This work provides evidence of a direct interaction of apo-DmeR with the corresponding DNA operator site *in vitro*. The recognition site for apo-DmeR consists of 10-bp AT-rich inverted repeats separated by six C bases (5′-ATATAGTATACCCCCCTATAGTATAT-3′). Cobalt and nickel cause DmeR to dissociate from the *dmeRF* promoter, which leads to expression of the metal efflux gene *dmeF*. This work also revealed a connection between iron homeostasis and cobalt/nickel resistance in *A. tumefaciens*.

Cobalt is required by coenzyme B_{12}-dependent enzymes and several proteins (1, 2). However, cobalt overload can cause cellular toxicity by catalyzing the generation of reactive oxygen species (3, 4), which leads to iron and glutathione depletion, and thus disturbing iron homeostasis (4–6). Cobalt competes with iron in heme proteins (7) and inhibits the activity of iron-sulfur (Fe-S) proteins as shown in *Escherichia coli* (5) and *Salmonella enterica* (6). To avoid cobalt toxicity, levels of intracellular cobalt must be properly controlled. Cobalt trafficking systems in the cell, including uptake systems, efflux systems, and metallochaperones, help maintain cobalt at levels suitable for growth (8).

To prevent intracellular cobalt overload-mediated toxicity, excessive amounts of cobalt are eliminated by efflux systems involving components such as the major facilitator superfamily (MFS), P_{1B-4}-ATPase, resistance nodulation cell division (RND), cation/proton antiporter, and cation diffusion facilitator (CDF). The *E. coli* RcnA (resistance to cobalt and nickel) efflux pump belongs to a unique family that is responsible for the detoxification of cobalt and nickel (9). The expression of *rcnA* is negatively regulated by RcnR (10). CoaT is a P_{1B-4}-ATPase that is responsible for cobalt export in *Synechocystis* (11). Induction of *coaT* expression is mediated by the MerR-like transcriptional activator CoaR in the presence of cobalt, while the vitamin B_{12} pathway represses *coaT* transcription (11). *Mycobacterium smegmatis* CtpD (12) and *Mycobacterium tuberculosis* CtpJ (13) are also cobalt-exporting P_{1B-4}-ATPases that have been shown to play an important role in controlling cobalt homeostasis. *Cupriavidus metallidurans* CH34 extrudes cobalt using two RND systems (the cobalt and nickel resistance system [CnrCBA] [14] and the cobalt, zinc, and cadmium resistance system [CzcABC] [15]), the CDF protein CzcD (16), and the P_{1B-4}-ATPase CzcP (17). The CzcD protein negatively regulates CzcCBA by extruding the inducing cations (16), while CzcP functions as a metal-resistant enhancer (17). In addition to CzcD, *C. metallidurans* CH34 contains another CDF protein, DmeF (divalent metal efflux), which plays a role in control-

Received 23 April 2016 **Accepted** 20 May 2016

Accepted manuscript posted online 27 May 2016

Citation Dokpikul T, Chaoprasid P, Saninjuk K, Sirirakphaisarn S, Johnrod J, Nookabkaew S, Sukchawalit R, Mongkolsuk S. 2016. Regulation of the cobalt/nickel efflux operon *dmeRF* in *Agrobacterium tumefaciens* and a link between the iron-sensing regulator RirA and cobalt/nickel resistance. Appl Environ Microbiol 82:4732–4742. doi:10.1128/AEM.01262-16.

Editor: A. M. Spormann, Stanford University

Address correspondence to Rojana Sukchawalit, rojana@cri.or.th.

T.D. and P.C. contributed equally to this article.

Supplemental material for this article may be found at http://dx.doi.org/10.1128/AEM.01262-16.

TABLE 1 Bacterial strains and plasmids used in this work

Strain or plasmid	Characteristic(s)[a] or genotype	Reference or source
A. tumefaciens strains		
NTL4	Wild-type strain, a Ti plasmid-cured derivative of strain C58	48
DF156	*dmeF*::pKNOCK-Km, Km^r	This study
DR151	*dmeR*::pKNOCK-Gm, Gm^r	This study
PN094	*rirA*::pKNOCK-Km, Km^r	20
WK074	*irr*::pKNOCK-Gm, Gm^r	37
E. coli strains		
BW20767	Host for plasmids pKNOCK-Gm and pKNOCK-Km	49
DH5α	Host for general DNA cloning	50
Plasmids for gene inactivation		
pKNOCK-Gm	Suicide vector, Gm^r	51
pKNOCK-Km	Suicide vector, Km^r	51
pKNOCKmDMEF	Internal coding region of *dmeF* cloned into pKNOCK-Km, Km^r	This study
pKNOCKDMER	Internal coding region of *dmeR* cloned into pKNOCK-Gm, Gm^r	This study
Plasmids for complementation		
pBBR1MCS-4	Expression vector, Ap^r (pBBR)	30
pDmeF	Full-length *dmeF* cloned into pBBR1MCS-4, Ap^r	This study
pDmeR	Full-length *dmeR* cloned into pBBR1MCS-4, Ap^r	This study
pRirA	Full-length *rirA* cloned into pBBR1MCS-4, Ap^r	20
Promoter-*lacZ* fusions		
pUFR027lacZ	Promoter probe vector, Tc^r	31
pDmeRF-lacZ	The *dmeRF* promoter fused to *lacZ* of pPR9TT, Ap^r	This study
Plasmid for the virulence assay		
pCMA1	pTiC58*traM*::*nptII*, Km^r	52
Plasmids for protein expression and purification		
pASK-IBA7	Protein expression vector, Ap^r	IBA
pStep-tag-DmeR	Coding region of *dmeR* cloned into pASK-IBA7, Ap^r	This study

[a] Ap^r, ampicillin resistance; Gm^r, gentamicin resistance; Km^r, kanamycin resistance; Tc^r, tetracycline resistance.

ling cobalt homeostasis (18). Disruption of the *dmeF* gene causes the CnrCBA and CzcCBA RND systems to become ineffective in cobalt transport. This suggests that cobalt is exported from the cytoplasm to the periplasm via the CDF proteins and that cobalt is then transported by the RND systems from the periplasm to outside the cell (18).

Agrobacterium tumefaciens is a soilborne plant pathogen that causes crown gall tumor disease. Cobalt transporters have not been characterized in *A. tumefaciens*. *Rhizobium leguminosarum*, a close relative of *A. tumefaciens*, belongs to the *Alphaproteobacteria* and contains the *dmeRF* operon that is responsible for exporting cobalt and nickel (19). *R. leguminosarum* DmeR represses *dmeRF* transcription. Expression of *dmeRF* is inducible in response to increased levels of cobalt and nickel. The *R. leguminosarum dmeRF* mutant is hypersensitive to cobalt and nickel. The *dmeRF* genes have been shown to play an important role in *R. leguminosarum* during free-living and symbiotic interactions with legume plants under high-cobalt and high-nickel conditions (19). Cobalt stress and iron homeostasis are linked. Induction of the ferric uptake regulator (Fur) regulon has been observed in response to cobalt stress, which may provide iron to out-compete cobalt (5, 6). Unlike *E. coli*, in which iron regulation is mediated by Fur, iron regulation in *A. tumefaciens* is controlled by the iron response regulator (Irr) and the rhizobial iron regulator (RirA) under low-iron and high-iron conditions, respectively (20, 21). In contrast to Irr, RirA is assumed to require the Fe-S cluster as its cofactor (22, 23). Disruption of an Fe-S cluster synthesis gene (*sufS2*) in the *suf* operon impairs RirA repression activity in *A. tumefaciens* (24). The *A. tumefaciens* genome contains genes that are homologous to *dmeR* (Atu0890) and *dmeF* (Atu0891) (25). Here, the molecular mechanism of the regulation of *A. tumefaciens dmeRF* and its role in controlling intracellular metal levels were determined. Furthermore, the effect of cobalt toxicity on the activities of Fe-S proteins, including RirA and SoxR, was investigated. A link between the control of iron homeostasis via RirA and cobalt/nickel tolerance was revealed.

MATERIALS AND METHODS

Bacterial strains, culture conditions, plasmids, and primers. The bacterial strains and plasmids used in this work are listed in Table 1. *E. coli* and *A. tumefaciens* were aerobically grown in Luria broth (LB) at 37°C and 28°C, respectively. LA refers to LB medium containing 1.5% agar. The growth conditions and antibiotic concentrations used were the same as those previously reported (24). Induction broth with a pH of 5.5 (IB 5.5; the *vir*-inducing condition) was used in the virulence assay (26). Primers are listed in Table S1 in the supplemental material. All mutant strains were confirmed by Southern blotting. The cloned DNA region was confirmed by sequencing (Macrogen). Plasmids were transferred into *A. tumefaciens* by electroporation (26). General molecular techniques were performed according to standard protocols (27).

RT-PCR. Total RNA was extracted from log-phase cells of wild-type *A. tumefaciens* strain NTL4 grown in LB medium and induced with 500 μM $CoCl_2$ for 15 min, and reverse transcription-PCR (RT-PCR) was performed using previously described protocols (20, 28). Primers BT4733 and BT4734 were used to amplify the junction of the *dmeR* and *dmeF* genes.

5′ RACE. The transcriptional start site of *dmeR* was determined using RNA that was isolated from log-phase NTL4 cells grown in LB and treated with 500 μM $CoCl_2$ for 15 min. The 5′ rapid amplification of cDNA ends (5′ RACE) (Roche) was performed according to the manufacturer's recommendations, using specific primers SP1 (BT4096) and SP2 (BT4619).

qRT-PCR analysis. RNA isolation, cDNA preparation, and quantitative real-time PCR (qRT-PCR) were performed as previously described (20, 24). The gene-specific primers for *dmeF*, *hmuT*, *shmR*, *fbpA*, *mbfA*, *hemA*, *fdx*, *irpA*, *sufS2*, *fssA*, and 16S rRNA are listed in Table S1 in the supplemental material. The amount of a specific mRNA target was normalized to the amount of a housekeeping gene 16S rRNA. Fold changes in gene expression are relative to untreated samples from wild-type NTL4 (WT) using the $2^{-\Delta\Delta CT}$ method (29). The data were reported as the means of biological triplicates plus or minus the standard deviation (SD).

Construction of *dmeF* and *dmeR* mutant strains (DF156 and DR151). *A. tumefaciens* mutant strains were constructed using an insertional gene inactivation method (20). The internal coding regions of *dmeF* (BT4569 and BT4570, 222 bp) and *dmeR* (BT4567 and BT4568, 176 bp) were PCR amplified from genomic wild-type NTL4 with the gene-specific primers. The PCR products were cloned into pKNOCK-Km and pKNOCK-Gm, generating pKNOCKmDMEF and pKNOCKDMER, respectively. The resulting plasmids were individually electroporated into the wild-type NTL4 strain. The mutant strains, DF156 and DR151, were selected on LA plus 30 μg/ml of kanamycin (Km) and LA plus 60 μg/ml of gentamicin (Gm) plates, respectively.

Cloning of functional *dmeF* and *dmeR* genes for complementation. The PCR fragments containing full-length *dmeR* (BT4618 and BT4619) and *dmeF* (BT4620 and BT4621) genes were individually cloned into the SmaI site of pBBR1MCS-4 (30), generating the plasmids pDmeR and pDmeF, respectively.

Construction of a *dmeRF* promoter-*lacZ* transcriptional fusion and β-galactosidase activity assay. To construct the pDmeRF-lacZ plasmid, DNA fragments (108 bp) that contained the *dmeRF* promoter region were amplified from *A. tumefaciens* NTL4 genomic DNA using PCR with the primers BT4618 and BT4735 and then cloned into the promoter probe vector pUFR027lacZ, a derivative of pUFR027 (31), as previously reported (24). The β-galactosidase (β-Gal) activity assay (32) was performed as previously described (24) using log-phase cells carrying pDmeRF-lacZ grown in LB. The results are presented as specific activity, which was calculated in units per milligram of protein.

Overexpression and purification of rDmeR. The coding region of *dmeR* was amplified via PCR using the primers BT5406 and BT5407, which contain a BsaI site. The PCR products were digested with BsaI and cloned into BsaI-digested pASK-IBA7 (IBA, Germany), generating the plasmid pStrep-tag-DmeR, to produce Strep-tag II fused to the N terminus of DmeR (recombinant DmeR protein [rDmeR]).

Log-phase *E. coli* DH5α cells carrying the pStrep-tag-DmeR plasmid grown in LB at 37°C were induced with 200 ng/ml anhydrotetracycline for 1 h. The cells were then harvested, washed, and resuspended in buffer W (100 mM Tris-HCl pH 8.0, 250 mM NaCl). The cell suspension was sonicated, and cell debris was removed via centrifugation. The clear lysate was allowed to bind to a Strep-Tactin Sepharose column and then washed with buffer W. The rDmeR protein was subsequently eluted with elution buffer (100 mM Tris-HCl pH 8.0, 250 mM NaCl, 2.5 mM desthiobiotin). The eluted fractions were concentrated using Amicon Ultra centrifugal filters, with a molecular weight cutoff (MWCO) of 10,000 (Millipore). The rDmeR protein with the expected molecular size (11.8 kDa) was detected, and protein purity was assessed via SDS-PAGE and Coomassie blue staining (see Fig. S1 in the supplemental material).

Electrophoretic mobility shift assay. The DNA fragment that contained the *dmeRF* promoter region (108 bp) was amplified via PCR using the primers BT4618 and BT4735. The DNA fragment (2 pmol) was end labeled with [γ-^{32}P]dATP and T4 polynucleotide kinase. The ^{32}P-labeled DNA probe was then purified using Sephadex G-50. Electrophoretic mobility shift assays were carried out in 20-μl reaction mixtures containing 1× binding buffer (20 mM Tris-HCl pH 7, 50 mM KCl, 1 mM dithiothreitol [DTT], 5% glycerol, 0.5 μg/ml calf thymus DNA, and 0.05 mg/ml bovine serum albumin [BSA]), purified rDmeR protein (0.25, 0.5, 0.75, or 1 μM), and 1 μl of diluted ^{32}P-labeled DNA probe (1:2,000) in the absence or presence of 1 mM EDTA and 200 μM metals ($CoCl_2$, $CuSO_4$, $FeCl_3$, $MnCl_2$, $NiCl_2$, or $ZnCl_2$). Following incubation at room temperature for 30 min, the reaction mixtures were resolved in 8% nondenaturing polyacrylamide gels in 1× TB buffer (89 mM Tris-HCl and 89 mM boric acid) at 4°C at a constant voltage of 120 V for 1 h. After electrophoresis, the gels were dried and then subjected to autoradiography using the Typhoon FLA 7000 phosphor imaging system (GE Healthcare Life Sciences).

DNase I footprinting assay. The ^{32}P-labeled *dmeRF* promoter probe (^{32}P-P_{dmeRF}, 108 bp) was generated via PCR using the primers ^{32}P-end-labeled BT4618 and nonlabeled BT4735. The ^{32}P-P_{dmeRF} PCR products were separated on a 1.8% agarose gel, and the 108-bp band was cut out and purified using a Qiagen PCR purification column. The DNase I footprinting experiment was carried out in a 50-μl binding reaction mixture containing 1× binding buffer (20 mM Tris-HCl pH 7, 50 mM KCl, 1 mM DTT, 5% glycerol, 0.5 μg/ml calf thymus DNA, and 0.05 mg/ml BSA), 1 mM EDTA, ^{32}P-P_{dmeRF} probe, and rDmeR. The binding reaction mixture was incubated at room temperature for 30 min before digestion in a total reaction mixture volume of 100 μl with 0.2 units of DNase I (Promega), 5 M $CaCl_2$, 10 mM $MgCl_2$ and 1 μg/ml salmon sperm at 37°C for 35 s. The DNase I digestion reaction was stopped by adding 700 μl of stop solution (650 μl of absolute ethanol, 50 μl of 3 M sodium acetate, and 1 μl of 1 mg/ml yeast tRNA), and then the reaction mixture was incubated at −20°C for 1 h. The digested DNA products were harvested via centrifugation at 10,000 rpm for 15 min. The resultant DNA pellet was washed with 70% ethanol, resuspended in Milli-Q water, and separated on an 8% polyacrylamide and 8 M urea sequencing gel in 1× TBE buffer (89 mM Tris-HCl, 89 mM boric acid, and 2 mM EDTA [pH 8]) at room temperature at a constant voltage of 1,800 V for 1.15 h. Dideoxy DNA sequencing of the 108-bp *dmeRF* promoter was carried out using the primer BT4618 and was run alongside the DNase I footprint.

Inductively coupled plasma mass spectrometry. Cells were grown in LB that was individually supplemented with 100 μM $CoCl_2$, $CuSO_4$, $FeCl_3$, $MnCl_2$, $NiCl_2$, or $ZnCl_2$ at 28°C for 24 h. Samples were prepared, and the metals were measured in parts per billion (ppb) as previously described (33).

Virulence assay. *A. tumefaciens* strains carrying the plasmid pCMA1 were used to infect young *Nicotiana benthamiana* plants according to a previously described protocol (28, 34). Tumor formation was observed 3 weeks after inoculation.

RESULTS

The *A. tumefaciens dmeRF* operon is inducible by cobalt and nickel. The arrangement of the *dmeR* (Atu0890) and *dmeF* (Atu0891) genes is shown in Fig. 1A. *A. tumefaciens dmeRF* is flanked by the Atu0889 and Atu0892 genes encoding proteins with unknown functions. The *dmeR* and *dmeF* genes are cotranscribed as confirmed through RT-PCR analysis (Fig. 1B). The expression of the *A. tumefaciens dmeF* ($dmeF_{At}$) gene was increased by cobalt and nickel treatment (10, 100, and 250 μM) in a dose-dependent manner (Fig. 1C), with cobalt serving as a better inducer. The expression of $dmeF_{At}$ in response to various metals was determined using qRT-PCR (Fig. 1D). At the high concentration of 500 μM, $CoCl_2$ and $NiCl_2$ caused induction of $dmeF_{At}$ expression by ~30-fold and ~20-fold, respectively, while other metals, includ-

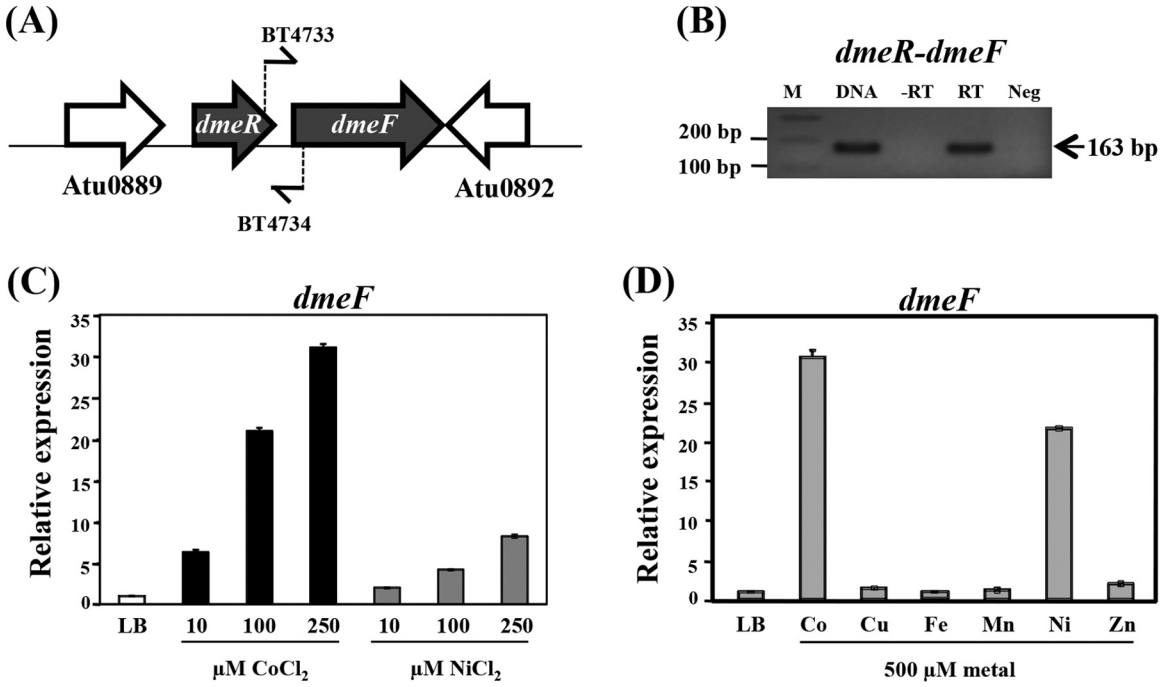

FIG 1 (A) Gene organization of *A. tumefaciens dmeRF*. The *dmeR* (Atu0890) gene is located upstream of the *dmeF* (Atu0891) gene and is separated by 78 bp. The Atu0889 and Atu0892 genes encode proteins of unknown function. The locations of the primers BT4733 and BT4734 used for RT-PCR analysis are indicated. (B) RT-PCR analysis. RNA was isolated from log-phase cells of the wild-type NTL4 strain grown in LB medium and induced with 500 μM $CoCl_2$ for 15 min and was then treated with DNase I, which was followed by treatment with reverse transcriptase (RT) or no treatment (−RT, a DNA-contamination control). Chromosomal DNA from NTL4 cells was amplified using the primers BT4733 and BT4734 and was used as a positive control (DNA). Neg indicates a reaction mixture without a template that is used as a negative control. The expected size of the PCR product is indicated. M indicates a 100-bp ladder marker. (C and D) Induction of *dmeF* by various metals examined through quantitative real-time PCR (qRT-PCR) analysis. Log-phase NTL4 cells grown in LB were either untreated or treated with 500 μM $CoCl_2$, $CuSO_4$, $FeCl_3$, $MnCl_2$, $NiCl_2$, or $ZnCl_2$ for 15 min. The fold changes in *dmeF* expression are expressed relative to the untreated control (LB, regarded as 1). The experiment was performed in biological triplicate, and the error bars indicate the standard deviations.

ing $CuSO_4$, $FeCl_3$, $MnCl_2$, and $ZnCl_2$, caused a less than 2-fold induction.

The *dmeRF* promoter is negatively regulated by DmeR. The *A. tumefaciens dmeR* ($dmeR_{At}$) gene encodes a protein that belongs to the RcnR/CsoR transcriptional regulator family (35). The upstream region of the $dmeR_{At}$ gene contains a predicted regulatory binding site for the RcnR/CsoR family that consists of a C-tract flanked by an AT-rich inverted repeat (5′-ATATAGTATACCCC CCTATAGTATAT-3′) (36), suggesting that the $dmeRF_{At}$ operon may be regulated by the $DmeR_{At}$ protein. The features of the $dmeRF_{At}$ promoter are shown in Fig. 2A. The transcriptional start site of $dmeRF_{At}$ at the adenine (A) residue was determined via 5′ RACE (Fig. 2A). The potential −35 and −10 sequences (TG TGCA and TAGTAT, respectively) were found with respect to the transcriptional start site.

The DR151 (*dmeR* mutation) and DF156 (*dmeF* mutation) strains were generated to determine the functions of the transcriptional regulator $DmeR_{At}$ and the CDF-type $DmeF_{At}$ transporter. To test whether $DmeR_{At}$ regulates the expression of $dmeRF_{At}$, the pDmeRF-lacZ (*dmeRF* promoter-*lacZ* transcriptional fusion) plasmid was constructed and transferred into the wild-type NTL4 (WT), mutant, and complemented strains, and β-galactosidase (β-Gal) activity was measured. The β-Gal activity obtained from the mutant strain DR151 (DR151/pBBR, ~1.25 U/mg protein) was higher than that from untreated WT cells (WT/pBBR, ~0.27 U/mg protein) (Fig. 2B) and WT cells treated with 500 μM $CoCl_2$ for 30 min (~0.59 U/mg protein). The high levels of β-Gal activity observed in DR151 could be suppressed by expressing the functional *dmeR* gene from the multicopy plasmid pDmeR (DR151/pDmeR, ~0.03 U/mg protein) but not pDmeF (DR151/pDmeF, ~1.24 U/mg protein) (Fig. 2B). In contrast to DR151, the level of β-Gal activity produced from DF156 (DF156/pBBR, ~0.33 U/mg protein) was similar to that from WT. These results demonstrated that $DmeR_{At}$ is the repressor of the $dmeRF_{At}$ operon.

DmeR binds to the *dmeRF* promoter, and the interaction is specifically inhibited by cobalt and nickel. The electrophoretic mobility shift assay demonstrated that the purified recombinant DmeR protein (rDmeR, Strep-tagged DmeR) bound to the ^{32}P-end-labeled 108-bp *dmeRF* promoter probe (Fig. 2C; see also Fig. S1B in the supplemental material). A single shifted band (rDmeR-probe complex) was observed with increasing rDmeR concentrations when 1 mM EDTA was present in the reactions (see Fig. S1B). When $CoCl_2$ or $NiCl_2$ (1, 10, 100, 250, 500, or 1,000 μM) was added instead of EDTA, the shifted band was not observed starting at a 100 μM concentration of the metal (see Fig. S1C). At a 200 μM concentration of various metals, the retarded band disappeared in the reaction mixtures containing $CoCl_2$ and $NiCl_2$ but was detected in the reaction mixtures containing $CuSO_4$, $FeCl_3$, $MnCl_2$, and $ZnCl_2$ (Fig. 2C). Among the retarded bands, the band from the reaction mixture containing $FeCl_3$ moved slightly more slowly, which may reflect differences in the conformation of the rDmeR-probe complexes. The results from the electrophoretic mobility shift assay supported the view that DmeR represses the *dmeRF* operon in the absence of cobalt and nickel by directly bind-

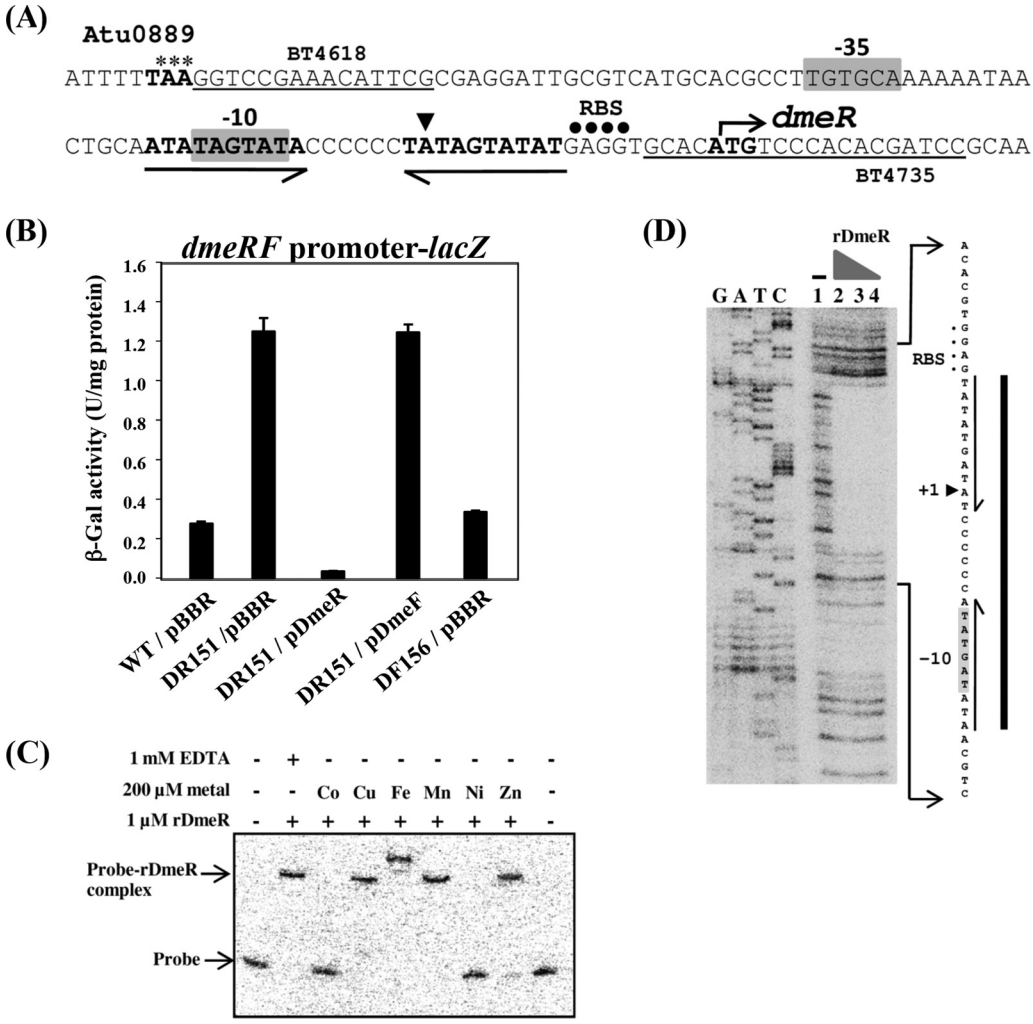

FIG 2 (A) The *A. tumefaciens dmeRF* promoter. The ATG start codon for *dmeR* is shown in bold with the bent arrow. The putative ribosome-binding site (RBS) is marked with black dots. The potential −35 and −10 sequences are indicated in the gray boxes. The transcriptional start site of *dmeR* at the adenine (A) residue, determined using 5′ RACE, is indicated with a black triangle. The AT-rich inverted repeat (arrows), separated by 6 bp of C-tract, is a predicted regulatory binding site for the RcnR/CsoR family. The TAA stop codon for Atu0889 is marked with asterisks. The locations of the primers BT4618 and BT4735 used for construction of the pDmeRF-lacZ plasmid (*dmeRF* promoter-*lacZ* transcriptional fusion) are underlined. (B) β-Gal activity assay. β-Gal activities were determined from log-phase cells that carry the pDmeRF-lacZ plasmid grown in LB medium. The cells were wild-type NTL4 (WT) and the mutant strain DR151 (*dmeR* mutation), containing a plasmid vector (pBBR) or functional *dmeR* and *dmeF* genes from the multicopy plasmids pDmeR and pDmeF, respectively. The error bars indicate the standard deviations. (C) Electrophoretic mobility shift assay. Effect of Co(II) and Ni(II) on the interaction of rDmeR and the *dmeRF* promoter. The DNA fragment that contains the *dmeRF* promoter region (108 bp) amplified by PCR with the primers BT4618 and BT4735 was end labeled with ^{32}P. The ^{32}P-labeled *dmeRF* promoter (Probe) was incubated with purified rDmeR protein in the absence (−) and presence (+) of 1 mM EDTA or a 200 μM concentration of various metals ($CoCl_2$, $CuSO_4$, $FeCl_3$, $MnCl_2$, $NiCl_2$, or $ZnCl_2$). The free probe and the probe-rDmeR complex are indicated with arrows. (D) DNase I footprint of rDmeR bound to the ^{32}P-end-labeled 108-bp *dmeRF* promoter. Lanes GATC, dideoxy DNA sequencing of the 108-bp *dmeRF* promoter using primer ^{32}P-end-labeled BT4618; lane 1, no rDmeR added; lanes 2 to 4, rDmeR added (10, 5, and 1 μM, respectively). The region of the promoter protected by rDmeR from DNase I digestion is marked with a thick line. The predicted −35 and −10 sequences, RBS, and the AT-rich inverted repeat are indicated.

ing to its promoter region. A DNase I footprinting assay was performed to determine the rDmeR binding site in the *dmeRF* promoter. The rDmeR protein protected an approximately 26-bp region (5′-ATATAGTATACCCCCCTATAGTATAT-3′) of the *dmeRF* promoter, spanning the predicted −10 sequence and the AT-rich inverted repeat (Fig. 2D).

The *dmeF* mutant strain is hypersensitive to cobalt and nickel and exhibits an increased cellular accumulation of these metals. The sensitivities of the WT and DF156 (*dmeF* mutation) strains to various metals were determined. The DF156 strain was more sensitive to 600 μM $CoCl_2$ (10^3-fold) and 1.2 mM $NiCl_2$ (10^3-fold) than the WT strain (Fig. 3A). However, the levels of sensitivity to other metals, including $CuSO_4$, $FeCl_3$, $MnCl_2$, and $ZnCl_2$, were similar in the WT and DF156 strains (data not shown). The hypersensitive phenotype of DF156 can be reversed by complementation with functional *dmeF* from the multicopy plasmid pDmeF (Fig. 3A). Inductively coupled plasma mass spectrometry analysis was performed to determine the accumulation of metals in WT and DF156. The results showed that DF156 exhibited apparently greater increases in intracellular cobalt (4-fold) and nickel (3-fold) contents than WT (Fig. 3B). The iron content in DF156 was slightly lower than that in WT, whereas the levels of

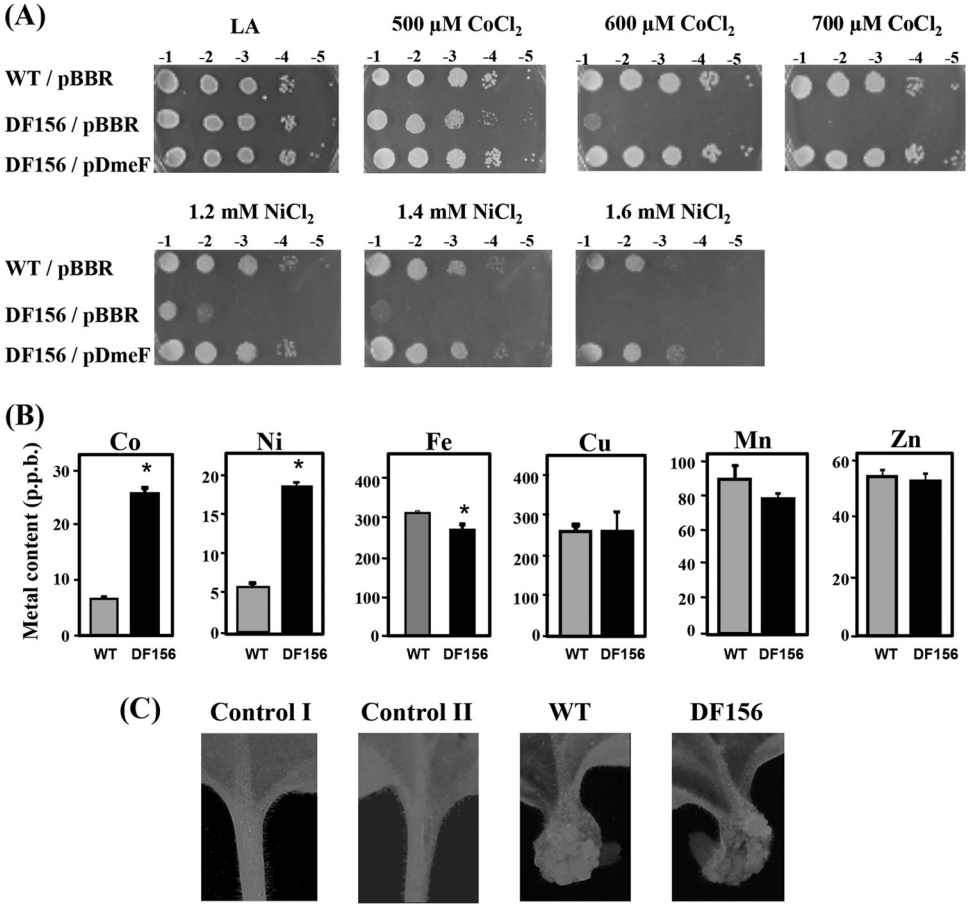

FIG 3 (A) Sensitivity to cobalt and nickel. Log-phase cells grown in LB were adjusted, serially diluted, and spotted onto LA plates containing $CoCl_2$ (500, 600, or 700 μM) and $NiCl_2$ (1.2, 1.4, or 1.6 mM). WT and DF156 (*dmeF* mutation) strains contained a plasmid vector (pBBR) or a functional *dmeF* from the multicopy plasmid pDmeF. Tenfold serial dilutions are indicated. (B) Measurement of intracellular metal contents using inductively coupled plasma mass spectrometry. WT and DF156 (*dmeF* mutation) cells were grown in LB that was individually supplemented with 100 μM $CoCl_2$, $NiCl_2$, $FeCl_3$,$CuSO_4$, $MnCl_2$, or $ZnCl_2$. Bars marked with an asterisk are significantly different from WT ($P < 0.05$ in an unpaired Student's *t* test). The error bars indicate the standard deviations. (C) Virulence assay. The images show tumor formation in *N. benthamiana* plants that were infected with the WT and DF156 (*dmeF* mutation) strains carrying the pCMA1 plasmid. Log-phase cells of *A. tumefaciens* grown in LB and then resuspended in IB 5.5 medium containing 300 μM acetosyringone (AS) were used to inoculate wounded *N. benthamiana* petioles. Control I, without infection; control II, inoculation of wounded petioles with IB 5.5 plus 300 μM AS. Fifteen petioles were inoculated for each bacterial strain, and representative petioles are shown.

copper, manganese, and zinc were similar in DF156 and WT (Fig. 3B). These results demonstrated that DmeF plays an important role in the detoxification of cobalt and nickel in *A. tumefaciens* and supported the view that $DmeF_{At}$ acts as an exporter of cobalt and nickel.

It was found that insertional inactivation of $dmeR_{At}$ (DR151, *dmeR*::pKNOCK-Gm) also disrupted the downstream gene $dmeF_{At}$. This was supported by the fact that the DR151 strain showed hypersensitivity to cobalt and nickel similar to that shown by DF156 (see Fig. S2 in the supplemental material). Furthermore, the hypersensitive phenotype of DR151 could be completely reversed by pDmeF but not by pDmeR (see Fig. S2).

Disruption of *dmeF* does not affect the virulence of *A. tumefaciens*. The effect of inactivation of *dmeF* on *A. tumefaciens* virulence was tested. *N. benthamiana* plants were infected with log-phase WT and DF156 cells grown in LB medium. Tumor formation results were similar in plants that were infected with WT and DF156 (Fig. 3C), suggesting that the loss of *dmeF* does not affect the ability of *A. tumefaciens* to cause disease in the host plant *N. benthamiana* under the tested conditions.

Cobalt stress causes increased expression of iron-responsive genes. *A. tumefaciens* iron homeostasis is regulated by RirA and Irr (20, 21). The promoter regions of *hmuT* (Atu2460, hemin ABC transporter substrate-binding protein), *shmR* (Atu2287, hemin receptor), and *fbpA* (Atu0407, ferric cation ABC transporter substrate-binding protein) contain the iron-responsive operator (IRO) motifs (RirA binding site); therefore, these genes were predicted to be regulated by *A. tumefaciens* RirA ($RirA_{At}$) (22). In contrast, *mbfA* (Atu0251, iron exporter), *hemA* (Atu2613, heme biosynthesis), *fdx* (Atu1350, ferredoxin), and *irpA* (Atu0288, iron-regulated protein A) were predicted to be regulated by Irr_{At} due to the presence of the iron control element (ICE) motifs (Irr binding site) in their promoters, while the *sufS2* (Atu1825, Fe-S cluster biosynthesis) and *fssA* (Atu0351, Fe-S scaffold protein) promoters contain both IRO and ICE motifs (22).

Cobalt toxicity in *E. coli* and *S. enterica* has been shown to disturb iron homeostasis (4–6). To investigate whether iron homeostasis in *A. tumefaciens* may be perturbed by stress from other metals, WT cells were exposed to a 500 μM concentration of various metals ($CoCl_2$, $CuSO_4$, $FeCl_3$, $MnCl_2$, $NiCl_2$, or $ZnCl_2$) for 15

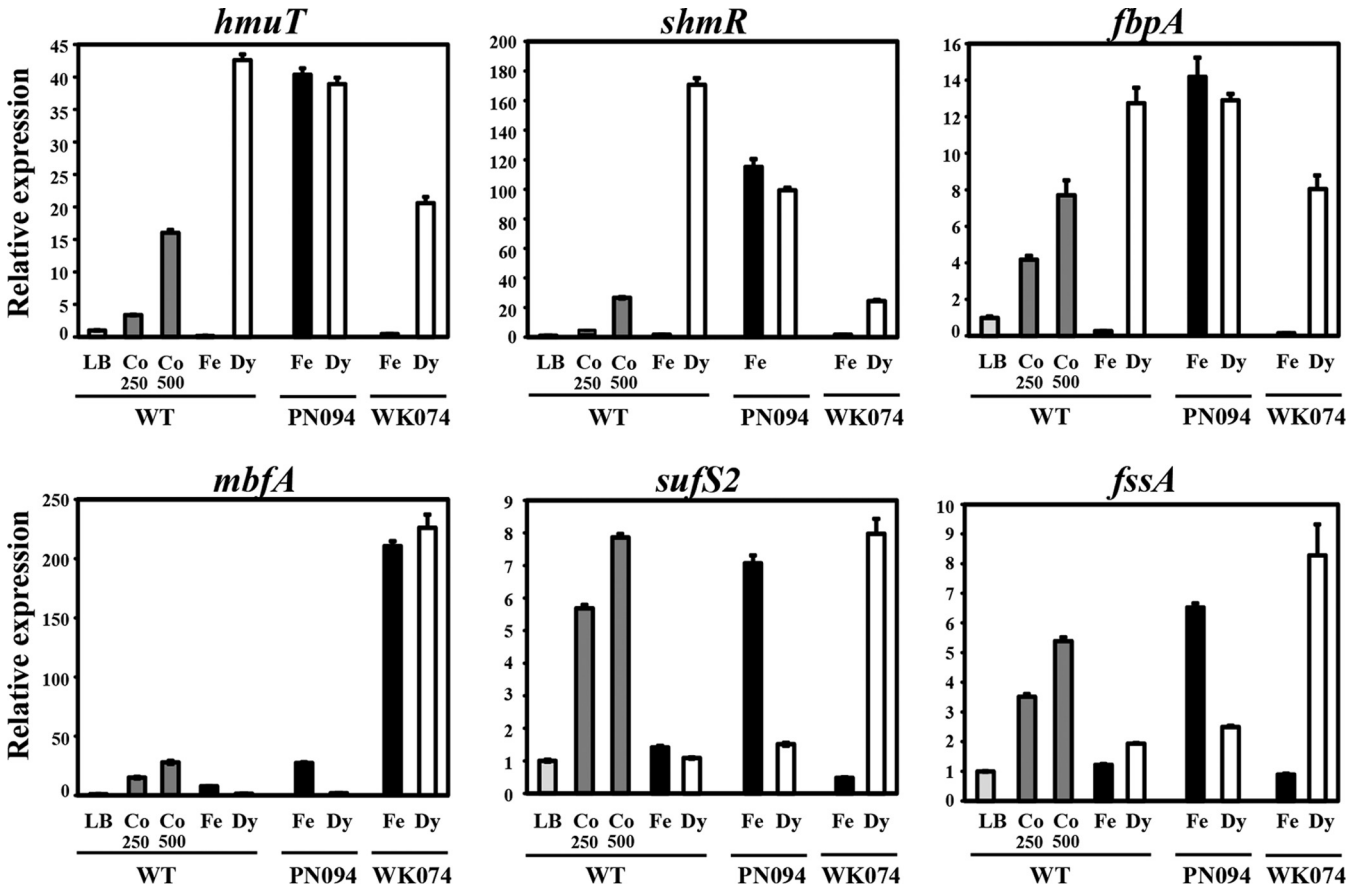

FIG 4 Effect of cobalt stress on the expression of iron-responsive genes determined using qRT-PCR. Log-phase cells of the NTL4 (WT), PN094 (*rirA* mutation), and WK074 (*irr* mutation) strains grown in LB were either untreated or treated with $CoCl_2$ (250 or 500 μM), $FeCl_3$ (50 μM), or Dy (200 μM) for 15 min. The fold changes in gene expression (*hmuT*, *shmR*, *fbpA*, *mbfA*, *sufS2*, and *fssA*) are expressed relative to the untreated WT sample (LB, regarded as 1). The experiment was performed in biological triplicate, and the error bars indicate the standard deviations.

min, and expression of the iron-responsive genes was determined using qRT-PCR. It was found that Co, but not Cu, Mn, Ni, and Zn, induced the expression of iron-responsive genes, including *hmuT* (14-fold), *shmR* (30-fold), *fbpA* (5-fold), *mbfA* (35-fold), *sufS2* (7-fold), and *fssA* (4-fold) (see Fig. S3 in the supplemental material). These genes were inducible in a concentration-dependent manner, where 500 μM $CoCl_2$ caused greater induction than 250 μM $CoCl_2$ (Fig. 4). In contrast, the expression of the *hemA*, *fdx*, and *irpA* genes was not strikingly inducible by Co (Fig. S3). These results demonstrated that cobalt stress perturbs iron homeostasis in *A. tumefaciens*.

In WT, the level of induction of the iron-repressed genes *hmuT* (42-fold), *shmR* (170-fold), and *fbpA* (13-fold) by an iron chelator (200 μM 2,2′-dipyridyl [Dy]) was higher than Co induction (Fig. 4). The iron-dependent repression of these genes was lost in the PN094 (*rirA* mutation) strain, with similar expression levels observed under high-Fe (50 μM $FeCl_3$) and low-Fe (200 μM Dy) conditions (Fig. 4) in accordance with the view that $RirA_{At}$ is the repressor of these genes under high-Fe conditions. In contrast, the Dy-induced levels of *hmuT* (20-fold), *shmR* (24-fold), and *fbpA* (8-fold) in the WK074 (*irr* mutation) strain were decreased relative to those from the WT strain treated with Dy, suggesting that *A. tumefaciens* Irr (Irr_{At}) is an activator of these genes under low-Fe conditions. The level of *shmR* activation by 200 μM Dy was also decreased in PN094 (*rirA* mutation), suggesting the existence of unidentified regulation in addition to Irr_{At} under low-Fe conditions (Fig. 4).

A. tumefaciens mbfA is negatively regulated by Irr and is inducible in response to high Fe (37). In WT, the expression of *mbfA* was also inducible by 500 μM $CoCl_2$ (30-fold) to an even greater extent than induction by 50 μM $FeCl_3$ (7-fold) (Fig. 4). The level of *mbfA* expression in PN094 (*rirA* mutation) grown in high-Fe conditions (27-fold) was similar to that in the WT strain treated with 500 μM $CoCl_2$. In contrast, WK074 (*irr* mutation) showed higher constitutive expression of *mbfA* (210-fold) under high- and low-Fe conditions (Fig. 4).

In WT, the expression of *sufS2* and *fssA* was not markedly responsive to either high-Fe (50 μM $FeCl_3$) or low-Fe (200 μM Dy) conditions, with the observed expression levels lower than those under Co-treated conditions (Fig. 4). The expression of *sufS2* and *fssA* was derepressed in PN094 (*rirA* mutation) grown in high Fe and in WK074 (*irr* mutation) grown in low Fe (Fig. 4), which is consistent with the notion that $RirA_{At}$ and Irr_{At} are repressors of *sufS2* and *fssA* under high-Fe and low-Fe conditions, respectively.

Cobalt impairs the activation of the SoxR-regulated gene *sodBII*. SoxR is a superoxide-sensing transcriptional regulator that requires 2Fe-2S for its activation function (23). *A. tumefaciens* SoxR ($SoxR_{At}$) activates *sodBII* expression as a defense response to

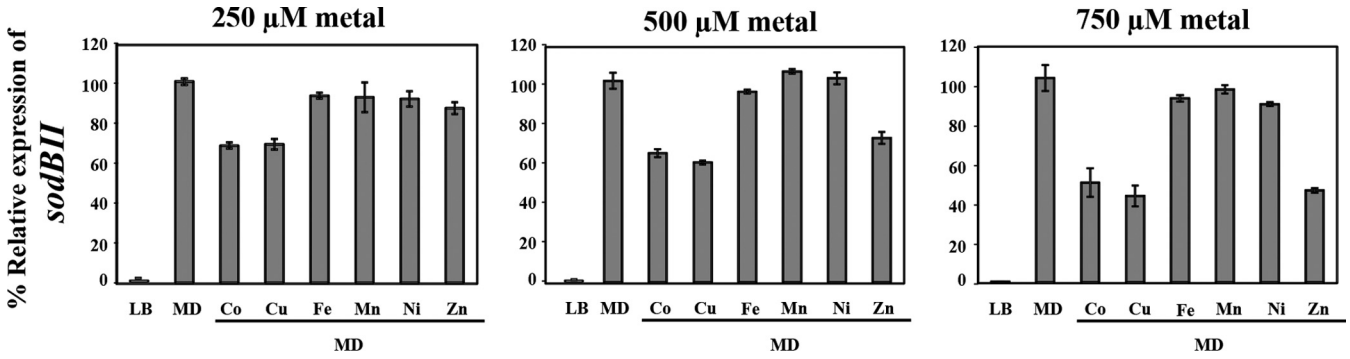

FIG 5 qRT-PCR analysis of *sodBII* induction by menadione in the presence of various metals. Log-phase NTL4 cells grown in LB were either uninduced or induced with 500 μM menadione (MD) in the absence or presence of 250, 500, or 750 μM concentrations of various metals ($CoCl_2$, $NiCl_2$, $FeCl_3$,$CuSO_4$, $MnCl_2$, or $ZnCl_2$) for 15 min. The expression levels are presented as a percentage, relative to those in cells grown in LB induced with 500 μM MD (100%).

detoxify superoxide anions (38). Cobalt inhibits the activity of Fe-S proteins as shown in *E. coli* (5) and *S. enterica* (6). It is possible that Fe-S clusters may be damaged during cobalt stress in *A. tumefaciens*, as many iron-responsive genes under the control of the Fe-S protein RirA were derepressed under high-cobalt conditions (Fig. 4). To test whether cobalt stress may also affect Fe-S-dependent $SoxR_{At}$ activity, the induction of *sodBII* by the superoxide generator menadione (MD; 500 μM) in the absence and presence of $CoCl_2$, $CuSO_4$, $FeCl_3$, $MnCl_2$, $NiCl_2$, or $ZnCl_2$ was measured via qRT-PCR using RNA isolated from the WT cells (Fig. 5). *sodBII* expression was inducible by ~1.4×10^3-fold by MD but not by cobalt treatment (250, 500, or 750 μM $CoCl_2$; data not shown). The MD activation of *sodBII* was reduced by ~30%, 35%, and 50% in the presence of 250, 500, and 750 μM $CoCl_2$, respectively (Fig. 5). These results demonstrated that Co has a negative effect on the induction of *sodBII* in response to MD exposure. In addition, Cu and Zn could also inhibit the MD activation of *sodBII*, while Fe, Mn, and Ni caused a slight effect (Fig. 5).

RirA plays a role in coping with cobalt and nickel toxicity. Iron can protect *E. coli* from cobalt toxicity (4). An *E. coli fur* mutant strain exhibits the derepression of iron uptake genes and increases in intracellular iron, leading to increased resistance to cobalt (4). Mutations in *A. tumefaciens rirA* and *irr* ($rirA_{At}$ and irr_{At}) cause higher and lower levels, respectively, of nonprotein-bound iron (21). Inactivation of either of the iron-sensing regulators $rirA_{At}$ and irr_{At} (PN094 and WK074 strains, respectively) has no effect on the metal induction of *dmeF* (Fig. 6A). However, the loss of $RirA_{At}$, but not Irr_{At}, decreased the ability of *A. tumefaciens* to cope with cobalt and nickel toxicity (Fig. 6B). The PN094 (*rirA* mutation) strain was more sensitive to cobalt and nickel than the WT strain (Fig. 6B). These results revealed a link between iron and cobalt/nickel homeostasis in *A. tumefaciens* via the iron-sensing transcriptional regulator RirA. At lower concentrations of cobalt (250 and 350 μM $CoCl_2$) and nickel (0.8 mM $NiCl_2$), PN094 (*rirA* mutation) was apparently more sensitive to the metals than DF156 (*dmeF* mutation) (Fig. 6B). In contrast, at higher concentrations of cobalt (600 and 700 μM $CoCl_2$) and nickel (1.4 and 1.8 mM $NiCl_2$), DF156 was more sensitive to the metals than PN094 (Fig. 6B).

DISCUSSION

The DmeF protein is a member of the metal exporter CDF family, and very little is known about its function and gene regulation. Thus far, only two DmeF proteins have been studied, from *Cupriavidus metallidurans* CH34 ($DmeF_{Cm}$) (18) and *Rhizobium leguminosarum* ($DmeF_{Rl}$) (19). DmeF is classified into the subgroup I Zn-CDFs (39). However, the DmeF proteins have been shown to exhibit broad metal specificity, with the ability to extrude Co(II) and Ni(II) (18, 19). Like $DmeF_{Cm}$ and $DmeF_{Rl}$, *Agrobacterium tumefaciens* DmeF ($DmeF_{At}$) exhibits six predicted transmembrane (TM) domains that contain two motifs, which are characteristic of the CDF family (the HX_3H motif at TM2 and the HX_3D motif at TM5) and are a unique characteristic of the subgroup I CDFs, in the histidine-rich stretch located between TM4 and TM5 (see Fig. S4 in the supplemental material). $DmeF_{At}$ shares 39% and 65% amino acid identity with $DmeF_{Cm}$ and $DmeF_{Rl}$, respectively. Similar to $DmeF_{Cm}$ and $DmeF_{Rl}$, $DmeF_{At}$ was shown to be involved in the detoxification of cobalt and nickel in the present study.

The regulation of *dmeF* gene expression differs in *C. metallidurans* CH34 and *R. leguminosarum*. The $dmeF_{Cm}$ gene is constitutively expressed and is not inducible by metals (18), whereas $dmeF_{Rl}$ is specifically inducible by cobalt and nickel, with cobalt acting as a more potent inducer (19). $dmeF_{Rl}$ is cotranscribed with an upstream gene, *dmeR*. The transcription of the $dmeRF_{Rl}$ operon is negatively controlled by *dmeR*, which encodes a metal-responsive transcriptional regulatory protein that belongs to the RcnR/CsoR family (19). RcnR senses Co(II) and Ni(II) in the metal-responsive repression of *rcnA* and encodes a cobalt and nickel efflux protein (10, 40), while CsoR is the Cu(I)-responsive repressor of the copper efflux gene *copA* (41–43). The predicted DNA operator sites recognized by RcnR/CsoR proteins contain a G or C tract of three to eight bases flanked by AT-rich inverted repeats (36).

The arrangement of the *dmeR* and *dmeF* genes and the potential DmeR-binding boxes is conserved in members of *Rhizobiaceae*, including *R. leguminosarum*, *Sinorhizobium meliloti*, and *A. tumefaciens* (19). Although negative regulation of the *dmeRF* operon by DmeR has been observed in *R. leguminosarum*, the molecular mechanism of the regulation has not been previously demonstrated. In the present study, we provide the first evidence of the molecular mechanism by which $DmeR_{At}$ regulates *dmeRF* expression. The use of a promoter-*lacZ* transcriptional fusion, electrophoretic mobility shift assay, and a DNase I footprinting assay revealed that $DmeR_{At}$ exerts repression of *dmeRF* transcription through direct binding to the promoter region upstream of

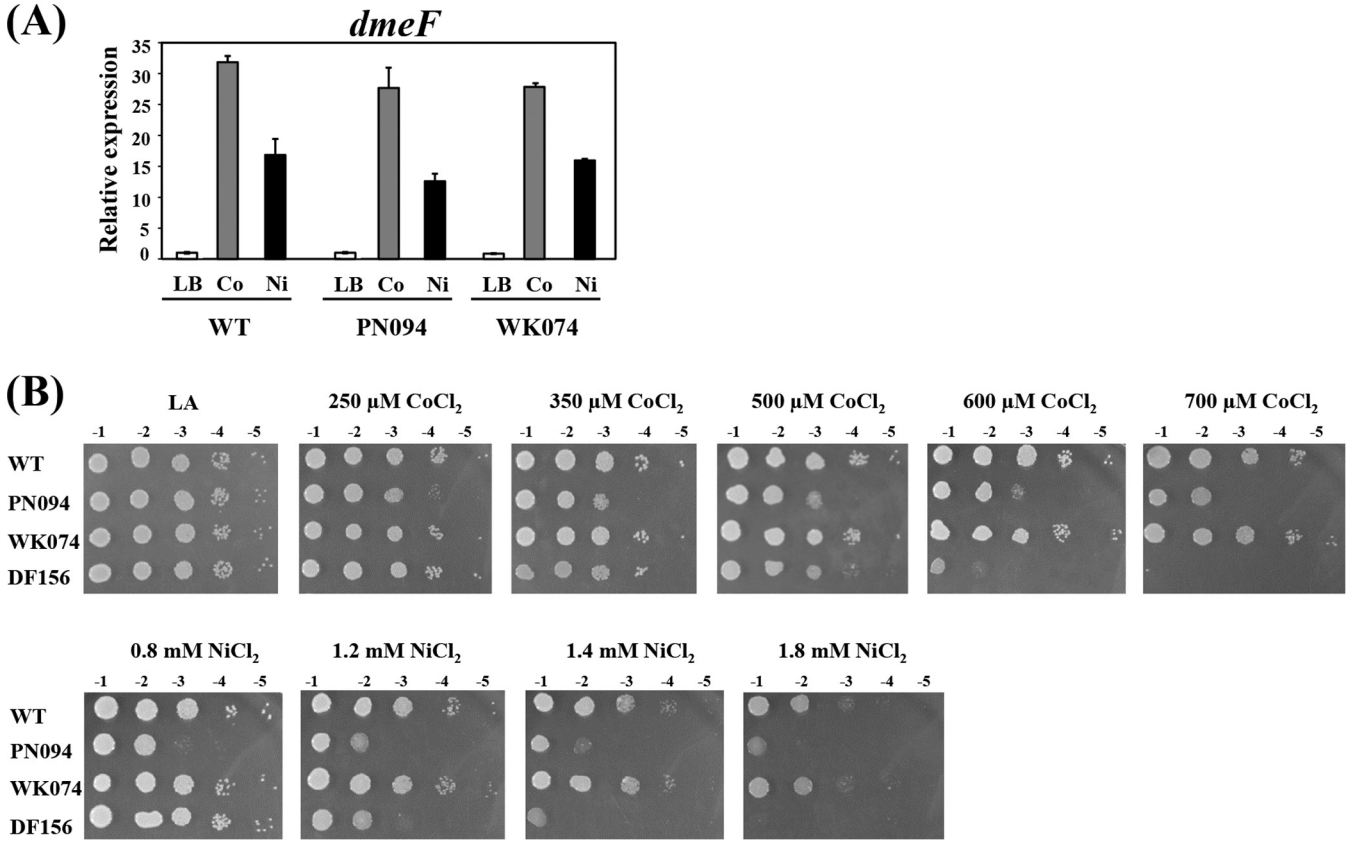

FIG 6 (A) qRT-PCR analysis of *dmeF* induction in NTL4 (WT), PN094 (*rirA* mutation), and WK074 (*irr* mutation). Log-phase cells grown in LB were either uninduced or induced with 500 μM $CoCl_2$ or $NiCl_2$ for 15 min. The fold changes in *dmeF* expression are expressed relative to the untreated WT sample (LB, regarded as 1). The experiment was performed in biological triplicate, and the error bars indicate the standard deviations. (B) Sensitivity to cobalt and nickel. Log-phase cells of NTL4 (WT), PN094 (*rirA* mutation), WK074 (*irr* mutation), and DF156 (*dmeF* mutation) grown in LB were adjusted, serially diluted, and spotted onto LA plates containing $CoCl_2$ (250, 350,500, 600, or 700 μM) or $NiCl_2$ (0.8, 1.2, 1.4, or 1.8 mM). Tenfold serial dilutions are indicated.

dmeR. The apo-$DmeR_{At}$ form recognizes the 5′-ATATAGTATA CCCCCCTATAGTATAT-3′ DNA sequence, while *E. coli* RcnR ($RcnR_{Ec}$) in the apo form binds to 5′-TACTGGGGGGAGTA-3′ (36). The inverted AT repeats are proposed to form sequence-specific recognition sites for the regulators, while the G or C tracts may be important for providing a unique DNA structural feature to facilitate protein-DNA interaction for the RcnR/CsoR family (36). The location of the $DmeR_{At}$ binding site overlaps that of the predicted −10 sequence of the RNA polymerase recognition site, supporting the view that $DmeR_{At}$ is a transcriptional repressor. The mechanism of metal-responsive repression of $DmeR_{At}$ is similar to that for $RcnR_{Ec}$ in that the regulatory switch occurs upon binding to Co(II) and Ni(II). The binding of these metals may cause conformational changes in $DmeR_{At}$, resulting in dissociation from DNA and thus triggering the transcription of the *dmeRF* operon. $DmeR_{At}$ shares 43% amino acid identity with $RcnR_{Ec}$ and exhibits the putative metal-binding residues His3-Cys35-His60-His64, which are the same as those of $RcnR_{Ec}$ used for Co(II)/Ni(II) coordination (10) (see Fig. S5 in the supplemental material). The metal-binding residues of the Co(II)/Ni(II)-sensing regulators $RcnR_{Ec}$ and $DmeR_{At}$ are different from those of CsoR (Cys36-His61-Cys65), a protein from the same family that responds specifically to Cu(I) (41). $DmeR_{At}$ represses its own transcription, which provides feedback regulation to help rapidly respond to fluctuations in cobalt and nickel concentrations in the environment. In contrast to the *dmeRF* system, the *E. coli rcnR* gene is transcribed in the opposite direction relative to *rcnA*. The expression of the *rcnR* and *rcnA* genes is negatively regulated by RcnR (10); moreover, *rcnR* expression is inducible by Fur in response to iron (44). However, iron has no effect on the induction of the $dmeRF_{At}$ operon. In some members of the *Alphaproteobacteria*, including *A. tumefaciens*, the RirA protein has evolved to carry out the typical Fur function in the regulation of iron-responsive genes (22). Unlike that observed regarding the connection of *E. coli* Fur and the *rcn* system, *A. tumefaciens* RirA ($RirA_{At}$) plays no role in the induction of the *dmeRF* operon.

Cobalt toxicity is caused by direct competition with iron, resulting in impaired Fe-S biogenesis, a defect in Fe-S enzymes, and deregulation of iron homeostasis (4–7). Another aim of this study was to investigate the effect of cobalt stress on the activity of Fe-S proteins (RirA and SoxR) and the expression of iron-responsive genes in *A. tumefaciens*. RirA and Irr sense iron in the form of Fe-S and heme, respectively, to control iron homeostasis in *Alphaproteobacteria* (22). Similar to observations made in *E. coli* (5) and *S. enterica* (6), cobalt caused increased expression of many iron-responsive genes in *A. tumefaciens*. Derepression of *hmuT*, *shmR*, and *fbpA* may result from direct damage to the Fe-S regulator $RirA_{At}$ and/or disruption of the Fe-S supply by cobalt. Impair-

ment of the function of another Fe-S regulator, *A. tumefaciens* SoxR ($SoxR_{At}$), in activating *sodBII* transcription was also observed at high concentrations of cobalt. In addition to cobalt, copper and zinc were also shown to reduce the activity of $SoxR_{At}$. The effects of copper and zinc on $SoxR_{At}$ are not surprising because these metals have also been reported to damage Fe-S clusters (45, 46). In contrast, copper and zinc had no effect on the expression of *hmuT*, *shmR*, and *fbpA*. One possible explanation is that there are differences in the sensitivities of Fe-S clusters in $RirA_{At}$ and $SoxR_{At}$ to be damaged by different metals. Cobalt also caused derepression of the iron exporter gene *mbfA*, which is under the negative control of *A. tumefaciens* Irr (Irr_{At}). Unlike Rir_{At}, Irr_{At} is not an Fe-S protein. Whether cobalt directly or indirectly damages Irr_{At} remains unknown. Iron has been shown to induce the oxidation and degradation of *Bradyrhizobium japonicum* Irr (47). Determination of whether the stability of Irr_{At} is affected by iron- and cobalt-induced oxidative damage awaits further study. Derepression of *sufS2* and *fssA* under high cobalt conditions may be a consequence of the inactivation of $RirA_{At}$ and/or Irr_{At}, as these genes are negatively regulated by both $RirA_{At}$ and Irr_{At}.

The upregulation of gene products involved in iron uptake in an *E. coli fur* mutant strain was found to lead to an increased intracellular iron content, which in turn protects *E. coli* from cobalt toxicity (4). An *A. tumefaciens rirA* mutant strain was shown to exhibit derepression of iron uptake genes and higher levels of intracellular iron (21); however, in the present study, this strain was shown to be hypersensitive to cobalt and nickel. These observations reflect the different mechanisms used by *E. coli* and *A. tumefaciens* to respond to the toxic effects of metals. Interestingly, the iron regulator $RirA_{At}$ played a more dominant role in bacterial survival at lower concentrations of cobalt/nickel than the metal efflux protein $DmeF_{At}$, whereas $DmeF_{At}$ became more important than $RirA_{At}$ in coping with the metals at higher concentrations. These results suggested the existence of differential modes of cellular responses to the toxic effects of cobalt/nickel at low and high concentrations in *A. tumefaciens*. Furthermore, the control of the homeostasis of a particular metal may also affect the ability of bacteria to resist other metals, although the exact mechanism through which the iron-responsive regulator $RirA_{At}$ mediates cobalt/nickel resistance is still not known.

One of the common strategies for bacteria to avoid metal toxicity is to pump excess metal ions out of the cell. It was demonstrated in *C. metallidurans* CH34 that DmeF interacts with the CnrCBA and CzcCBA RND systems (18). Cobalt must be first transferred from the cytoplasm to the periplasm via the CDF protein DmeF, and cobalt can subsequently be transported from the periplasm to the outside of the cell by the RND systems (18). The identification and characterization of the RND system(s) working in cooperation with $DmeF_{At}$ for metal efflux will be of interest in future studies aimed at obtaining a better understanding of metal transport systems and metal tolerance in *A. tumefaciens*.

ACKNOWLEDGMENTS

We thank S. K. Farrand for the plasmid pCMA1. We also thank P. Srifah Huehne and K. Bhinija for technical assistance with the virulence assay.

This work was supported by the Chulabhorn Research Institute and the Thailand Research Fund grant RSA5880010.

REFERENCES

1. **Kobayashi M, Shimizu S.** 1999. Cobalt proteins. Eur J Biochem **261:**1–9. http://dx.doi.org/10.1046/j.1432-1327.1999.00186.x.
2. **Banerjee R, Ragsdale SW.** 2003. The many faces of vitamin B_{12}: catalysis by cobalamin-dependent enzymes. Annu Rev Biochem **72:**209–247. http://dx.doi.org/10.1146/annurev.biochem.72.121801.161828.
3. **Leonard S, Gannett PM, Rojanasakul Y, Schwegler-Berry D, Castranova V, Vallyathan V, Shi X.** 1998. Cobalt-mediated generation of reactive oxygen species and its possible mechanism. J Inorg Biochem **70:**239–244. http://dx.doi.org/10.1016/S0162-0134(98)10022-3.
4. **Fantino JR, Py B, Fontecave M, Barras F.** 2010. A genetic analysis of the response of *Escherichia coli* to cobalt stress. Environ Microbiol **12:**2846–2857.
5. **Ranquet C, Ollagnier-de-Choudens S, Loiseau L, Barras F, Fontecave M.** 2007. Cobalt stress in *Escherichia coli*. The effect on the iron-sulfur proteins. J Biol Chem **282:**30442–30451.
6. **Thorgersen MP, Downs DM.** 2007. Cobalt targets multiple metabolic processes in *Salmonella enterica*. J Bacteriol **189:**7774–7781. http://dx.doi.org/10.1128/JB.00962-07.
7. **Majtan T, Frerman FE, Kraus JP.** 2011. Effect of cobalt on *Escherichia coli* metabolism and metalloporphyrin formation. Biometals **24:**335–347. http://dx.doi.org/10.1007/s10534-010-9400-7.
8. **Okamoto S, Eltis LD.** 2011. The biological occurrence and trafficking of cobalt. Metallomics **3:**963–970. http://dx.doi.org/10.1039/c1mt00056j.
9. **Rodrigue A, Effantin G, Mandrand-Berthelot MA.** 2005. Identification of *rcnA* (*yohM*), a nickel and cobalt resistance gene in *Escherichia coli*. J Bacteriol **187:**2912–2916. http://dx.doi.org/10.1128/JB.187.8.2912-2916.2005.
10. **Iwig JS, Leitch S, Herbst RW, Maroney MJ, Chivers PT.** 2008. Ni(II) and Co(II) sensing by *Escherichia coli* RcnR. J Am Chem Soc **130:**7592–7606. http://dx.doi.org/10.1021/ja710067d.
11. **Rutherford JC, Cavet JS, Robinson NJ.** 1999. Cobalt-dependent transcriptional switching by a dual-effector MerR-like protein regulates a cobalt-exporting variant CPx-type ATPase. J Biol Chem **274:**25827–25832. http://dx.doi.org/10.1074/jbc.274.36.25827.
12. **Raimunda D, Long JE, Sassetti CM, Argüello JM.** 2012. Role in metal homeostasis of CtpD, a Co^{2+} transporting P_{1B4}-ATPase of *Mycobacterium smegmatis*. Mol Microbiol **84:**1139–1149. http://dx.doi.org/10.1111/j.1365-2958.2012.08082.x.
13. **Raimunda D, Long JE, Padilla-Benavides T, Sassetti CM, Argüello JM.** 2014. Differential roles for the Co^{2+}/Ni^{2+} transporting ATPases, CtpD and CtpJ, in *Mycobacterium tuberculosis* virulence. Mol Microbiol **91:**185–197. http://dx.doi.org/10.1111/mmi.12454.
14. **Liesegang H, Lemke K, Siddiqui RA, Schlegel HG.** 1993. Characterization of the inducible nickel and cobalt resistance determinant *cnr* from pMOL28 of *Alcaligenes eutrophus* CH34. J Bacteriol **175:**767–778.
15. **Nies DH.** 1995. The cobalt, zinc, and cadmium efflux system CzcABC from *Alcaligenes eutrophus* functions as a cation-proton antiporter in *Escherichia coli*. J Bacteriol **177:**2707–2712.
16. **Anton A, Grosse C, Reissmann J, Pribyl T, Nies DH.** 1999. CzcD is a heavy metal ion transporter involved in regulation of heavy metal resistance in *Ralstonia* sp. strain CH34. J Bacteriol **181:**6876–6881.
17. **Scherer J, Nies DH.** 2009. CzcP is a novel efflux system contributing to transition metal resistance in *Cupriavidus metallidurans* CH34. Mol Microbiol **73:**601–621. http://dx.doi.org/10.1111/j.1365-2958.2009.06792.x.
18. **Munkelt D, Grass G, Nies DH.** 2004. The chromosomally encoded cation diffusion facilitator proteins DmeF and FieF from *Wautersia metallidurans* CH34 are transporters of broad metal specificity. J Bacteriol **186:**8036–8043. http://dx.doi.org/10.1128/JB.186.23.8036-8043.2004.
19. **Rubio-Sanz L, Prieto RI, Imperial J, Palacios JM, Brito B.** 2013. Functional and expression analysis of the metal-inducible *dmeRF* system from *Rhizobium leguminosarum* bv. *viciae*. Appl Environ Microbiol **79:**6414–6422. http://dx.doi.org/10.1128/AEM.01954-13.
20. **Ngok-Ngam P, Ruangkiattikul N, Mahavihakanont A, Virgem SS, Sukchawalit R, Mongkolsuk S.** 2009. Roles of *Agrobacterium tumefaciens* RirA in iron regulation, oxidative stress response, and virulence. J Bacteriol **191:**2083–2090. http://dx.doi.org/10.1128/JB.01380-08.
21. **Hibbing ME, Fuqua C.** 2011. Antiparallel and interlinked control of cellular iron levels by the Irr and RirA regulators of *Agrobacterium tumefaciens*. J Bacteriol **193:**3461–3472. http://dx.doi.org/10.1128/JB.00317-11.
22. **Rodionov DA, Gelfand MS, Todd JD, Curson AR, Johnston AW.** 2006. Computational reconstruction of iron- and manganese-responsive transcriptional networks in *Alphaproteobacteria*. PLoS Comput Biol **2:**e163. http://dx.doi.org/10.1371/journal.pcbi.0020163.
23. **Crack JC, Green J, Thomson AJ, Le Brun NE.** 2012. Iron-sulfur cluster

sensor-regulators. Curr Opin Chem Biol **16:**35–44. http://dx.doi.org/10.1016/j.cbpa.2012.02.009.
24. **Bhubhanil S, Niamyim P, Sukchawalit R, Mongkolsuk S.** 2014. Cysteine desulphurase-encoding gene *sufS2* is required for the repressor function of RirA and oxidative resistance in *Agrobacterium tumefaciens*. Microbiology **160:**79–90. http://dx.doi.org/10.1099/mic.0.068643-0.
25. **Wood DW, Setubal JC, Kaul R, Monks DE, Kitajima JP, Okura VK, Zhou Y, Chen L, Wood GE, Almeida NF, Jr, Woo L, Chen Y, Paulsen IT, Eisen JA, Karp PD, Bovee D, Sr, Chapman P, Clendenning J, Deatherage G, Gillet W, Grant C, Kutyavin T, Levy R, Li MJ, McClelland E, Palmieri A, Raymond C, Rouse G, Saenphimmachak C, Wu Z, Romero P, Gordon D, Zhang S, Yoo H, Tao Y, Biddle P, Jung M, Krespan W, Perry M, Gordon-Kamm B, Liao L, Kim S, Hendrick C, Zhao ZY, Dolan M, Chumley F, Tingey SV, Tomb JF, Gordon MP, Olson MV, Nester EW.** 2001. The genome of the natural genetic engineer *Agrobacterium tumefaciens* C58. Science **294:**2317–2323. http://dx.doi.org/10.1126/science.1066804.
26. **Cangelosi GA, Best EA, Martinetti G, Nester EW.** 1991. Genetic analysis of *Agrobacterium*. Methods Enzymol **204:**384–397. http://dx.doi.org/10.1016/0076-6879(91)04020-O.
27. **Sambrook J, Fritsch EF, Maniatis T.** 1989. Molecular cloning: a laboratory manual. Cold Spring Harbor Laboratory, Cold Spring Harbor, NY.
28. **Bhubhanil S, Sittipo P, Chaoprasid P, Nookabkaew S, Sukchawalit R, Mongkolsuk S.** 2014. Control of zinc homeostasis in *Agrobacterium tumefaciens* via *zur* and the zinc uptake genes *znuABC* and *zinT*. Microbiology **160:**2452–2463. http://dx.doi.org/10.1099/mic.0.082446-0.
29. **Livak KJ, Schmittgen TD.** 2001. Analysis of relative gene expression data using real-time quantitative PCR and the $2^{-\Delta\Delta CT}$ method. Methods **25:**402–408. http://dx.doi.org/10.1006/meth.2001.1262.
30. **Kovach ME, Elzer PH, Hill DS, Robertson GT, Farris MA, Roop RM, II, Peterson KM.** 1995. Four new derivatives of the broad-host-range cloning vector pBBR1MCS, carrying different antibiotic-resistance cassettes. Gene **166:**175–176. http://dx.doi.org/10.1016/0378-1119(95)00584-1.
31. **DeFeyter R, Kado CI, Gabriel DW.** 1990. Small, stable shuttle vectors for use in *Xanthomonas*. Gene **88:**65–72. http://dx.doi.org/10.1016/0378-1119(90)90060-5.
32. **Miller JH.** 1972. Experiments in molecular genetics. Cold Spring Harbor Laboratory, Cold Spring Harbor, NY.
33. **Bhubhanil S, Chamsing J, Sittipo P, Chaoprasid P, Sukchawalit R, Mongkolsuk S.** 2014. Roles of *Agrobacterium tumefaciens* membrane-bound ferritin (MbfA) in iron transport and resistance to iron under acidic conditions. Microbiology **160:**863–871. http://dx.doi.org/10.1099/mic.0.076802-0.
34. **Kamoun S, Hamada W, Huitema E.** 2003. Agrosuppression: a bioassay for the hypersensitive response suited to high-throughput screening. Mol Plant Microbe Interact **16:**7–13. http://dx.doi.org/10.1094/MPMI.2003.16.1.7.
35. **Iwig JS, Rowe JL, Chivers PT.** 2006. Nickel homeostasis in *Escherichia coli*-the *rcnR-rcnA* efflux pathway and its linkage to NikR function. Mol Microbiol **62:**252–262. http://dx.doi.org/10.1111/j.1365-2958.2006.05369.x.
36. **Iwig JS, Chivers PT.** 2009. DNA recognition and wrapping by *Escherichia coli* RcnR. J Mol Biol **393:**514–526. http://dx.doi.org/10.1016/j.jmb.2009.08.038.
37. **Ruangkiattikul N, Bhubhanil S, Chamsing J, Niamyim P, Sukchawalit R, Mongkolsuk S.** 2012. *Agrobacterium tumefaciens* membrane-bound ferritin plays a role in protection against hydrogen peroxide toxicity and is negatively regulated by the iron response regulator. FEMS Microbiol Lett **329:**87–92. http://dx.doi.org/10.1111/j.1574-6968.2012.02509.x.
38. **Saenkham P, Eiamphungporn W, Farrand SK, Vattanaviboon P, Mongkolsuk S.** 2007. Multiple superoxide dismutases in *Agrobacterium tumefaciens*: functional analysis, gene regulation, and influence on tumorigenesis. J Bacteriol **189:**8807–8817. http://dx.doi.org/10.1128/JB.00960-07.
39. **Montanini B, Blaudez D, Jeandroz S, Sanders D, Chalot M.** 2007. Phylogenetic and functional analysis of the cation diffusion facilitator (CDF) family: improved signature and prediction of substrate specificity. BMC Genomics **8:**107. http://dx.doi.org/10.1186/1471-2164-8-107.
40. **Blaha D, Arous S, Blériot C, Dorel C, Mandrand-Berthelot MA, Rodrigue A.** 2011. The *Escherichia coli* metallo-regulator RcnR represses *rcnA* and *rcnR* transcription through binding on a shared operator site: insights into regulatory specificity towards nickel and cobalt. Biochimie **93:**434–439. http://dx.doi.org/10.1016/j.biochi.2010.10.016.
41. **Liu T, Ramesh A, Ma Z, Ward SK, Zhang L, George GN, Talaat AM, Sacchettini JC, Giedroc DP.** 2007. CsoR is a novel *Mycobacterium tuberculosis* copper-sensing transcriptional regulator. Nat Chem Biol **3:**60–68. http://dx.doi.org/10.1038/nchembio844.
42. **Smaldone GT, Helmann JD.** 2007. CsoR regulates the copper efflux operon *copZA* in *Bacillus subtilis*. Microbiology **153:**4123–4128. http://dx.doi.org/10.1099/mic.0.2007/011742-0.
43. **Corbett D, Schuler S, Glenn S, Andrew PW, Cavet JS, Roberts IS.** 2011. The combined actions of the copper-responsive repressor CsoR and copper-metallochaperone CopZ modulate CopA-mediated copper efflux in the intracellular pathogen *Listeria monocytogenes*. Mol Microbiol **81:**457–472. http://dx.doi.org/10.1111/j.1365-2958.2011.07705.x.
44. **Koch D, Nies DH, Grass G.** 2007. The RcnRA (YohLM) system of *Escherichia coli*: a connection between nickel, cobalt and iron homeostasis. Biometals **20:**759–771. http://dx.doi.org/10.1007/s10534-006-9039-6.
45. **Macomber L, Imlay JA.** 2009. The iron-sulfur clusters of dehydratases are primary intracellular targets of copper toxicity. Proc Natl Acad Sci U S A **106:**8344–8349. http://dx.doi.org/10.1073/pnas.0812808106.
46. **Xu FF, Imlay JA.** 2012. Silver(I), mercury(II), cadmium(II), and zinc(II) target exposed enzymic iron-sulfur clusters when they toxify *Escherichia coli*. Appl Environ Microbiol **78:**3614–3621. http://dx.doi.org/10.1128/AEM.07368-11.
47. **Yang J, Panek HR, O'Brian MR.** 2006. Oxidative stress promotes degradation of the Irr protein to regulate haem biosynthesis in *Bradyrhizobium japonicum*. Mol Microbiol **60:**209–218. http://dx.doi.org/10.1111/j.1365-2958.2006.05087.x.
48. **Luo ZQ, Clemente TE, Farrand SK.** 2001. Construction of a derivative of *Agrobacterium tumefaciens* C58 that does not mutate to tetracycline resistance. Mol Plant Microbe Interact **14:**98–103. http://dx.doi.org/10.1094/MPMI.2001.14.1.98.
49. **Metcalf WW, Jiang W, Daniels LL, Kim SK, Haldimann A, Wanner BL.** 1996. Conditionally replicative and conjugative plasmids carrying *lacZ* alpha for cloning, mutagenesis, and allele replacement in bacteria. Plasmid **35:**1–13. http://dx.doi.org/10.1006/plas.1996.0001.
50. **Grant SG, Jessee J, Bloom FR, Hanahan D.** 1990. Differential plasmid rescue from transgenic mouse DNAs into *Escherichia coli* methylation-restriction mutants. Proc Natl Acad Sci U S A **87:**4645–4649. http://dx.doi.org/10.1073/pnas.87.12.4645.
51. **Alexeyev MF.** 1999. The pKNOCK series of broad-host-range mobilizable suicide vectors for gene knockout and targeted DNA insertion into the chromosome of gram-negative bacteria. Biotechniques **26:**824–826, 828.
52. **Hwang I, Cook DM, Farrand SK.** 1995. A new regulatory element modulates homoserine lactone-mediated autoinduction of Ti plasmid conjugal transfer. J Bacteriol **177:**449–458.